ROLE OF ASTROCYTE-SECRETED THROMBOSPONDIN-1 IN THE FRAGILE X MOUSE

THE ROLE OF ASTROCYTE-SECRETED THROMBOSPONDIN-1 IN THE FRAGILE X MOUSE

By

CONNIE CHENG, B.Sc.

A Thesis
Submitted to the School of Graduate Studies
in Partial Fulfillment of the Requirements for the Degree
Doctor of Philosophy

McMaster University
© Copyright by Connie Cheng, June 2016

DOCTOR OF PHILOSOPHY (2016) McMASTER UNIVERSITY

Science—Neuroscience Hamilton, ON

TITLE:	The Role of Astrocyte-Secreted Thrombospondin-1 in the Fragile X Mouse Model
AUTHOR:	Connie Cheng, B.Sc. (McMaster University)
SUPERVISOR:	Dr. Laurie C. Doering
NUMBER OF PAGES:	xvi, 203

Abstract

Fragile X syndrome (FXS) is the most common inherited form of intellectual disability and autism spectrum disorders. The disorder is typically caused by decreased or absent levels of the fragile X mental retardation protein (FMRP) due to a loss-of-function mutation in the fragile X mental retardation 1 (*FMR1*) gene. Astrocytes are key participants in various aspects of brain development and function, many of which are executed via secreted proteins. Specifically, the astrocyte-secreted matricellular protein thrombospondin-1 (TSP-1) has been highly implicated in the regulation of neuronal synaptogenesis. Previously, we have shown that astrocytes can prevent the abnormal dendrite morphology and dysregulated synapses that characterize FXS. While we have identified that astrocytes affect synapse development *in vitro*, the role of secreted factors has not been elucidated. Utilizing a Fragile X mouse model and a neuron-astrocyte, non-contact co-culture system, we investigated the contributions of soluble TSP-1 in spine and synapse development. We found that TSP-1 protein levels were reduced in *Fmr1* knockout (KO) cultured astrocytes and astrocyte-conditioned media (ACM). TSP-1 levels were also downregulated in the cortex and hippocampus of Fragile X mice in contrast to their wildtype (WT) counterparts. Additionally, *Fmr1* KO hippocampal neurons exhibited significant deficits in dendritic spine morphology and excitatory synapse formation following long-term culture. However, all spine and synaptic abnormalities were prevented in the presence of either ACM or a feeder layer derived from WT astrocytes, or following the application of exogenous TSP-1, thereby suggesting a role for soluble glial factors in the formation and maturation of spines and synapses. These findings presented here provide strong evidence for astroglia-derived TSP-1 as a strong promoter of neuronal development in FXS. Therefore, defects in astrocyte function and secreted molecules during early development may contribute to the abnormal neurobiology in FXS.

Preface

This doctoral dissertation is presented as a *sandwich thesis* and is comprised of author-generated versions of three manuscripts prepared for publication during the author's Ph.D. candidacy. One manuscript has been published (Chapter 2), and two manuscripts have been submitted for publication (Chapters 3 & 4). Due to the common focus of the manuscripts, the reader will encounter a significant degree of overlap, specifically the general introduction of the dissertation and introduction/discussion sections of each article.

Following a review of the relevant literature (Chapter 1), the hypotheses and specific aims of the thesis will be stated (Chapter 2). Then, each manuscript will be presented as an individual chapter (Chapters 3-5). Each chapter will include a preface detailing the contributions of each author to the work therein, and outlining the background and rationale for the manuscript. Following the presentation of the three manuscripts, a concluding chapter (Chapter 6) will summarize the major findings from each article, discuss the significant advances in knowledge gained from the work and provide considerations for future research directions.

Literature citations are included in the style required by the journal to which each manuscript was submitted, and refer only to the reference list within that paper. Elsewhere, the references will adhere to the formatting guidelines described by the Council of Science Editors (CSE), with a list of citations appearing in a separate references section at the end of the dissertation.

Acknowledgements

First, and foremost, I would like to take this opportunity to express my sincere gratitude to my supervisor, Dr. Laurie C. Doering. Thank you for your guidance, wisdom and the endless encouragement I received over the years under your mentorship. I would not have come this far if it were not for your leadership, support and faith in me. Thank you for believing in me and for always making yourself available to clarify my doubts. It truly has been a privilege and a pleasure to learn from you.

I would also like to acknowledge my supervisory committee members, Dr. Ram Mishra and Dr. Joseph Gabriele, who have both kindly advised and guided me in my scientific endeavours. I appreciate your guidance with my research project, all of your helpful input and genuine support throughout the process.

A very special thanks goes out to my lab mates and colleagues, Dr. Mary Sourial, Dr. Angela Scott, Jessica Wallingford, Sharon Ralph, Dr. Alexander Ball, Dr. Thomas Sabljic and Dr. Ahad Siddiqui. You have all truly been the most amazing source of support and humour. I am incredibly grateful and fortunate to have been able to work alongside you. I would also like to acknowledge the many undergraduate students and volunteers whom I had the pleasure of working with. You have all made my time in the Doering lab an unforgettable experience.

Next, I would like to extend my gratitude to the West-Mays lab - present and former, Scott Bowman, Paula Deschamps, Dr. Christine Kerr, Dr. Joe Pino, Dr. Madhuja Gupta and Dr. Aftab Taiyab. Thank you for the times spent at lunch and for never turning me away whenever I needed experimental advice, equipment or reagents.

I would also like to thank my dear friends and fellow graduate students, Mizna Zaveri, Dr. Elyse Rosa, Ritesh Daya, Anna Korol and Vanessa Martino, who have helped to keep me grounded over the years. You have all been there and supported me during my failures, yet celebrated even harder during my successes. This work would not have been possible without your support and friendship.

Last but certainly not least; I would like to express my heartfelt gratitude to my parents, family and s/o David. You have all been my motivation and my reason for being where I am today. This accomplishment marks a milestone I had never thought to reach. My achievements are directly attributable to your unwavering support and encouragement, for which I will always be grateful.

Table of Contents

List of Figures

Chapter 1

Chapter 3

Chapter 4

Chapter 5

List of Tables

Chapter 1

Chapter 3

Chapter 5

List of Publications

1. **Cheng C**, Lau KMS, Doering LC. (2016) Developmental expression of thrombospondin-1 diminishes in Fragile X astrocytes. *Neuroscience.* (Submission #: NSC-16-833).

2. **Cheng C,** Lau KMS, Doering LC. (2016) Astrocyte-secreted thrombospondin-1 modulates synapse and spine defects in the Fragile X mouse model. *Molecular Brain.* 9:74.

3. Jacobs S, **Cheng C**, Doering LC. (2016) Hippocampal neuronal subtypes develop abnormal dendritic arbors in the presence of Fragile X astrocytes. *Neuroscience.* 324:202-217.

4. **Cheng C**, Trzcinski O, Doering LC. (2014) Fluorescent labeling of dendritic spines in cell cultures with the carbocyanine dye "DiI." *Frontiers in Neuroanatamy*. 8:30.

5. Sourial M, **Cheng C**, Doering LC. (2013) Progress toward therapeutic potential for AFQ056 in Fragile X syndrome. *Journal of Experimental Pharmacology.* 5:45-54.

6. **Cheng C**, Sourial M, Doering LC. (2012) Astrocytes and Developmental Plasticity in Fragile X. *Neural Plasticity*. 96-107.

7. Jacobs S, **Cheng C**, Doering LC. (2012) Probing Astrocyte Function in Fragile X. *Results and Problems in Cell Differentiation*. 54:15-31.

List of Abbreviations

ACM	astrocyte-conditioned media
ADAMTS	a disintegrin and metalloproteinase with thrombospondin motifs
ASD	autism spectrum disorder
AFL	astrocyte feeder layer
ALDH1L1	aldehyde dehydrogenase 1 family, member L1
AMPA	a-amino-3-hydroxyl-5-methyl-4-isoazole-propionate
ANOVA	analysis of variance
ASD	autism spectrum disorder
BBB	blood brain barrier
BSA	bovine serum albumin
CNS	central nervous system
DAPI	4',6-diamidino-2-phenylindole
dH_20	distilled water
DiI	1, l ',di-octadecyl-3,3,3 '3'-tetramethylindocarbocyanine perchlorate
DIV	days *in vitro*
DS	Down Syndrome
ECM	extracellular matrix
EDTA	ethylenediaminetetraacetic acid
ELISA	enzyme-linked immunosorbent assay
Eph	ephrin
FDH	10-formyltetrahydrofolate dehydrogenase

FITC	fluorescein isothiocyanate
FMR1	*fragile X mental retardation gene 1*
FMRP	fragile X mental retardation protein
FXPOI	fragile X-associated primary ovarian insufficiency
FXS	fragile X syndrome
FXTAS	fragile X-associated tremor/ataxia syndrome
GBP	gabapentin
GFAP	glial fibrillary acidic protein
GLAST	glutamate aspartate transporter
GLT-1	glutamate transporter 1
GM	glial media
HBSS	Hanks' buffered saline solution
H.I.	heat inactivated
ICC	immunocytochemistry
ID	intellectual disability
KO	knockout
LTP	long-term potentiation
MAP-2	microtubule associated protein-2
MEM	minimum essential media
mGluR	metabotropic glutamate receptor
mRNA	messenger RNA (ribonucleic acid)
NES	nuclear export signal

NGM	neural growth media
NL-1	neuroligin-1
NLS	nuclear localization signal
NMDAR	N-methyl-D-aspartate receptor
NT-3	neurotrophin-3
PBS	phosphate buffered saline
PLL	poly-$_{L}$-lysine
PSD-95	postsynaptic density protein 95
RT	room temperature
RGC	retinal ganglion cell
rTSP-1	recombinant thrombospondin-1
SEM	standard error of mean
TSP-1	thrombospondin-1
UTR	untranslated region
vWF_A	von Willebrand Factor A
WT	wildtype

Chapter 1: Introduction

1.1 Fragile X Syndrome

1.1.1. Clinical Presentation

Fragile X syndrome (FXS), an X-linked condition first described by Martin-Bell, is the leading cause of inherited intellectual disability and autism spectrum disorders (Bagni et al. 2012). The prevalence of FXS is estimated to be 1/4000 males and 1/6000 females (Coffee et al. 2009). Patients affected by FXS experience a wide range of symptoms including cognitive deficits, social anxiety, attention deficit and hyperactivity disorder, repetitive stereotyped behaviors, seizures, and sensory hypersensitivity (Bardoni et al 2000; Wijetunge et al. 2013). Physical features may include a long, narrow face, prominent ears, and flat feet (Berry-Kravis 2014). In general, females display a less severe phenotype, with the severity of impairments correlated to the degree of inactivation of the abnormal X-chromosome.

1.1.2. Genetics of Fragile X Syndrome

Named for the cytogenic "fragile" site visible at the tip of the long arm of the X chromosome, the constriction arises from the unstable expansion of a trinucleotide repeat sequence (CGG) in the 5' untranslated region (UTR) of the fragile X mental retardation 1 (*FMR1)* gene. This results in the transcriptional silencing of the *FMR1* gene (Verkerk et al. 1991) and near complete loss of the encoded protein product, fragile x mental retardation protein (FMRP) (Ashley et al. 1993). In unaffected individuals, the CGG

repeat range is between 5-54 repeats, while expansions of 200 or more result in the full mutation. Individuals with 55-199 repeats are considered to have the premutation allele, which tends to expand when transmitted (Oostra and Willemsen 2009). When passed to the offspring, the premutation allele can either undergo a relatively small expansion that is still within the premutation range, or it can undergo a massive expansion to 200 or more repeats, resulting in the full mutation (Willemsen et al. 2011). Premutation carriers show elevated levels of *FMR1* mRNA with a minor reduction in protein levels and generally have only mild, if any, typical symptoms of FXS (Hagerman and Hagerman 2004). Trinucleotide expansions in the intermediate range result in the formation of toxic intra-nuclear inclusions and is associated with the neurodegenerative disorder Fragile X-associated Tremor and Ataxia Syndrome (FXTAS) (Bagni et al. 2012; LaFauci et al. 2013; Ludwig et al. 2014). Additionally, females with the premutation exhibit an increased risk for Fragile X-Associated Primary Ovarian Insufficiency (FXPOI), a condition that is characterized by reduced function of the ovaries (Gallagher and Hallahan 2012).

Although the most prevalent etiology of FXS is characterized by trinucleotide expansions, missense point mutations and deletions in the *FMR1* gene coding region have been found to lead to the development of the disease (De Boulle et al. 1993; Coffee et al. 2008; Myrick et al. 2015). Reduced levels of FMRP expression have also been reported in other mental disorders including autism, schizophrenia, bipolar disorder, and major depression (Fatemi and Folsom 2011).

1.1.3. The Fragile X Mental Retardation Protein (FMRP)

1.1.3.1. Molecular Structure

FMRP is a 70-80 kDa protein that is one of three paralogous proteins (with the FXR1 and FXR2 proteins) in mammals. FMRP has three RNA-binding domains, including two K homology domains (KH1 and KH2) and an arginine-glycine-glycine (RGG) box, and binds a subset of neuronal mRNAs (Darnell 2005). KH domains bind tertiary motifs in mRNAs, which are generally known as "kissing-complexes" (Darnell et al. 2005). Furthermore, RGG boxes recognize stem-G-quartet loops, potentially in a methylation-dependent mechanism (Blackwell et al. 2010). The primary transcript of the *FMR1* gene spans ~38 kb and is composed of 17 exons (Eichler et al. 1993). Similar to many transcripts in the central nervous system (CNS), it undergoes alternative splicing and possesses alternative transcription start sites such that at least 12 isoforms are generated (Tassone et al. 2011; Brackett et al. 2013). Isoform 1 is known to account for about 40% of total FMRP in the human brain (Huang et al. 1996). FMRP isoform 1 is the full-length protein, which contains both a nuclear localization signal (NLS) and a nuclear export signal (NES), and sites for post-translational modification through phosphorylation and methylation (Sittler et al. 1996; Ceman et al. 2003). Nuclear localization of FMRP is isoform dependent (Dury et al. 2013). Lack of the NES signal, in FMRP isoforms 4, 6, 10 and 12, results in the predominant nuclear localization of these FMRP isoforms, indicating its functional significance (Sittler et al. 1996; Dury et al. 2013). In contrast, the most common FMRP isoforms (1 and 7), which are associated with translational machinery (Ascano et al. 2012), are mainly cytoplasmic (Dury et al. 2013). These

observations suggest that the nuclear FMRP isoforms might have independent functions from the dominant cytoplasmic FMRP isoforms.

1.1.3.2. FMRP Function

FMRP is a polyribosome-associated RNA-binding protein that controls the expression of hundreds of genes in the CNS (Darnell and Klann 2013). FMRP binds to more than 800 different identified gene transcripts in mouse brain tissue and human cell lines (Darnell et al. 2011; Ascano et al. 2012), which is equivalent to approximately 4% of total mRNAs that are expressed in the human brain (Darnell et al. 2011). For many of these substrates, FMRP has been shown to act as a translational repressor. However, FMRP has been shown to also act as a positive modulator of protein translation for some of its mRNA substrates (Bechara et al. 2009), possibly by enhancing mRNA stability (Zalfa et al. 2007) or potentiating the actions of the translational activating gene Sod1 (Bechara et al. 2009). FMRP targets distinct mRNA sequence elements to regulate protein expression (Ascano et al. 2012). Interestingly, many of the mRNA targets of FMRP encode several proteins that are implicated in autism spectrum disorders (ASDs) (Darnell et al. 2011).

Although FMRP is commonly acknowledged as a regulator of mRNA translation, the precise mechanism by which FMRP influences the translational machinery remains to be further identified. Considering the fact that FMRP co-sediments with polyribosomes, it was initially believed that FMRP might inhibit translation by blocking elongation (Ceman et al. 2003). In support of this hypothesis, it was shown using ribosomal run-off assays that FMRP binds the vast majority of its 842 mRNA substrates within the coding

sequence, instead of the 5' or 3' untranslated regions, stalling ribosomes and inhibiting translation (Darnell et al. 2011). Putative FMRP target mRNAs have been found to be both up- and downregulated, suggesting that FMRP could both activate and repress translation. FMRP could shift between these roles during development and/or in different parts of the brain, or, perhaps more likely, it could serve as a repressor until activated by phosphorylation and/or other signaling mechanisms (Bagni and Greenough 2005). Another mechanism by which FMRP could affect translation is through selective delivery of mRNAs to dendritic translation sites in response to synaptic activity; however the contribution of FMRP localization remains poorly understood (Dictenberg et al. 2008).

1.1.3.3. FMRP Distribution & Expression

FMRP is ubiquitously expressed throughout the body in humans, mice and rats, with the highest levels in in the brain, testes and ovaries (Devys et al. 1993; Hinds et al. 1993). FMRP is widely expressed throughout embryonic brain development and peak levels of FMRP are reached at the end of the first postnatal week, with expression gradually declining thereafter (Wang et al. 2004). Within the brain, the highest expression of FMRP is found in the hippocampus, cerebellum and cortex (Devys et al. 1993; Hinds et al. 1993; Bakker et al. 2000). In neurons, FMRP resides largely in the cytoplasm, with high concentrations of FMRP found in regions rich with ribosomes (>85%, (Khandjian et al. 1996). In the cytoplasm, FMRP is localized in the cell body, dendrites and axons in synaptic spines where it plays a role in spine maturation (Cruz-Martin et al. 2010). FMRP is also located in a subset of presynaptic compartments. FMRP is highly abundant in "fragile X granules" in neuronal axons and pre-synaptic terminals where it is involved in

regulating recurrent neuronal activity (Akins et al. 2012). A portion of total cellular FMRP is also present in the nucleus (less than 5%), where its role is less well-characterized. The correlation of peak levels of FMRP expression with periods of synaptic formation, coupled with its localization to synaptic structures, suggests potential important roles for FMRP in the formation, maturation, stabilization and elimination of synapses.

In contrast to the expression of FMRP of neurons, relatively little is known about the types of glial cells that express FMRP during CNS development. FMRP was once thought to reside exclusively in neurons (Bakker et al. 2000). However, Wang and colleagues (2004) provided evidence of a possible role for FMRP in oligodendrocytes in development. FMRP is expressed in oligodendrocyte precursor cells in the immature cerebellum, where it appears to play a role in the proper progression of myelination (Pacey et al. 2013). Our laboratory also provided evidence for FMRP in cells of the early glial lineage (Pacey and Doering 2007). In the mouse hippocampus, FMRP is expressed in astrocytes within the first week of birth and then its expression declines to low or undetectable levels (Pacey and Doering 2007; Gholizadeh et al. 2015). These findings highlight the important role for FMRP expression in astrocytes during early postnatal weeks of development, which coincide with synaptogenesis. FMRP is also expressed in neural stem cells (Luo et al. 2010), where it has been shown to control hippocampal-dependent neurogenesis and learning in the mature brain (Guo et al. 2011).

1.1.4. The Fragile X Mouse Model

To better study the underlying neurobiology surrounding the FMRP protein and investigate potential treatments for FXS, an appropriate animal model was necessary (Bakker 2000). In 1994, Bakker and colleagues developed the Fragile X transgenic mouse model and has enhanced the possibilities for neuron-glia research immensely. The *Fmr1* knockout (KO, null) mouse *FMR1* gene has 97% amino acid homology with the human gene (Ashley et al. 1993). Furthermore, FMRP expression shows similar tissue and cell specific patterns in both humans and mice (Hinds et al. 1993). The *Fmr1* KO mouse was created by the transfection of a neomycin cassette into exon 5 of the *Fmr1* gene in embryonic stem cells (Dutch-Belgian Consortium 1994). FMRP is absent in the resulting homozygous KO, and although the mouse model results from a knockout, whereas the human condition results from an expansion, the result is similar in that no FMRP is produced. Parallel to human FXS, *Fmr1* KO mice exhibit deficits consistent with their human counterparts, including learning and memory impairments, autistic-like behaviours, hyperactivity and seizures (Bakker et al., 1994).

1.1.5. Dendritic Spine Characterization

Dendritic spine dysgenesis has been characterized most extensively in FXS (Penzes et al. 2011). Dendritic spines are dynamic structures, particularly during early development with experience stabilizing a mature set of spines as development proceeds (Bourne and Harris 2007). Studies examining spine morphology in postmortem brain tissues from adult FXS patients showed normal neuronal number and size. However, evaluation of Golgi-impregnated neurons revealed an increase in long, thin spines in

multiple cortical areas, which is indicative of delayed dendritic development (Rudelli et al. 1985; Irwin et al. 2001).

Parallel to human studies, neuroanatomical spine abnormalities are mirrored in *Fmr1* knockout (KO) mice. In normal mice, there is a rapid decrease in spine turnover on layer 2/3 neurons in the barrel cortex with immature filopodia replaced by mature mushroom spines during the first two postnatal weeks. In contrast, *Fmr1* KO mice exhibit a developmental delay in the downregulation of spine turnover, as well as in the stabilization of spines and in the transition from immature to mature subtypes (Cruz-Martin et al. 2010; He and Portera-Cailliau 2012).

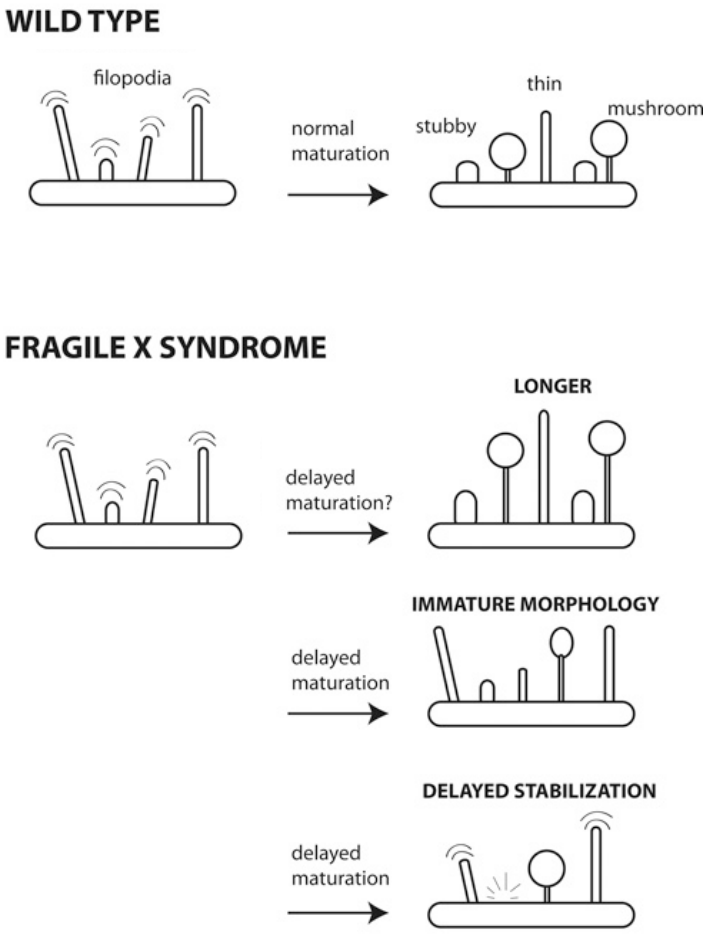

Figure 1.1: Schematic comparing spine development during synaptogenesis in wildtype versus Fragile X mice. During early brain development in wildtype (WT) mice, dendrites are studded with headless protrusions called filopodia. These are highly motile and transient protrusions that play a role in early synaptogenesis. In the adult, dendritic spines can be classified morphologically into three main types: thin, stubby and mushroom. Thin spines tend to be smaller and have shorter lifetimes (days), whereas mushroom spines tend to be the largest and most stable (weeks to months). In FXS, a delayed maturation of dendritic protrusions results in an overabundance of spines with immature morphologies or higher than normal turnover. Adapted from He & Portera-Caillau (2013).

Interestingly, reports on spine phenotypes show a wide range and differ significantly within the literature. The existence and/or magnitude of the spine alterations in the *Fmr1* KO mouse vary according to brain region, developmental age, and genetic background indicating the complex and multi-factorial regulation of spines (Beckel-Mitchener and Greenough 2004) (**Table 1.1**). For example, in the hippocampus, mutant mice have been reported to have either a lower spine density (Braun and Segal 2000), which is the opposite of what is traditionally seen in the neocortex, or a normal spine density (Grossman 2006; Pfeiffer and Huber 2007), regardless of age. Similarly, the length of spines on hippocampal neurons from *Fmr1* KO mice has been reported to be either normal (Braun and Segal 2000) or increased (Irwin et al. 2001; Comery et al. 1997; Grossman et al. 2006) compared to wildtype (WT) mice. Despite the inconsistencies in the reported literature, most studies show an excess of long, thin spines that resemble immature spines (Pfeiffer and Huber 2009), suggesting that FMRP may be involved in facilitating synaptic pruning and the formation and/or maturation of synapses. Since dendritic spines are the primary sites of excitatory synapses and information exchange in the CNS, perturbations in their structure and function can result in synaptic and neural circuit alterations that lead to disrupted brain function and cognitive deficits in FXS.

Table 1.1: Summary of reports examining dendritic spine morphology.

Result (in FXS)	Preparation/ Method	Source	Brain Region	Age	Reference
↑ Long, thin spines	Golgi analysis	Human	Parieto-occiptal; Neocortex	Adult	Rudelli et al. (1985)
↑ Long, thin spines	Golgi analysis	Human	Parieto-occiptal; Neocortex	Adult	Hinton et al. (1991)
↑ Long, thin spines	Golgi analysis	Human	Neocortex	Adult	Wiskniewski et al. (1991)
↑ Spine length	Golgi analysis	Mouse C57Bl/6	Visual cortex	Adult	Irwin et al. (2001)
↑ Filopodia No difference in spine density or length	Di-Olistic labeling for slice preparations	Mouse C57Bl/6	Hippocampus (CA1) Hippocampus (CA3)	Adult	Levenga et al. (2011)
↑ Spine length ↑ Spine density	Golgi analysis	Mouse FVB	Visual cortex	Adult	Comery et al. (1997)
↑ Spine length	Golgi analysis	Mouse FVB	Visual cortex	Adult	Irwin et al. (2002)
↑ Spine length ↑ Spine density No difference in spine density or spine length	GFP transfection of slice preparations	Mouse FVB	Somatosensory cortex	1 week 2 weeks 4 weeks	Nimchinsky et al. (2001)
↑ Spine length ↑ Long, thin spines	Golgi analysis	Mouse FVB	Hippocampus	Adult	Grossman et al. (2006)
↓ Spine density	DiI labeling in primary neurons	Mouse FVB	Hippocampus	7 and 21 *DIV*	Braun & Segal (2000)

1.1.6. The Autistic Phenotype of Fragile X Syndrome

Fragile X syndrome (FXS) is one of the most prevalent and well-studied monogenetic causes of intellectual disability and autism and, although rare, its high penetrance makes it a desirable model for the study of neurodevelopmental disorders more generally. Autism is a complex neurodevelopmental disorder with variable clinical presentation (Gürkan and Hagerman 2012), including functional impairment in social communication, language and sensory motor outcomes. Diagnostic criteria from the DSM-5 define autism spectrum disorder (ASD) with two core symptom dimensions: (1) impairments in social communication and (2) repetitive behaviours (American Psychiatric Association, 2013). This disorder is heterogeneous in presentation and in etiology, likely a result of multigenic interactions and environmental contributions (Won et al. 2013). As a result, the high genetic heterogeneity of ASD poses an enormous challenge for understanding disease etiology. Both ASD and FXS share considerable deficits in social interactions and communication (Hagerman et al. 2010). Approximately 46% of males and 16% of females with FXS meet clinical criteria for autism, while up to 90% of FXS patients display autistic symptoms. 1–2% of people diagnosed with ASD are also diagnosed with FXS (Bailey et al. 2008), making FXS the leading heritable single gene cause of ASD. However, the clinical overlap between the two conditions extends beyond behavioral similarities to include genetic or biological components.

Recent studies suggest that there is functional convergence of a number of genes that are implicated in FSX and ASDs, indicating that an understanding of the cellular and biochemical dysfunction of the disorders are likely to reveal common targets for

therapeutic intervention. For instance, FMRP regulates the translation for hundreds of genes, many of which are associated with autism. High-throughput sequencing of RNAs isolated by crosslinking immunoprecipitation (CLIP) to identify FMRP interactions with mouse brain polyribosomal mRNAs revealed a highly significant overlap of FMRP targets with several well-studied autism candidate genes (Darnell et al. 2011). In fact, a comparison of FMRP's 842 target genes with 117 known autism candidate genes (Basu et al. 2009) revealed an overlap of 28 FMRP targets (Darnell et al. 2011). Many of these genes encode various synaptic proteins including synaptic cell adhesion molecules and postsynaptic scaffolding proteins, such as neuroligin, neurexin and SHANK (Zoghbi and Bear 2012). Understanding the neurobiology of FXS provides an avenue to understanding the developmental processes gone awry in ASDs.

1.1.7. Treatments for Fragile X Syndrome

Currently there is no cure for FXS, and as such, pharmacological treatments of the disorder are used to mediate the symptoms and maximize functioning of the individuals with FXS (Gross et al. 2015). Early diagnosis and intensive intervention offer the best prognosis for individuals with FXS. Behavioural therapy and specialized learning programs are implemented in an attempt to minimize cognitive disabilities, and pharmaceuticals such an anti-convulsants are used to alleviate seizures (Lipton and Sahin 2013). Various pharmacological treatments have been investigated as a potential means to address the underlying neural defect resulting from the absence of FMRP. Recent clinical trials have tested the use of mGluR5 antagonists such as AFQ056 (Mavoglurant) (Levenga et al. 2011) and $GABA_B$ agonists, including STX209 (R-baclofen) (Berry-

Kravis et al. 2012). Although compelling pre-clinical evidence was demonstrated by these interventions in rodent models of the disease, the therapeutic benefits did not translate in human patients. In relation to AFQ056, this drug advanced to phase 3; however, all trials were eventually terminated, mostly due to a lack of efficacy (Schaefer et al. 2015). Other reasons why the clinical trials may have failed include inappropriate inclusion criteria, inadequate outcome measures, inadequate dosing or development of drug tolerance (Mullard 2015). The failure of these clinical trials has prompted the consideration of other therapeutic approaches.

1.2. Neurons

1.2.1. Dendritic Spines

Dendritic spines are small protrusions visible on dendrites of neurons that serve as postsynaptic sites for excitatory input (Rochefort and Konnerth 2012). Spines consist of three distinct basic compartments: (1) a delta-shaped base at the junction with the dendritic shaft, (2) a constricted neck in the middle, and (3) a bulbous head contacting the axon (Bourne and Harris 2008). Dendritic spines consist of small protrusions scattered along the dendrites of many neurons and are approximately 0.5 μm in diameter and 0.5-2.0 μm in length (Hotulainen and Hoogenraad 2010). Spines occur at a density of 1–10 spines per micrometer of dendrite length, and some neurons contain thousands of spines throughout the dendritic arbors (Frotscher et al. 2014).

Spines develop around the time of synaptogenesis and are dynamic structures that continue to undergo remodeling over time. Developmental changes in the shape of

dendritic protrusions reflect the progressive replacement of thin, elongated, and highly motile filopodia, characteristic of immature neurons, with more stable spines that acquire a mature morphology (Dansie and Ethell 2011). Spine shapes are structurally diverse and include thin, filopodia-like protrusions ('thin spines'), short spines without a well-defined spine neck ('stubby spines') and spines with a large bulbous head ('mushroom spines').

Spine morphogenesis is fundamental to the development of neuronal networks and the regulation of synaptic plasticity (Ethell and Pasquale 2005). Activity patterns that induce long-term potentiation (LTP), one of the major cellular mechanisms underlying learning and memory, causes enlargement of spine heads, suggesting that changes in dendritic spine morphology play an important role in memory formation (Yuste 2011). Although *de novo* formation of dendritic spines in adult mice has been described, most spines are thought to arise from dendritic filopodia during early postnatal life (Holtmaat and Svoboda 2009).

Spine dynamics are largely controlled through changes in cytoskeletal proteins (Pontrello and Ethell 2009). In contrast to the microtubule-based cytoskeleton of dendrites, dendritic spines are typically composed of a filamentous network of actin and actin-regulating proteins (Hotulainen and Hoogenraad 2010; Shirao and González-Billault 2013). Spine number and morphology are largely controlled by signaling pathways initiated by regulatory Rho family GTPases, which are able to "switch on" signal transduction pathways when in a GTP-bound (i.e. active) state (De Filippis et al. 2014). Once triggered by GTPase-activating proteins (GAPs) or guanine exchange factors (GEFs), active GTPases including Rac1 and RhoA go on to induce downstream effectors

including various actin polymerizing/depolymerizing factors. This pathway ultimately triggers reorganization of the actin cytoskeleton in dendrites, contributing to the initial contact and stabilization of synapses (Ebrahimi and Okabe 2010).

1.2.2. Synapse Formation

In most regions of the developing brain, the formation of dendritic spines coincides with the main period of synaptogenesis in the first few weeks after birth (García-López et al. 2010). The establishment of the correct number and types of synapses is essential for the formation of neural circuits and for information processing in the brain. Neural circuit formation occurs in three distinct stages. First, immature synapses form between axons and dendrites (Knott & Holmaat 2008). Once a contact is made, the challenge of the new synapse is to become stabilized, a process that is likely to be regulated by neural activity (Matus 2005). Newly formed spines are usually thin and elongated and in general have a small head. They have often been referred to as learning spines in opposition to classical mushroom-shape spines that are representing more stable structures (Bourne and Harris 2007).

Second, synapses undergo maturation, which involves the conversion of silent synapses to active ones (through the recruitment of AMPA-type glutamate receptors) (Hotulainen and Hoogenraad 2010). During this early phase of stabilization, when newly formed spines acquire a postsynaptic density (PSD), their spine head enlarges, a phenomenon that probably shows similarities with the spine head enlargement associated with LTP induction (Sala and Segal 2014). The PSD functions as a postsynaptic organizing structure where it clusters ionotopic (NMDAR and AMPAR) and

metabotropic glutamate receptors (mGluRs), adhesion molecules and channels, and assembles a variety of signaling molecules at the postsynaptic membrane (Gold 2012). Some of the proteins enriched in this excitatory postsynaptic region include, but are not limited to Homer, Shank1-3, CaMKII, SynGAP, and postsynaptic density protein 95 (PSD-95) (Shinohara 2011).

Given that dendritic spines lie opposite presynaptic boutons in excitatory synapses, a tight structure-function relationship exists between spines and neuronal activity. Increases in spine volume closely correlate with the accumulation of additional AMPA receptors, the reorganization of the actin cytoskeleton, and larger PSDs that express more adhesion and cross-linking molecules, indicative of increased spine stability (Sala and Segal 2014). Therefore, immature spines that are thin and long tend to lack a PSD, AMPAR currents and synaptic input.

Lastly, excess synapses are eliminated or pruned to refine the neuronal connections within the circuit (Riccomagno & Kolodkin 2015). However, the cellular and molecular mechanisms that underlie synapse elimination are largely unknown.

1.2.3. Fluorescent Labeling with Lipophilic DiI

Analyzing cell morphology is a key component to understand neuronal function. Classical staining methods have been used to investigate the anatomy of neurons *in vivo,* but are not appropriate for visualization of cultured living neurons. Several methods have been developed to overcome the limitations of Golgi stains for spine analysis, including the use of various commercially available tracer dyes, fluorochrome-labeled antibodies,

and genetically encoded fluorescent proteins such as green fluorescent protein (GFP) or yellow fluorescent protein (YFP) (Malinow et al. 2010; Staffend and Meisel 2011). Due to the excellent specificity of GFP, it is one of the most well-accepted neuronal labeling techniques. Among these methods, viral-transfected fluorescent protein engineering, immunolabeling techniques, and transgenic animal engineering have been helpful in elucidating the detailed structure and dynamics of dendritic spines of different brain diseases (Sala and Segal 2014). However, a similar level of neuronal labeling can be achieved using fluorescent lipophilic tracer dyes, such as DiI (1,1′-dioctadecyl-3,3,3′,3′-tetramethylindocarbocyanine perchlorate) and its derivatives, with lower cost and a shorter time frame (Maiti et al. 2015). DiI is a cationic carbocyanine membrane dye that exhibits enhanced fluorescence upon insertion of its lipophilic hydrocarbon chains into the lipid membrane of cells (Staffend and Meisel 2011). Once bound to the membrane, the dye diffuses laterally to stain the entire cell (Honig and Hume 1989). DiI, which is well retained in the cell membrane, is considered one of the most effective methods for labeling and detecting spines in cultured neurons.

1.3. Astrocytes

1.3.1. Astrocyte Morphology

Astrocytes, or astroglia, are named with the Greek root word 'astro', which means star (Zhang and Barres 2010). In the late nineteenth century and the early twentieth century, Camillo Golgi and Santiago Ramón y Cajal noticed that although different astrocytes share a stellate feature, their morphology is extremely diverse, perhaps as diverse as neurons (García-Marín et al. 2007). Since Cajal's time, modern scientists have confirmed the morphological diversity of astrocytes *in vitro* and *in vivo* (Kettenmann and Verkhratsky 2008). Astrocytes are the predominant glial cell type in central nervous system (CNS), constituting approximately one-third of mouse brain cells and nearly half of human brain cells (Cahoy et al. 2008). Astrocytes are divided into two main classes and can be distinguished on the basis of their morphology, primary location and function (Bushong et al. 2004; Bayraktar et al. 2015). Protoplasmic astrocytes are classically found in the grey matter of the brain. Their processes, which are long, thick and highly ramified, are closely associated with synapses as well as blood vessels (Kettenmann and Verkhratsky 2008). Their processes intensively ensheath synapses and contact blood vessels (Parri and Crunelli 2003). Fibrous astrocytes are found mainly in the white matter of the brain, where their processes contact blood vessels and nodes of Ranvier on neuronal axons. In contrast to protoplasmic astrocytes, fibrous astrocyte processes are long, cylindrical, smooth and branch infrequently (Halassa et al. 2007).

1.3.2 Antigenic Astrocyte Markers

Defining diverse astrocyte morphology and functionality has been limited by the lack of immunological markers to identify and distinguish astrocyte subtypes. Until recently, our understanding has been predominantly based on classical immunostaining with the widely used astrocyte marker GFAP (glial fibrillary acidic protein, an intermediate filament protein), which grossly underestimates the complexity of astrocytes and their interactions with neurons and other cells (Eliasson et al. 1999; Verkhratsky et al. 2014). GFAP, which selectively reveals the structure of primary branches, represents ~15% of the total volume of the astrocyte (Bushong et al. 2004). Furthermore, GFAP is expressed predominantly in mature astrocytes, restricting its use for the identification of immature astrocytes in postnatal development (McCall et al. 1996).

Recent studies on astroglial gene expression profiles have characterized the molecular identity of astrocytes *in vivo* and identified ALDH1L1 (aldehyde dehydrogenase 1 family, member L1) as a highly specific antigenic marker for astrocytes (Cahoy et al. 2008). ALDH1L1 is expressed by both immature and mature astrocytes (Yang et al. 2010) and has a substantially broader pattern of astrocyte expression than the conventional astrocyte marker GFAP (Cahoy et al. 2008; Fiacco et al. 2008). ALDH1L1, also known as 10-formyltetrahydrofolate dehydrogenase (FDH), is a folate enzyme that converts 10-formyltetrahydrofolate (10-formyl-THF) to tetrahydrofolate, playing an important role in many reactions like *de novo* nucleotide biosynthesis and the regeneration of methionine, thus having a major impact on cell division and growth (Yang et al. 2010). Other non-stage-specific markers of astrocytes include the astrocyte-

specific glutamate transporters Glt-1 (glial glutamate transporter 1) and GLAST (glutamate-aspartate transporter) (Molofsky et al. 2012).

1.3.3. Astrocyte Functions

Astrocytes play many diverse roles within the CNS. The functions of astrocytes can be divided into three groups: those that provide housekeeping functions necessary to maintain neuronal function, those that actively shape synaptic function, and those that act as neural precursors in adult neurogenic regions (Jacobs et al. 2012). Astrocytes are actively involved in providing structural and metabolic support to neurons (Kreft et al. 2012). In particular, astrocytes are responsible for buffering excess K+ ions (Walz 2000) and glutamate (Okabe et al. 2012) released at the synapse. Astrocytes induce the formation of the blood-brain barrier (BBB), maintain BBB integrity, and regulate angiogenesis (Abbott et al. 2006). Additionally, they regulate functions in synaptic transmission, synapse strength and information processing by neural circuits (Perea and Araque 2010). Astrocytes are organized into discreet domains, with a single astrocyte contacting between 300-600 dendrites and as many as 100,000 synapses (Halassa et al. 2007). This extensive synaptic interaction not only ensures that astrocytes are able to fulfill their metabolic support roles, but also positions astrocytes to directly influence the structure and function of the synapse. Astrocytes are often found in close opposition to the pre- and postsynaptic machinery of neurons at excitatory glutamatergic connections, an arrangement that has come to be known as the “tripartite synapse” (Araque et al. 2001). Astrocytes, which are bidirectional, communicate and exchange information with both pre- and postsynaptic elements. Communication is primarily controlled by the

change in Ca^{2+} concentrations, causing excitability within the astrocyte (Volterra and Meldolesi 2005). Networks of astrocytes act in concert to influence transmission among neighbouring synapses (Haydon 2006). Through this close contact with neurons, astrocytes modulate the efficacy of synapses through release and uptake of neuroactive substances (Eroglu et al. 2008). Of these gliotransmitters, the best characterized are glutamate, ATP, and D-serine (Newman 2003).

Astrocytes are also crucial for the survival and health of neurons, both in culture and *in vivo* (Banker 1980). For instance, the deletion of Mek1 and Mek2 in radial glia in the mouse cortex eliminates astrocyte and oligodendrocyte precursors, thus obliterating gliogenesis (Li et al. 2012). Consequently, the majority of the mice born are unable to survive past the first two postnatal weeks, as a result of extensive neurodegeneration due to the absence of glia, thereby reinforcing the crucial importance of astrocytes during early development.

1.3.4. Astrocyte Involvement in Synaptogenesis

Astrocytes are integral for the proper formation, growth and maintenance of neurons and synaptic connections. In the developing CNS, synapse formation is spatiotemporally controlled, suggesting the presence of regulatory mechanisms (Freeman 2010). Although most neurons are produced during embryonic stages, the major waves of synaptogenesis follow and depend on the production of astrocytes. Newly generated immature astrocytes are typically formed between postnatal day P1-P8 *in vivo*, whereas astrocyte proliferation and maturation are largely complete by P17-P21 (Bushong et al. 2004). Correspondingly, the majority of excitatory synapses in the brain form during the

second and third postnatal weeks, even though neuronal maturation and axon path-finding events are mostly completed by birth (Eroglu et al. 2008; Eroglu and Barres 2010). This delay between target innervation by neurons and the establishment of synapses correlates with the appearance and maturation of astrocytes in the brain, which suggests that astrocytes may provide instructive cues that contribute to the initiation of excitatory synapse formation. Given their proximity to synapses, astrocytes can directly promote and regulate these processes through both secreted and contact-mediated signals (Clarke and Barres 2013a).

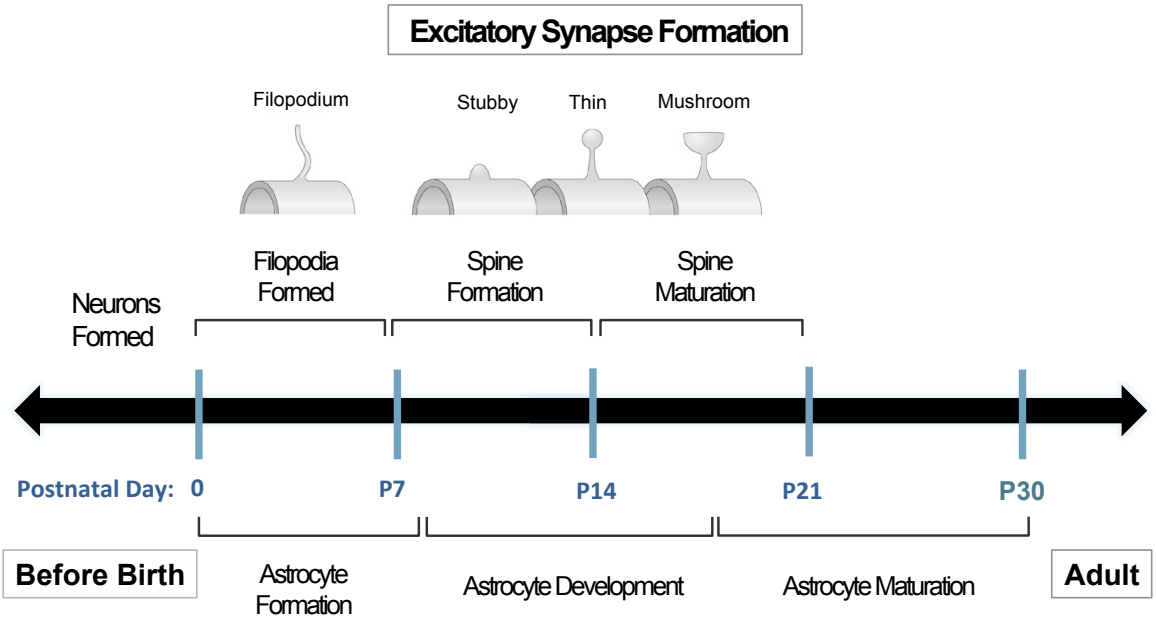

Figure 1.2: Timeline of astrocyte and neuron development *in vivo* (rodent). In the developing CNS, synapse formation is spatiotemporally controlled, suggesting the presence of regulatory mechanisms. The majority of neurons are formed before birth. Excitatory synapses subsequently form during the second and third postnatal weeks. During spine development, filopodia typically emerge within the first week. Spine formation and maturation occur between postnatal day P7 and P21 (Yuste 2004). In contrast, newly generated immature astrocytes are formed between P1 and P8 (Bushong et al. 2004). These astrocytes acquire their mature morphology at later stages when development is nearly complete by approximately P17 and P30 (Cahoy et al. 2008). This (1-week) delay period between P0 and P7, which correlates with synaptogenesis and astrocyte appearance, strongly suggests the possibility that extracellular signals from astrocytes could provide a signal necessary to trigger synapse formation.

1.3.4.1. Cell-Mediated Contact

The formation of synaptic contacts is paramount for the proper development and function of the CNS. Astrocyte processes, which are highly mobile, contribute to the stabilization of new synapses during synaptogenesis. Hama et al. (2004) provided data to show that astrocytes affect neuronal synaptogenesis by the process of adhesion. They showed that local contact of neurons with astrocytes via integrin receptors elicited molecular events that facilitated the formation of excitatory synaptogenesis. Astrocytes also induce local structural and functional modifications of dendritic segments or individual synapses through a contact-mediated mechanism involving bi-directional ephrin (ligand)/EphA (receptor) signaling (Murai et al. 2002). Membrane-bound ligands on astrocytes, such as ephrin-A3, have been shown to upregulate spine morphology in the hippocampus, via local activation of EphA receptors on spines by astrocytic ephrin-A3 (Carmona et al. 2009). EphB family ligand/receptors expressed on astrocytes also play a role in regulating the formation of dendritic spines in the hippocampus (Henkemyer et al. 2003) through the recruitment of NMDA receptors to the post-synaptic specialization (Huroy et al. 2016). Live imaging of organotypical hippocampal slice preparations demonstrated that astrocytes rapidly extend and retract fine processes to engage and disengage from postsynaptic dendritic spines (Haber 2006). Studies with two-photon microscopy that track the dynamics of astrocyte processes and the fate of dendritic protrusions also revealed contributions of astrocyte contact (Nishida and Okabe 2007). Dendritic protrusions with astrocyte contacts had a longer lifetime and were morphologically more mature. Thus, dendritic protrusive activity and transient contacts

with astrocytes act to stabilize newborn synapses and promote subsequent spine maturation.

The development of inhibitory synapses can also be modulated by astrocyte contact. A study by Liu et al. (2004) showed that local contact between neurons and astrocytes significantly increased the amplitude and density of $GABA_A$ currents in developing hippocampal neurons. This contact-dependent increase in GABAergic synaptic activity relied on Ca^{2+} signaling in astrocytes. In addition, astrocytes and astrocyte-conditioned media (ACM) were shown to regulate the Cl^- gradient in cultured spinal cord neurons and convert GABAergic synapses from excitatory to inhibitory (Li et al. 1998). This finding is particularly exciting given the importance of local GABAergic inhibitory circuits in both activity-dependent wiring of developing neural circuits and the consolidation of critical period plasticity.

Overall, these studies reveal that contact-mediated signaling between astrocytes and neurons is important for the structure and maintenance of synaptic connections. This suggests a model in which physical and molecular interactions between neurons and astrocytes provide instructive cues that control synapse formation, morphology and plasticity. Although membrane-bound factors have been identified as participants in synaptogenesis, the contributions of diffusible astrocyte factors in regulating neural development have not been extensively explored.

1.3.4.2. Secreted Factors

While astrocyte-contact induces the formation and function of synapses, other evidence proposes further regulatory roles for astrocytes through non-contact-mediated

mechanisms. During early studies of the development of synapse formation in primary neuronal cultures, it was apparent that 'feeder layers' of glial cells, in particular astrocytes, were critical to drive synapse assembly between various populations of neurons (Banker 1980; Pfrieger and Barres 1997). Astrocytes are now known to release many trophic factors, many which promote synaptogenesis and enhance synaptic function (Barres, 2008). In fact, 187 putative astrocyte-secreted proteins have been identified in astrocyte-conditioned media (ACM) derived from murine cultures using a combination of shotgun proteomics and bioinformatics (Dowell et al. 2009).

The first evidence that astrocytes instruct synapse formation came from a study that used purified rodent retinal ganglion cells (RGCs). Retinal neurons that were cultured in the complete absence of astrocytes formed very few synapses and had low synaptic activity (Pfrieger and Barres 1997). Conversely, RGCs that were cultured with astrocyte feeder layers or ACM exhibited a 3-7 fold increase in the number of excitatory synapses and 10x higher synaptic activity (Christopherson et al. 2005). These results demonstrated that synaptogenesis is not only controlled by intrinsic mechanisms of neurons, but are stimulated by astrocyte-secreted prosynaptogenic signals. Further investigation identified one of these signals as none other than thrombospondin-1 (TSP-1) (Christopherson et al. 2005), the extracellular matrix molecule (ECM) whose synthesis and secretion by astrocytes had been discovered nearly two decades earlier (Asch et al. 1986) (See Section 1.4 Thrombospondins). Consistent with these findings, immunodepletion of TSP-1 from ACM inhibited the synapse-inducing effect of astrocytes (Christopherson et al 2005).

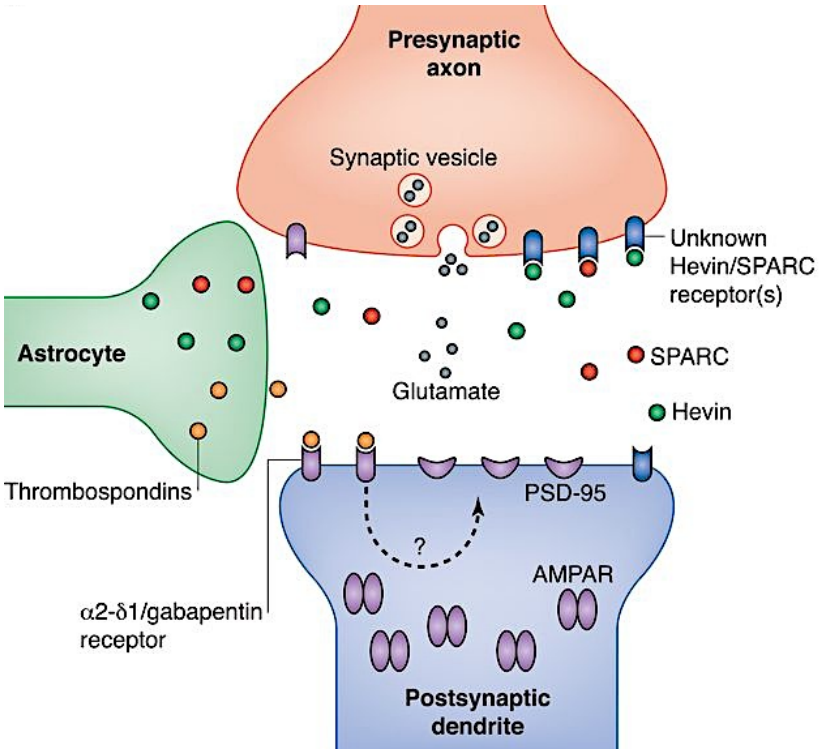

Figure 1.3: Model of astrocyte-neuron interactions during synapse formation and maturation. Astrocytes secrete several factors to promote structural synapse formation. Astrocytes secrete thrombospondins (TSPs), which act through α2–δ1 calcium channel subunit/gabapentin receptor to drive the formation of structurally intact glutamatergic synapses (Eroglu et al. 2009). The synapses formed in response to TSPs are typically structurally intact with docked vesicles and PSD-95 correctly localized; however, they lack surface expression of AMPARs at the post-synapse and are therefore not fully functional (Christopherson et al. 2005). The mechanism by which TSPs induce synapse formation remains elusive. Many factors since have also been implicated in the involvement of synaptogenesis, including Hevin and SPARC (Kucukdereli et al. 2011). Adapted from Corty & McFreeman (2013).

It has also been shown that astrocytes also help to control synapse elimination in the developing CNS by inducing neurons to express and secrete C1q, a subunit of the first component of the classical complement pathway. C1q becomes synaptically localized and leads to the activation of the classical complement cascade (Stevens et al. 2007). In adult CNS, neuronal C1q is normally downregulated. Upon injury or disease, reactive astrocytes induce C1q expression in neurons to tag unwanted synapses for elimination (Stevens et al. 2007). Together, these studies indicate that soluble and contact-mediated signals between astrocytes and neurons are important for the formation, maturation and maintenance of synaptic connections for the optimal development of neural circuits.

1.4. Thrombospondins (TSPs)

1.4.1. TSP Structure and Function

Thrombospondins (*THBS*) have been identified as key regulators of synaptogenesis in the CNS. The thrombospondin (TSP) family of matricellular, multidomain glycoproteins is widely expressed in the developing and adult CNS, although their function remains poorly defined. Matricellular proteins are a family of structurally unrelated proteins that are secreted into the extracellular space. They act as nonstructural regulators of the ECM and cell-matrix interactions through the modulation of growth factor signaling, cytokines, hormones and proteases (Jones et al. 2014). TSPs were initially described in platelet alpha granules as a large (~450 kDa), trimeric glycoprotein that functioned in platelet aggregation and clot formation (Lawler et al. 1978). Further investigation established that TSPs are secreted by a number of cells,

including astrocytes in the human brain (Asch et al. 1986). Some of these cells include endothelial cells (Mosher et al. 1982), macrophages (Jaffe et al. 1983), fibroblasts and smooth muscle cells (Raugi et al. 1982), indicating a broader spectrum of functions than that initially recognized in coagulation. Mammalian TSPs have many complex tissue-specific roles, including activities in wound healing and angiogenesis, vessel wall biology, connective tissue organization, cancer, and synaptogenesis (reviewed by Adams and Lawler 2004).

The TSP family consists of 2 subgroups organized by oligomerization state and domain structure: subgroups A and B. Subgroup A includes the trimeric TSP-1 and TSP-2, while the pentameric TSP-3, TSP-4 and TSP-5 comprise subgroup B (Adams and Lawler 2004). All of the TSPs have epidermal growth factor-(EGF-) like repeats followed by calcium-binding type 3 repeats, and all share a highly conserved C-terminal region. Unlike many ECM proteins that play structural roles, TSPs are primarily involved in regulating cell–cell and cell–matrix interactions (Bornstein 2001). TSPs act through a number of ECM proteins and cell surface receptors to control cytoskeletal dynamics, cell migration and cell attachment (O'Shea et al. 1990; Tucker 2004; Resovi et al. 2014). In the CNS, TSP-1 is cleaved by a disintegrin and metalloproteinase with thrombospondin motifs (ADAMTS) and released from the ECM (Gotschall & Howell 2015).

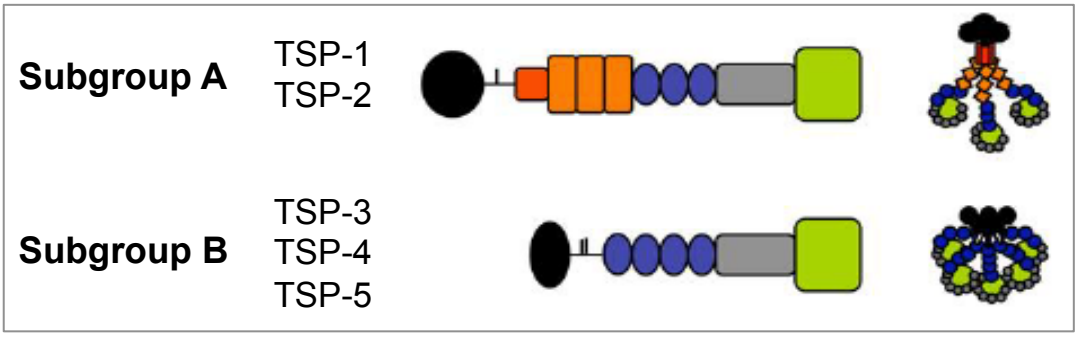

Figure 1.4: Structural organization of thrombospondins. The TSP family consists of 2 subgroups organized by oligomerization state and domain structure: subgroups A and B. Subgroup A includes the trimeric TSP-1 and TSP-2, while the pentameric TSP-3, TSP-4 and TSP-5 comprise subgroup B. The domain structures of thrombospondins (TSPs) include: N-terminal (black), procollagen (red) and properdin-like repeats (orange), epidermal growth factor-like repeats (blue), calcium-binding repeats (grey) and C-terminal L-lectin like globular domains (green). Adapted from Wang et al. (2012).

1.4.2. Thrombospondins Promote Excitatory Synapse Formation in the CNS

TSPs have been identified as important contributors to synapse formation within the CNS. TSP-1 is secreted by cultured astrocytes and abundantly expressed by astrocytes *in vivo* (Clarke & Barres 2013). The first postnatal weeks of the mammalian brain are characterized by extensive plasticity with rapid synapse formation and elimination. Accordingly, TSP-1 is synthesized and secreted by immature astrocytes (postnatal day P5-10) during the peak period of synaptogenesis and its expression declines as the brain matures (Christopherson et al. 2005). Although the expression of TSP-1 is downregulated after the peak of synaptogenesis, the closely related protein TSP-4 is expressed in the adult brain (Bornstein et al. 2005). Both TSP-1 and TSP-4 are involved in supporting neurite outgrowth and survival (O'Shea et al. 1990). These expression patterns suggest that immature astrocytes provide a permissive environment during a critical developmental window in which synapses can form.

Investigation of synaptic development *in vivo* in TSP-1 mice confirmed the *in vitro* findings showing a role for TSPs in excitatory synaptogenesis. TSP-1-null mice demonstrated 30% fewer excitatory synapses in the cortex compared to their wildtype littermates by P8 (Christopherson et al. 2005). Single gene knockout mice of TSP-1 were viable, as were double null TSP-1 mice (Agah et al. 2002). However, these mice recovered poorly following experimentally-induced stroke, with reduced synaptic recovery and axonal sprouting, indicative of lifelong roles for TSPs in synaptic plasticity (Liauw et al. 2008).

1.4.3. TSP-1 Mechanism

The expression of TSP-1 correlates closely with the time interval when the rodent brain normally forms synapses during the first 3 postnatal weeks. Mechanistically, TSP-1 may act as a transynaptic organizer, acting as a permissive switch that times CNS synaptogenesis and enables neuronal molecules to assemble into synapses within a specific window of development (Johnson-Venkatesh and Umemori 2010). Both *in vitro* and *in vivo* data demonstrate the capacity of TSPs to increase synapse number, promote the localization of synaptic molecules, and refine the pre- and postsynaptic alignment. All TSPs secreted by mammalian astrocytes promote the assembly of excitatory glutamatergic synapses within the CNS. TSP-induced synapses in culture are ultrastructurally normal and presynaptically active, but lack postsynaptic activity (Christopherson et al. 2005; Eroglu et al. 2009). TSPs are not involved in promoting inhibitory GABAergic synaptogenesis (Hughes et al. 2010).

Recently, the gabapentin receptor α2δ-1 was identified as the TSP receptor responsible for mediating excitatory CNS synaptogenesis. This receptor is commonly known for its interaction with the anti-epileptic and analgesic drug gabapentin (Eroglu et al. 2009). Glutamatergic synapatogenic activity is mediated by interaction of the epidermal growth factor (EGF)-like domains of TSPs with the Von Willebrand Factor A (vWF_A) domain of α2δ-1, a ubiquitously expressed, nonessential subunit of L-type calcium channels (Eroglu et al. 2009). Excitatory neurons, including RGCs, express high levels of α2δ-1, which are localized to synapses. The overexpression of α2δ-1 both *in vitro* and *in vivo* leads to increases in synaptogenesis, while the knockdown of α2δ-1

results in the loss of TSP-1-induced synapse formation *in vitro*. The extracellular component of α2δ-1 is responsible for its synaptogenic effects. However, the synaptogenic properties do not involve global changes in calcium channel expression levels or function, despite the known roles of α2δ-1 in calcium channel function and trafficking (Eroglu et al. 2009). Synaptogenesis as a result of this interaction is independent of the cytoplasmic domain of α2δ-1; thus, it is likely that additional downstream processes are required for the necessary cytoskeletal and membrane reorganizations, the nature of which remain to be established.

In hippocampal neurons, a TSP-1/neuroligin-1 interaction was implicated in promoting synaptogenesis (Xu et al. 2009). Neuroligin-1 is a cell adhesion protein located on the postsynaptic membrane that mediates the formation and maintenance of synapses between neurons (Purves et al. 2012). Researchers found that TSP-1 accelerated synaptogenesis in young hippocampal neurons through neuroligin-1, but not the final density in mature neurons. Collectively, the data suggests that the synaptogenic activity of TSPs is mediated via a multi-protein complex on neuronal cell surfaces.

1.5. Astrocytes in Fragile X Neurobiology

Current models regarding the neurobiological changes that underlie FXS have largely focused around the synapse. Several studies have now linked astrocyte dysfunction to the altered neurobiology in FXS. Our laboratory was first to discover that FMRP is not expressed exclusively in neurons, but also in cells of the glial lineage (Pacey et al. 2007). Using a co-culture approach in which primary hippocampal neurons were

grown in direct contact with astrocytes, our laboratory demonstrated that the loss of FMRP in astrocytes induces profound developmental delays in dendrite maturation and altered synaptic protein expression (Jacobs et al. 2010). More specifically, WT neurons grown in the direct presence of FMRP-deficient astrocytes displayed increased dendritic branching and decreased pre-and postsynaptic proteins aggregates at 7, 14 and 21 days *in vitro* (*DIV*) (Jacobs and Doering 2010). Interestingly, normal astrocytes could rescue the alterations in dendritic branching and synapse development in the FXS neurons. More recently, we identified that hippocampal neurons with spiny stellate neuronal morphology exhibit pervasive developmental delays, with significant dendritic arbor alterations persisting at 21 days in culture (Jacobs et al. 2016). These results further dictate the critical role astrocytes play in governing neuronal morphology including altered dendrite development in FXS.

Consistent with our findings, Yang et al. (2012) identified that elevated levels of neurotrophin-3 secreted from *Fmr1 KO* astrocytes partially contribute to the abnormal neuronal dendritic development in the *Fmr1* KO mouse model. Recent work by Higashimori et al. (2013) also demonstrated a unique activation role of FMRP in regulating protein expression in astrocytes. In particular, astroglial glutamate transporter subtype GLT1 and glutamate uptake was significantly reduced in the cortex of *Fmr1* KO mice, which may contribute to enhanced cortical neuronal excitability. Together, these findings suggest that astrocytes contribute significantly to the abnormal neurobiology seen in FXS.

Chapter 2

2.1. Central Hypothesis, Objective and Specific Aims of the Thesis

2.1.1. Central Hypothesis

The central idea around which the experiments in this dissertation were designed can be summarized as:

An altered expression of astrocyte-secreted thrombospondin-1 (TSP-1) contributes to the abnormal neurobiology observed in Fragile X.

2.1.2. Objective

Examine the role of TSP-1 during early developmental periods in the brain that center on the proper formation and maturation of synapses in FXS.

2.1.3. Specific Aims

The hypothesis is addressed by the following Specific Aims:

1. To optimize the use of fluorescent lipophilic DiI labeling on cultured neurons to identify dendritic spines for morphological analysis.
2. To establish the role of non-contact astrocyte-mediated signaling effects on neuronal development in FXS.
3. To evaluate the protein expression levels of cellular and secreted TSP-1 in FXS astrocytes.
4. To assess the role of diffusible factors, specifically TSP-1 in the regulation of spine development and excitatory synapse formation in FXS.

5. To determine the differential expression patterns of TSP-1 between wildtype (WT) and FXS primary astrocytes.
6. To examine the developmental trajectory of TSP-1 in the hippocampus and cortex across various timepoints of early postnatal development.

CHAPTER 3:

FLUORESCENT LABELING OF DENDRITIC SPINES IN CELL CULTURES WITH THE CARBOCYANINE DYE "DiI"

Chapter 3

3.1. Preface to Chapter 3

This chapter consists of an author-generated version of a methods paper entitled, "Fluorescent labeling of dendritic spines in cell cultures with the carbocyanine dye 'DiI'". This paper was published in Frontiers in Neuroanatomy and used with permission from Frontiers.

Copyright Statement

"Copyright © 2014 Cheng, Trzcinski and Doering. This is an open-access article distributed under the terms of the Creative Commons Attribution License (CC BY). The use, distribution or reproduction in other forums is permitted, provided the original author(s) or licensor are credited and that the original publication in this journal is cited, in accordance with accepted academic practice. No use, distribution or reproduction is permitted which does not comply with these terms."

Front Neuroanat. 2014 May 9;8:30. doi: 10.3389/fnana.2014.00030

3.1.1. Declaration of Author Contributions

The author would like to acknowledge Olivia Trzcinski for her experimental contributions in assisting with the immunocytochemistry, imaging and in compiling the current literature on the applications of DiI labeling. The author designed and performed the experiments, wrote the manuscript and prepared the figures. Dr. Laurie C. Doering provided guidance in the designing of the experiments and the editing of the manuscript.

3.1.2. Rationale

The present protocol sought to define the optimal conditions for the fluorescent illumination of individual neurons, including the soma, dendritic arborizations, and spines in cell culture through the use of confocal microscopy. To date, very few procedures are available that permit the direct application of DiI to cultured cells. DiI labeling serves as a cost-effective and convenient means of assessing dendritic spines and results in high quality staining of dissociated neurons. This labeling technique was also utilized for the morphological spine analysis in ‘Chapter 4’ of the dissertation.

3.2 Fluorescent labeling of dendritic spines in cell cultures with the carbocyanine dye 'DiI'

Connie Cheng[1], Olivia Trzcinski[1], Laurie C. Doering[1*]

[1]*Department of Pathology & Molecular Medicine, McMaster University, Hamilton, Ontario, Canada*

***Correspondence:**
Dr. Laurie C. Doering
McMaster University
Department of Pathology and Molecular Medicine
1280 Main Street West, Hamilton, ON, L8S 4K1, Canada
E-mail: doering@mcmaster.ca
Tel: +1(905)525-9140 ext. 22913

Journal: Frontiers in Neuroanatomy

Research Topic: Dendritic spines: from shape to function

Keywords: DiI, carbocyanine dye, dendritic spine, morphology, confocal microscopy, paraformaldehyde, neuronal function

3.2.1. Abstract

Analyzing cell morphology is a key component to understand neuronal function. Several staining techniques have been developed to facilitate the morphological analysis of neurons, including the use of fluorescent markers, such as DiI (1,1'-dioctadecyl-3,3,3',3'-tetramethylindocarbocyanine perchlorate). DiI is a carbocyanine membrane dye that exhibits enhanced fluorescence upon insertion of its lipophilic hydrocarbon chains into the lipid membrane of cells. The high photostability and prominent fluorescence of the dye serves as an effective means of illuminating the cellular architecture in individual neurons, including detailed dendritic arborizations and spines in cell culture and tissue sections. Here, we specifically optimized a simple and reliable method to fluorescently label and visualize dissociated hippocampal neurons using DiI and high-resolution confocal microscopic imaging. With high efficacy, this method accurately labels neuronal and synaptic morphology to permit quantitative analysis of dendritic spines. Accurate imaging techniques of these fine neuronal specializations are vital to the study of their morphology and can help delineate structure-function relationships in the central nervous system.

3.2.2. Introduction

Dendritic spines are small protrusions from the dendritic shaft of various types of neurons that act as the postsynaptic compartments of most excitatory synapses in the central nervous system (CNS). They are known to play a significant role in neuronal plasticity and synaptic integration through their ability to undergo structural rearrangements during development (Rochefort and Konnerth, 2012). Morphological features of spines, such as size, shape and density, have been shown to reflect important synaptic functional attributes and the potential for plasticity. Spine morphology is highly variable and has been classified into several different types based on their structure: filopodia, long-thin, stubby, and mushroom-shaped (Yuste, 2011) **(Figure 3.1)**. On the same dendrite, a continuum of shapes can be observed and the morphology can change rapidly through activity-dependent and -independent mechanisms (Penzes and Rafalovich, 2012). The density of spines can be understood in terms of the levels of connectivity within the neuronal network, as well as the integrative capabilities of the neuron. As such, abnormalities in the shape and density of spines can often signify an aspect of disease (Fiala et al., 2002). Therefore, structural classifications of spines with accurate labeling and imaging techniques can spawn vital information on neuronal function, and in turn offer insight into the etiology of neurological diseases (Penzes et al., 2011; Lin and Koleske, 2010).

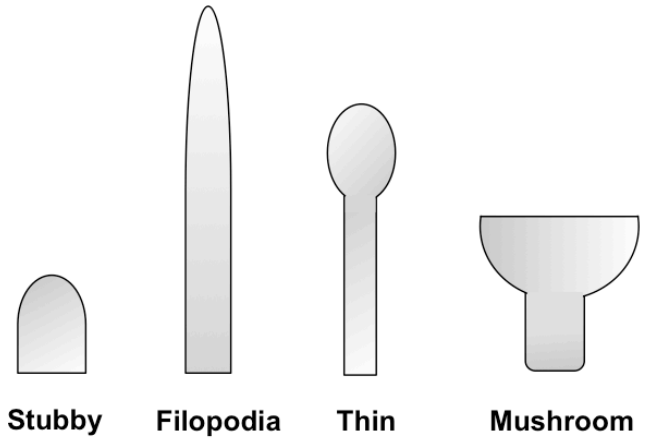

Figure 4.1: Schematic representation of spine morphologies. Spines display a wide diversity of morphologies. They are commonly classified into four different categories (as illustrated from left to right): stubby, filopodia, thin, and mushroom-shaped. Stubby spines are devoid of a neck and are particularly prominent during postnatal development. Thin spines are most common and have a thin, long neck and a small bulbous head, whereas mushroom spines are those with a large head. Lastly, dendritic filopodia are typically longer, normally have no clear head, and often represent immature spines.

For over a century, the Golgi staining technique has been the classical method for neuronal labeling and dendritic spine analysis (Neely et al., 2009). Although Golgi staining has played a crucial role in the advancement of anatomical neurobiology, a major drawback of this technique is that the tissue fixation used for Golgi is often incompatible with other methods to study morphology, such as immunocytochemistry. Furthermore, the Golgi method provides inconsistent, low frequency staining, which results in the insecurity of a selection bias (Staffend and Meisel, 2011b). In addition, long periods of time (often weeks) are required to reach the final product. Due to the lack of specificity and reproducibility, researchers have decreasingly relied on this technique (Ranjan and Mallick, 2010). A variety of methods have been developed to circumvent some of the limitations of the Golgi staining, most notably through the use of fluorescent markers. In fact, labeling cells and tissues with fluorescent markers is one of the most widely used methods of cellular examination employed to date (Colello et al. 2012). Fluorescence immunolabeling is a highly specific method that is commonly used to visualize cell structure, facilitate protein localization, and study cell interactions at the light microscopic level. Some of these other methods used to evaluate cellular morphology include various commercially available dyes, fluorochrome labeled antibodies, and genetically encoded fluorescent proteins, such as green fluorescent protein (GFP) (Staffend and Meisel, 2011a). Specifically with GFP, transgenic animals and cultured cells can be designed to drive fluorescent expression under specific promoters (Malinow et al., 2010). However, although GFP-labeling provides great specificity of fluorescent expression, a similar end result can be accomplished in a much shorter time frame and

with far fewer supplies/materials by employing lipophilic DiI labeling.

The fluorescent lipophilic dye dialkylcarbocyanine, also called 'DiI' (1,1'-dioctadecyl-3,3,3',3'-tetramethylindocarbocyanine perchlorate; $DiIC_{18}(3)$), has traditionally been used for anterograde and retrograde neuronal tracing (Honig and Hume, 1989). Structurally, the molecule consists of a hydrophilic head that lies above the plasma cell membrane and two lipophilic hydrocarbon side chains that insert into the hydrophobic plasma membrane (Bruce et al., 1997) (**Figure 3.2**). The orange-red fluorescent dye is weakly fluorescent until it is incorporated into the membrane. DiI partitions and diffuses through the cell membrane to sufficiently highlight dendrites and their spinous protrusions, providing a well-defined outline of neuronal processes (Sherazee and Alvarez, 2013). The fluorescence provided by the carbocyanine dye is very strong, robust and withstands illumination, e.g. in a confocal laser scanning microscope (Lanciego and Wouterlood, 2011; Gan et al., 1999). Typical applications of this technique include the study of neuronal morphology during development and altered development in neurological disorders (Li et al., 2010; Bruce et al., 1997; Braun and Segal, 2000; Smith et al., 2009). This dye can be applied to a variety of cell types, live or fixed tissue (Terasaki et al., 1994), as well as diverse species such as rodents, primates, and zebrafish (Gan et al., 2000; O'Brien and Lummis, 2006; Arsenault and O'Brien, 2013; Seabold et al., 2010). In slice preparations, DiI labeling is commonly known as 'DiOlistic labeling', in which beads coated with the lipohilic dye are 'ballistically' ejected with a gene gun on to brain tissue (Lo et al., 1994). This technique has been developed as a useful and simple means to label neurons and glia in their entirety, unveiling even the most detailed

structures, such as dendritic spines (Haber, 2006). To date, very few procedures are available that allow the direct application of DiI to cultured cells. Our protocol described here results in high quality staining and imaging of dissociated cell cultures with lipophilic DiI labeling and confocal microscopy. This visualization approach enables a detailed analysis of dendritic spine morphology, density, topographical distribution, and connectivity.

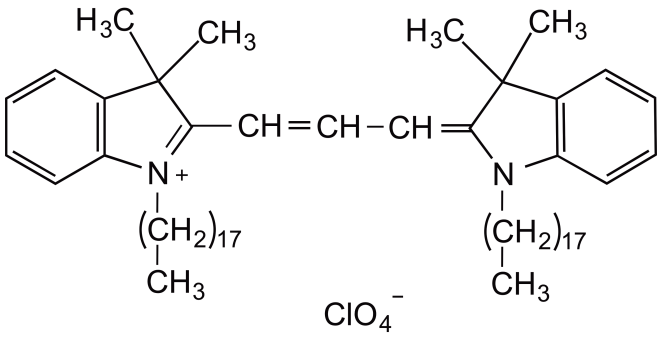

Figure 3.2: Chemical structure of carbocyanine dye DiI ($C_{59}H_{97}ClN_2O_4$). The fluorescent lipophilic dye 'DiI' (1,1'-dioctadecyl-3,3,3',3' tetramethylindocarbocyanine perchlorate; DiIC18(3)) is commonly used as an anterograde and retrograde neuronal tracer. DiI has 18-carbon-long straight alkyl hydrocarbon tails on each nitrogen of the two indoline rings, two methyl groups and a conjugated 3-carbon bridge connecting the aromatic rings symmetrically. DiI labels cell membranes by inserting its two long (C_{18} carbon) hydrocarbon chains into the lipid bilayers.

3.2.3. Materials and Methods

Animals

An in-house mouse breeding colony was used to generate primary cell cultures of hippocampal neurons for DiI labeling. The mice were housed and bred at the McMaster University Central Animal Facility. All experiments complied with the guidelines set out by the Canadian Council on Animal Care and were approved by the McMaster Animal Research Ethics Board.

Cell Culture Preparation

Primary hippocampal neurons were generated as previously described by our laboratory with minor modifications (Jacobs and Doering, 2010). Briefly, four embryonic day 15-17, E15-17 (day of sperm plug counted as E1) pups were randomly removed from the pregnant dam. Hippocampi were dissected in Calcium and Magnesium-Free Hank's Buffered Salt Solution (CMF-HBSS) and tissues were digested with 2.5% trypsin for 15 minutes in a 37°C water bath. The supernatant was removed, rinsed with three successive washes of CMF-HBSS and re-suspended in Neural Growth Media (NGM) containing 1X Neurobasal (Life Technologies), 0.5mM GlutaMAX (Life Technologies) and 2.0% B-27 Supplement (Invitrogen). Cells were subsequently plated on 12 mm glass coverslips (Bellco) in 24 multi-well plates, pre-treated with 1 mg/mL poly-$_L$-lysine (Sigma) and 10 ug/ml laminin (Life Technologies), immediately after dissociation at a density of 16 000 cells per well. Neurons were subsequently incubated at 37°C with 5% CO_2 and remained

in culture for 17 days *in vitro* (*DIV*) to allow for the development and maturation of dendritic spines. Every 3-4 days, the neurons were fed by replacing one half of the media with fresh NGM.

DiI Labeling Procedure

Dendritic spines were identified using the well-characterized fluorescent marker DiI (1,1'-dioctadecyl-3,3,3',3'-tetramethylindocarbocyanine perchlorate). Application of the dye was adapted from established protocols (Westmark et al., 2011). The neurons were fixed with freshly prepared 2.0% paraformaldehyde (PFA) for 15 minutes. Each well was gently washed with Dulbecco's Phosphate-Buffered Saline (DPBS, Invitrogen). For the staining, the wells were aspirated and sprinkled with solid DiI crystals (Life Technologies-Molecular Probes, Cat. #D-3911). Approximately 2-3 crystals were added using a pair of fine forceps to each well. To prevent dehydration of the cells, a small amount of DPBS was dispensed to the edge of the wells. Special care was taken to deliver the smallest crystals to prevent clumping of the dye. The neurons were exposed to the crystals for 10 minutes on an orbital shaker set at a low speed. The shaker motion ensured that the crystals were adequately distributed to augment complete staining across the surface of the coverslip. The plate was then removed from the shaker and the wells were copiously washed with DPBS to remove all crystals. This procedure was repeated until no crystals were visible. The cells were incubated with DPBS in the dark overnight at room temperature to allow for the diffusion of the dye. The following day, the coverslips were rinsed three times with dH_20 for 5-10 minutes each. The coverslips were removed,

completely air-dried, and mounted on slides with Prolong Gold Antifade (Life Technologies - Molecular Probes). Coverslips cured for a minimum of 24 hours *to allow the liquid mountant to form* a semi-rigid gel. Cells were visualized after 72 hours from the time of the initial staining to allow the dye to fully migrate across neuronal membranes and diffuse throughout the neurons to highlight spine structures. All images were taken within 7-10 days after staining to minimize fading.

Confocal Imaging

Visual imaging of the dendritic spines was acquired using a Zeiss 510 confocal laser-scanning microscope (LSM 510). All images were taken using a 63x/1.2 water immersion lens. A 543nm Hene-1 Rhodamine laser was utilized to visualize the fluorescence emitted by DiI. To view the specimen with reflected fluorescent light, the reflector turret was programmed to position F set 15 in correlation to the Rhodamine laser, and the single-track configuration was chosen. We used 1024 x 1024 pixels for image size and set the scan speed at a setting of 4. Scan direction and line averaging were also adjusted to a setting of 4. The pinhole diameter was configured to 1 Airy unit (124 μm). Series stacks were collected from the bottom to the top covering all dendrites and protrusions, with an optical slice thickness of 0.5 to 1 μm. The resulting images (4-6) were then reconstructed to identify hidden protrusions according to z-stack projections of the maximum intensity.

Dendritic Spine Analysis

ImageJ software (http://rsbweb.nih.gov/ij/) was used for viewing the confocal images and for spine quantification. In order to increase the magnification for a better view of the spines without loss of image quality, the resolution of the stack image was increased by a factor of 5 in the X and Y directions with the plug-in Transform J Scale (Pop et al., 2012). The length of a spine was obtained by drawing a line from its emerging point on the dendrite to the tip of its head. Approximately, 8-10 neurons selected at random were analyzed per condition across two coverslips. Density and morphology of spines were scored in dendritic segments 10 μm in length. Spines were classified into one of the four morphological subtypes: filopodial, thin, stubby, and mushroom-shaped.

Statistical Analysis

Spine density was determined by summing the total number of spines per dendritic segment length and then calculating the average number of spines per 10 μm. These values were then averaged to yield the number of spines per 10 μm for each animal. Statistics were performed using GraphPad Prism. Differences were detected with a one-way analysis of variance. Following one-way ANOVA, post hoc differences were resolved using the Tukey's multiple comparison test. A p-value of <0.05 was considered significant. All values are expressed as mean ± SEM.

3.2.4. Results

Laboratory Prepared versus Commercial Grade Paraformaldehyde Fixation

To determine an optimized protocol for the fluorescent visualization of dendritic spines with the carbocyanine dye in dissociated cultures, we explored patterns of DiI labeling in neurons fixed with laboratory prepared paraformaldehyde (PFA) in PBS or commercial grade formalin at 2.0%. When the cells were prepared with either fixative, the DiI crystals diffused efficiently along the neuronal membranes to permit the effective visualization of the somas and dendritic processes studded with delicate spinous protrusions. However, the laboratory prepared PFA samples facilitated enhanced staining and clarity for the crisp visualization of spines compared to formalin. Commercial grade formalin which typically contains ~10-15% methanol prevents polymerization in storage. Given that DiI is soluble in organic solvents, the use of methanol or acetone fixation is highly discouraged. Taking this into consideration, we investigated whether neurons fixed with acetone would be ineffectively labeled with DiI. We were able to confirm that cells had adhered to the coverslip (as visualized by DAPI) when fixed with acetone, but as expected, the dye unsuccessfully permeated throughout the dendritic segments (results not shown). Additionally, it is important to note that the use of any fixative stored for extended periods of time may risk decomposition and in turn yield poor fixation of samples.

Variations in Paraformaldehyde Concentration Alter Clarity

Labeling neurons with the fluorescent marker DiI provides a well-defined outline of neuronal cell bodies, dendritic arbors (**Figure 3.3),** and spine subtypes **(Figure 3.4).** To determine the most effective conditions for optimal DiI diffusion along dendritic segments, we tested varying concentrations of laboratory PFA fixative at 1.5%, 2.0% and 4.0%. Qualitative analysis revealed that the structural integrity of dendrites could not be maintained with a higher concentration of fixation. Namely, the extent of dendritic branching visualized by the dye in cells fixed with 4.0% PFA was hindered compared to cells fixed using 1.5% or 2.0% PFA (**Figure 3.5A**). In some cases, dye diffusion was limited to where the dye was applied, such that distal dendrites and spines on the same neuron were often not stained, including other neighbouring neurons. Swelling of the dendrites (varicosities) were also apparent often hindering accurate measurements of the spines **(Figure 3.5B)**. For instance, the dye would aggregate along the dendrites at spines, causing them to appear 'stubby' in shape. However, this often yielded a false morphological classification, as the shape or appearance of spines was attributed to the dye's inability to completely diffuse throughout the neuronal processes. Furthermore, higher concentrations of PFA typically yielded autofluorescence, which may explain the diffuse background fluorescence coupled with reduced illumination of the spines evident in **Figure 3.5B**.

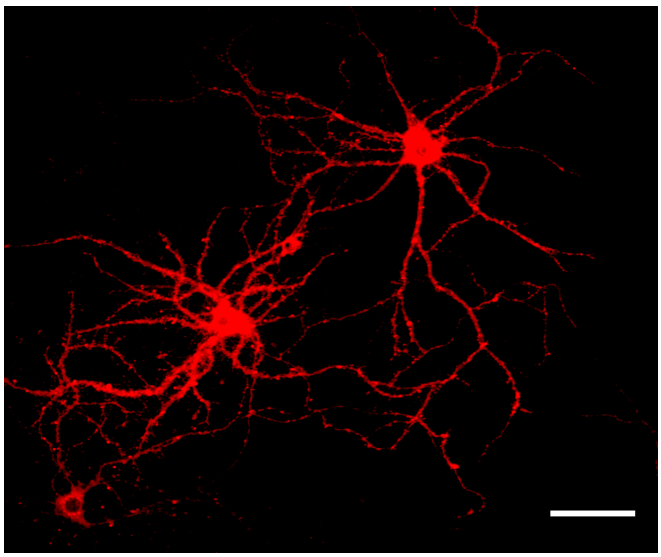

Figure 3.3: Representative image of DiI labeled neurons. DiI highlighting the dendritic complexity and topographical connectivity of neurons. Dendritic arbors and spines are sufficiently filled and visualized in their entirety with the fluorescent dye. Scale bar = 50 μm.

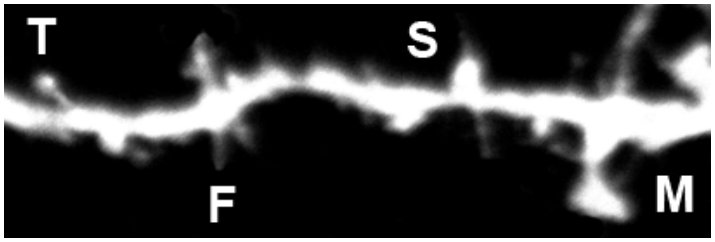

Figure 3.4: Representative image of DiI labeled spines. Filopodia-like (F), long-thin (T), stubby (S) and mushroom (M) spines are identified based on structural measures.

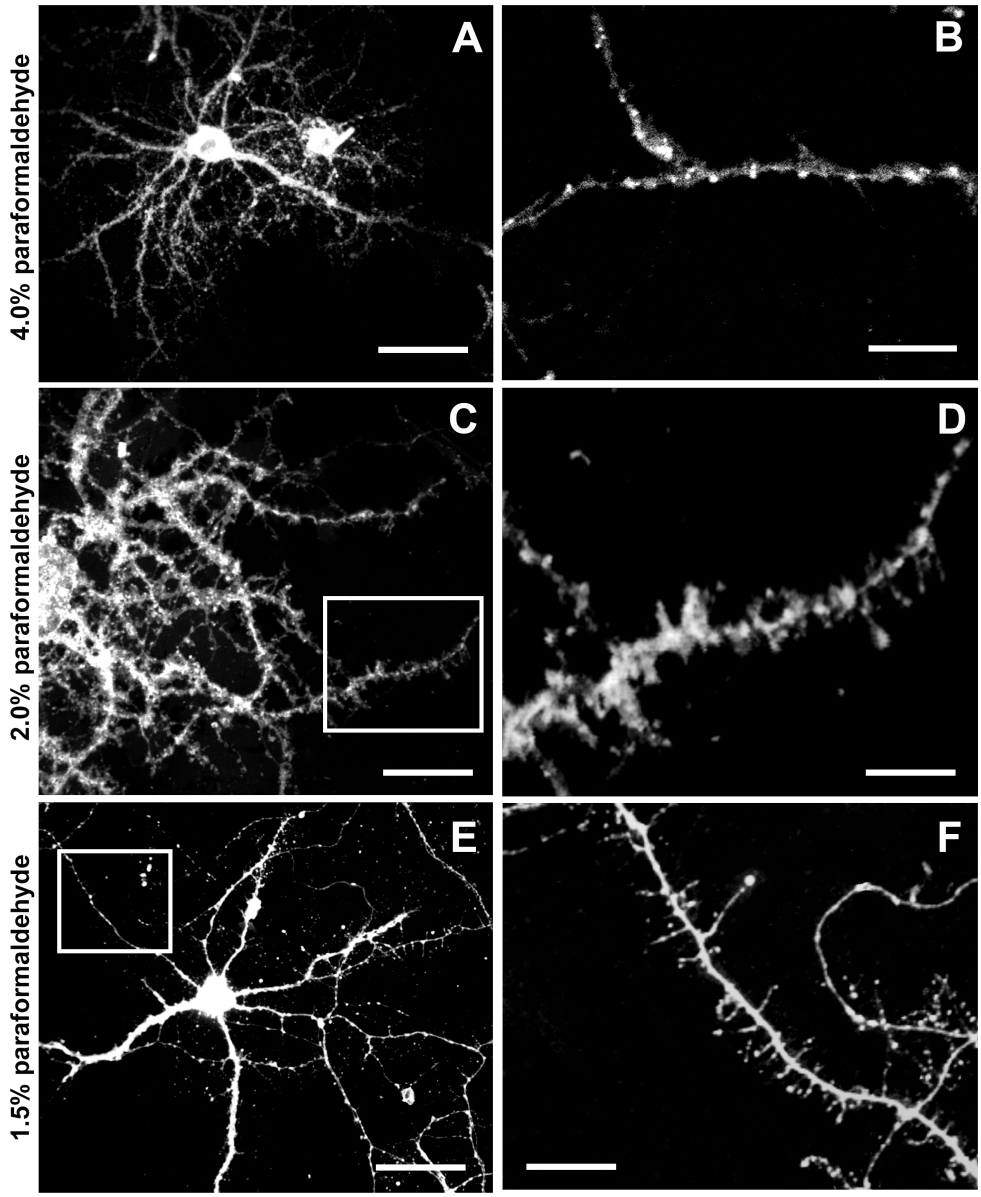

Figure 3.5: DiI labeled neurons fixed with varying concentrations of paraformaldehyde (PFA). Application of DiI crystals on fixed cells produces a very high degree of detail. **(A)** Cell fixed with 4.0% PFA. **(B)** The use of 4.0% PFA fixative

significantly compromises DiI diffusion through the dendrites. Multiple varicosities are highlighted along the dendrite and spines are poorly resolved. **(C)** Cell fixed with 2.0 % PFA. **(D)** The use of 2.0% PFA generates high quality DiI labeling of spines. Various subtypes of spines are evident along the dendritic segment. **(E)** Cell fixed with 1.5% PFA. **(F)** The use of 1.5% PFA yields comparable results to the use of 2.0% fixative. Fine, thin filopodial projections are resolved. Scale bar (A,C,E) = 50 μm; Scale bar (B,D,F) = 5 μm.

Ultimately, we discovered that laboratory prepared PFA utilized at lower concentrations was most effective, as it encouraged complete filling of the dendritic segments and finer processes through rapid dye diffusion. Specifically, the images obtained with 1.5-2.0% PFA delineated fine dendritic spines in comparable detail to the traditional Golgi staining method **(Figures 3.5C-F)**. Hence, optimal fixation can greatly improve the quality of DiI neuronal labeling.

Quantitative Analysis of Spine Density and Morphology

Spine density and morphology were assessed in DiI labeled neurons fixed with varying concentrations of PFA (1.5%, 2.0% and 4.0%) to investigate dye permeability. No significant differences in spine density were observed in neurons fixed with either 1.5% or 2.0% PFA (**Figure 3.6)**. Alternatively, neurons fixed with 2.0% PFA yielded significantly higher spine densities when compared to neurons fixed with 4.0% PFA (*p=0.012), potentially as a result of increased DiI labeling. These findings suggest and reinforce our observation that the use of a stronger fixative hinders the dye's ability to completely diffuse and fill fine processes, like spines. Notably, despite the appearance of an increased proportion of 'stubby' spines in neurons fixed with a higher concentration of fixative (**Figure 3.5B**), no significant differences resulted in any of the comparisons made in the composition of spine morphologies with varying concentrations of fixative (results not shown). Still, our recommendation holds that initial fixation with milder concentrations of PFA fixative at 1.5-2.0% generates the most consistent and superior results.

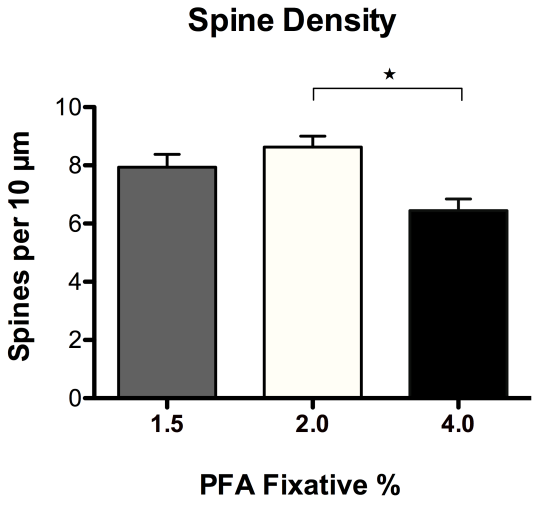

Figure 3.6: Spine density analysis of DiI labeled neurons fixed with varying concentrations of paraformaldehyde (PFA). No significant differences in spine density were observed in neurons fixed with 1.5% or 2.0% PFA. Neurons fixed with 2.0% PFA yielded significantly higher spine densities when compared to neurons fixed with 4.0% PFA (*$p<0.05$).

Summary of Findings

The results obtained through this protocol demonstrated that DiI staining in cells prepared with a lower percentage of fixative yielded the highest quality of images. The detailed images generated by this protocol allow us to perform an accurate quantitative analysis of spine structures and spine density. Stubby and mushroom shaped dendritic spines were most evident by their prominent 'pinhead' fluorescence directly on the dendritic spine when positioned perpendicularly to the plane of focus on the microscope slide, or as thick protrusions off the dendrite. Filopodial dendritic spines were most visible when their characteristic long and thin protrusions extended upwards/downwards from the dendritic branch. The high-resolution images that can be obtained using this technique allow us to delineate spine morphologies to provide insight into the areas of synapse formation, development and remodeling in the CNS.

3.2.5. Discussion

Several methods to study neuronal structure include histological stains, immunocytochemistry, electroporation of fluorescent dyes, transfection of fluorescent constructs, and the Golgi technique. Although the Golgi technique offers valuable results, this method is time consuming and often lacks reliability. DiI fluorescence labeling has gained popularity, but optimization of the method is essential to accurately quantitate and evaluate fine neuronal structures such as dendritic spines. In lieu of the DiOlistic literature, reported protocols differ vastly for cell/tissue fixation, dye delivery, and diffusion times, with no report on the impact that these different conditions have on the quality of labeling. Here, we outlined a procedure that allows the direct application of DiI to cells in culture; a method that has not been thoroughly explored. The present protocol sought to define the optimal conditions for the fluorescent illumination of individual neurons, including the soma, dendritic arborizations, and spines in cell culture through the use of confocal microscopy. Confocal microscopic analysis of fluorescently labeled neurons has improved resolution of dendritic morphology and has been suggested to provide a more accurate measurement of spines (Schmitz et al., 2011; Lee et al., 2009). Among the most important parameters of this procedure, fixation properties impacted the success of labeling most profoundly.

Optimization of Cell Fixation

Amid the DiOlistic literature, a variety of fixation conditions have been reported that produce acceptable levels of DiI labeling. The use of 4.0% PFA is most commonly

reported by standard immunohistochemical and immunocytochemical protocols, while many DiI labeling protocols indicate the use of both 1.5% or 4.0% PFA (i.e. Kim et al., 2007; Westmark et al., 2011; Staffend and Meisel, 2011b). To explore this range, we compared the image quality of neurons obtained from 1.5%, 2.0% and 4.0% concentrations of fixative. The use of 4.0% PFA fixative significantly compromised DiI diffusion through the dendritic processes (**Figure 3.5B**). This was apparent by reduced image quality due to increased background fluorescence and inconsistent labeling. However, fixation with both 1.5% and 2.0% PFA yielded similar results with superior diffusion of the lipophilic dye DiI along the neuronal membranes (**Figure 3.5C-F**). We determined this to be a significant finding since 4.0% PFA has been reported to yield successful results in both tissue slices and cell culture labeling. We discovered that a milder concentration of PFA fixative increased the extent of DiI diffusion, resulting in complete visualization of dendrites and spines. A higher concentration of fixative may interfere and prevent the dye from penetrating the membrane. We strived to further augment our cell fixation technique through a direct comparison of the effectiveness of using freshly prepared laboratory PFA versus commercially-produced formalin. Utilization of 1.5-2.0% laboratory PFA produced images with higher clarity and less background fluorescence. The use of commercially-produced formalin (containing methanol) may have adversely impacted the labeling. When evaluating spine density, we found that milder fixation conditions with 2.0% PFA more effectively incorporated DiI into the spines than their 4.0% PFA counterpart. With the use of a weaker fix, more spines were resolved and identified, resulting in an increase in spine density. Together,

our results suggest the use of 1.5-2.0% freshly prepared buffered PFA as the superior fixative. As a precaution, utilizing 2.0% (rather than 1.5%) PFA fixative ensures that the cells are effectively fixed and adhered to the coverslip.

Dendritic Order of Analysis

To quantitatively analyze the dendritic spines, we utilized confocal imaging of the cells. The resolution obtained with the confocal microscope permitted the study of individual spines. However, Z stack images with a step interval of 0.5 to 1 μm supplemented each XY image for accurate spine quantification. The sides of the dendrite were meticulously examined for vertical protrusions stretching upward and downward off the dendrite in addition to the spines extending upwards towards the observer. At higher magnification, we were able to morphologically classify some of the dendritic protrusions. However, the spines that extended vertically towards the observer were difficult to morphologically classify from an aerial perspective. Additionally, extra care was taken while examining possible protrusions positioned on the dendritic trunk that extended vertically upwards towards the observer; filopodia and thin shaped spines were likely to exhibit less fluorescence in comparison to stubby and mushroom-shaped counterparts, due to less absorption of the dye with reduced surface volume. This point was particularly significant in accurately deciphering the morphology of spines. Moreover, the aggregation of overlapping dendritic processes and complex branching/arborization at times hindered the accurate evaluation of spines. For instance, the areas of the dendritic trunk located closer to the soma-exhibited extreme intertwining

with numerous surrounding dendrites that complicated the isolation and differentiation of spines. Additionally, swellings of the dendritic trunk tended to conceal the presence of shorter spines even with a detailed analysis using a series of Z stack images.

Providing that spine density may vary across different order dendrites (primary, secondary tertiary, etc.), systematic sampling of dendritic order is necessary when analyzing spine density and morphology. Branch ordering schemes are frequently used, wherein the dendrites emerging from the cell soma are primary, their first branches are secondary and so on, with increasing order until the tips are reached. Branches may also vary in diameter. The total number of images collected will depend on the experimental requirements and the degree of variability within a neuron, and across neurons and animals (Ruszczycki et al., 2012). For the purpose of this study, image collection was restricted to the three-dimensional structure of secondary and tertiary dendrites. These parameters were consciously considered to improve accuracy in conducting spine measurements (Rosenzweig, 2011). Differences in spine measurements on different order dendrites could potentially draw further insight on neural connectivity in the brain.

Optimization of DiI delivery

Less than optimal cellular DiI labeling can be attributed to a variety of sources. For troubleshooting purposes, the most common problems, probable causes, and solutions are outlined in Table 1.

Table 2.1: Troubleshooting guide for optimal DiI labeling.

Problems	Potential Causes / Corrective Measures
High background is visible.	Residual crystals will result in high background. Avoid adding a surplus of DiI crystals. An excess of crystals will yield high autofluorescence and debris in the cultures. Ensure that coverslips are rinsed well with dH_20 until no DiI crystals are visible to the naked eye. Lastly, it is desirable to limit the duration of exposure of the sample to the laser to minimize the degree of phototoxic damage to the ultrastructure and any non-specific signal.
Dye bleeds upon exposure to light.	Glycerol-based mounting media (i.e. Prolong Gold, Vectashield, etc.) can extract membrane-bound dyes upon exposure to light. DiI is light sensitive and long-term exposure will cause fluorescence to fade. Higher magnification objectives (i.e. 63x) are necessary to produce better image resolution and enhance sensitivity of spine detection; however samples are subject to increased light exposure. High intensity light renders the dye to photobleaching. Minimize duration of light exposure if possible.
Slides are fading.	Ensure that images are captured as soon as possible after mounting. Illumination with light will cause fluorescence to diminish. Slides can be used at least 6 months to a year if stored in the dark at 4°C.
Coverslips appear cloudy.	Ensure that coverslips are rinsed well with dH_2O or salt residue/film will accumulate clouding the coverslip. Apply more washes if necessary.

Bubbles are apparent after mounting.	Avoid the formation of air bubbles. Ensure that coverslips are completely dry before mounting. Do not apply an excess of mounting medium. Apply a small amount using a dropper to the coverslip and gently pick up the coverslip using the slide. As the coverslip pulls against the slide, allow the mountant to gradually permeate without applying additional pressure.
Absence or lack of cells present.	Fixation of cells may have been unsuccessful. Higher concentration of fixative may be required if cells are not adhering to the coverslip. Always use freshly prepared fixative. Avoid rigorous washes that may cause cells to lift.
Low frequency staining of neurons.	Due to the dye's indiscriminate nature, this technique often generates sparse fluorescent labeling. During the application, DiI crystals must be thoroughly dispersed to maximize the staining of cells. High concentration of fixative may also obstruct dye diffusion. Do not extend the duration of fix, as it will affect labeling. Overfixation will disrupt the cell membrane integrity causing DiI to leak out of the cell.
Streaking across coverslips.	Scratching of the coverslip with the glass pipette during extraction of solutions from the well impacts image quality. Since this procedure involves numerous washes, it is important to slowly add or remove solutions from the wells to prevent lifting of the cells. One can practice gentle pipetting techniques using the sides of the wells to allow solutions to slowly cover the cells. Extract solutions from the side of the well to avoid contact with coverslip and prevent scratching.

Difficulty isolating single neuronal processes for analysis.	Overlapping of cells and processes may be caused by high density. Reduce plating density.
Dendritic spines are poorly resolved.	Confocal imaging parameters may not be optimal for assessing spine morphology. For high-resolution images obtained at high magnification, slower image acquisition should be used. Adjust settings for detector gain, line averaging, and speed of scanning to improve image quality. *Note*: The same imaging parameters should be used throughout the study.

Possible Limitations of this Method

Although this approach has proven to be effective, it is important to address some of the limitations to the technique. For instance, DiI labeling can be highly variable, because dye crystal size, density, and penetration are all very difficult factors to control. Despite the majority of cells being labeled, the application of extracellular solid DiI crystals often restricted complete staining of all neurons in its entirety within a culture well. Dye diffusion was constrained to neurons that were in close proximity to the crystals, whereas more distal neurons or terminal branches were not prominently stained or filled in. As such, this method is most appropriate for the structural analysis of dendritic spines rather than a comprehensive analysis of dendritic arborization. While these methods produce an accurate analysis on a single-cell resolution, extrapolating the acquired data to a larger neuronal population might prove inaccurate if the staining technique selectively labels only subsets of neurons. Additional selection bias might also occur in these cases if the researcher chooses to measure "convenient" cells, which are visualized more clearly and without overlap with other neurons. Therefore, it is of the utmost importance to ensure that cultures are grown at a sufficient density that limits overlapping processes and permits the isolation of single entities (spines). By using the appropriate concentration of fixative, this can ensure that most neuronal processes are appropriately filled in. Additionally, ensuring that the solid dye is thoroughly distributed during the staining procedure will highlight a larger proportion of cells per sample in a well.

As the morphology of dendritic spines is highly variable, a sufficient sampling size is essential for statistical analysis. With light or epifluorescent microscopy, the dendrite may obscure spines that lie above or below the visual plane, such that only spines extending laterally can be accurately counted. However, this problem cannot be completely remedied by three-dimensional confocal microscopy. To compensate, some studies have applied correction factors for hidden spines (Bannister and Larkman, 1995).

It is also desirable to combine DiI labeling with immunofluorescent staining, with which detailed co-localization can be analyzed using confocal microscopy. The two techniques, however, are often incompatible because Triton X-100, a conventional detergent or permeabilization reagent commonly used to enhance antibody penetration into tissues or cells, causes diffusion of DiI from the labeled structures (Neely et al., 2009). Since Triton X-100 solubilizes lipid molecules almost indiscriminately, it is most likely that Triton X-100 compromises the retention of DiI in the cellular membrane. As a result, the dye potentially leaks out of the membrane, causing the label to disappear after immunocytochemical procedures (Matsubayashi et al., 2008). The ability to perform a dual staining would better allow investigators to phenotypically characterize DiI labeled cells. In future studies, it may be valuable to couple DiI labeling with other fluorescent markers and/or antibodies to immunocytochemically identify other target proteins of interest within a neuron. Investigating appropriate fluorescent immunocytochemical protocols compatible with DiI neuronal tracing would serve as a useful tool in advancing current labeling techniques.

Advantages of this Method

The methods outlined above using DiI labeling offer a reproducible protocol that have several advantages for the analysis of dendritic spine structures using photostable fluorescence. This protocol offers the opportunity to systematically analyze a large quantity of dendritic spines in high detail, which cannot be achieved through other neuronal identification methods. Furthermore, fluorescent staining and imaging by confocal microscopy yields a series of Z stack images. Many densely compacted segments and spine protrusions often do not lie favourably in the plane of focus and thus cannot be reliably counted. Confocal imaging with DiI labeling permits the sensitive detection of spines by allowing a three-dimensional analysis of spines and dendrites to avoid over and undersaturated pixels. This is particularly vital for the identification of spinous protrusions on the dendritic trunk and most proximal to the soma, and in other cases where there is frequent overlap of the dendrites. Finally, our described methods are simple and do not increase the costs or effort, and more importantly do not compromise the integrity of the neurons or the quality of the staining and data acquired. Taken together, these characteristics make DiI a powerful technique for identifying and studying early events in neuronal development and brain connectivity with significant implications for neurological disease.

3.2.6. Conclusion

Given the literature, a variety of labeling and diffusion conditions can produce acceptable levels of fluorescent DiI labeling. Our goal was to explicitly compare specific methodological components to determine a DiI protocol that produces reproducible staining of dendritic spines in dissociated cultures. Dendritic spines are significant structural substrates for synaptic plasticity and in turn are vital to the proper functioning of the CNS. Spines serve as a functional integrative unit whose morphology is tightly correlated with its function. An accurate neuronal visualization method provides valuable insight into the neuronal organization of various areas of the brain. Importantly, our technique provides an alternative method to fluorescently label neurons and dendritic spines in a convenient and cost-effective manner. Our technique further enables the analysis of dendritic spine topographical distribution, quantitative measurement, and morphological assessment. Such findings would be highly applicable to the investigation of the etiology of various disorders in which spine pathology has been implicated. As a result, this accurate, efficient and economical staining technique has a wide array of applicability to the study of CNS neurobiology in normal and disease states.

3.2.7. Acknowledgements

This work has been supported by NSERC (National Sciences and Engineering Research Council of Canada) and the Fondation Jérôme LeJeune (Paris).

3.2.8. References

Arsenault, J., and O'Brien, J. A. (2013). Optimized heterologous transfection of viable adult organotypic brain slices using an enhanced gene gun. *BMC Res Notes* 6, 544. doi:10.1186/1756-0500-6-544.

Bannister, N. J., and Larkman, A. U. (1995). Dendritic morphology of CA1 pyramidal neurones from the rat hippocampus: II. Spine distributions. *J. Comp. Neurol.* 360, 161–171. doi:10.1002/cne.903600112.

Braun, K., and Segal, M. (2000). FMRP involvement in formation of synapses among cultured hippocampal neurons. *Cereb. Cortex* 10, 1045–1052.

Bruce, L. L., Christensen, M. A., and Fritzsch, B. (1997). Electron microscopic differentiation of directly and transneuronally transported DiI and applications for studies of synaptogenesis. *Journal of Neuroscience Methods* 73, 107–112.

Colello, R. J., Tozer, J., and Henderson, S. C. (2012). Confocal laser scanning microscopic photoconversion: a new method to stabilize fluorescently labeled cellular elements for electron microscopic analysis. *Curr Protoc Neurosci* Chapter 2, Unit2.15. doi:10.1002/0471142301.ns0215s58.

Fiala, J. C., Spacek, J., and Harris, K. M. (2002). Dendritic spine pathology: cause or consequence of neurological disorders? *Brain Research Reviews* 39, 29–54.

Gan, W. B., Bishop, D. L., Turney, S. G., and Lichtman, J. W. (1999). Vital imaging and ultrastructural analysis of individual axon terminals labeled by iontophoretic

application of lipophilic dye. *Journal of Neuroscience Methods* 93, 13–20.

Gan, W. B., Grutzendler, J., Wong, W. T., Wong, R. O., and Lichtman, J. W. (2000). Multicolor "DiOlistic" labeling of the nervous system using lipophilic dye combinations. *Neuron* 27, 219–225.

Honig, M. G., and Hume, R. I. (1989). Dil and diO: versatile fluorescent dyes for neuronal labelling and pathway tracing. *Trends in Neurosciences* 12, 333–5– 340–1.

Jacobs, S., and Doering, L. C. (2010). Primary dissociated astrocyte and neuron co-culture. 269–283. doi:10.1007/978-1-60761-292-6.

Kim, B. G., Dai, H.-N., McAtee, M., Vicini, S., and Bregman, B. S. (2007). Labeling of dendritic spines with the carbocyanine dye DiI for confocal microscopic imaging in lightly fixed cortical slices. *Journal of Neuroscience Methods* 162, 237–243. doi:10.1016/j.jneumeth.2007.01.016.

Lanciego, J. L., and Wouterlood, F. G. (2011). A half century of experimental neuroanatomical tracing. *Journal of Chemical Neuroanatomy* 42, 157–183. doi:10.1016/j.jchemneu.2011.07.001.

Lee, P.-C., Chang, H.-M., Lin, C.-Y., Chiang, A.-S., and Ching, Y.-T. (2009). Constructing neuronal structure from 3D confocal microscopic images. *Journal of Medical and Biological Engineering* 29, 1–6.

Li, M., Cui, Z., Niu, Y., Liu, B., Fan, W., Yu, D., and Deng, J. (2010). Synaptogenesis in

the developing mouse visual cortex. *Brain Research Bulletin* 81, 107–113. doi:10.1016/j.brainresbull.2009.08.028.

Lin, Y.-C., and Koleske, A. J. (2010). Mechanisms of Synapse and Dendrite Maintenance and Their Disruption in Psychiatric and Neurodegenerative Disorders. *Annu. Rev. Neurosci.* 33, 349–378. doi:10.1146/annurev-neuro-060909-153204.

Lo, D. C., McAllister, A. K., and Katz, L. C. (1994). Neuronal transfection in brain slices using particle-mediated gene transfer. *Neuron* 13, 1263–1268. doi:10.1186/1756-0500-6-544.

Malinow, R., Hayashi, Y., Maletic-Savatic, M., Zaman, S. H., Poncer, J.-C., Shi, S.-H., Esteban, J. A., Osten, P., and Seidenman, K. (2010). Introduction of green fluorescent protein (GFP) into hippocampal neurons through viral infection. *Cold Spring Harb Protoc* 2010, pdb.prot5406. doi:10.1101/pdb.prot5406.

Matsubayashi, Y., Iwai, L., and Kawasaki, H. (2008). Fluorescent double-labeling with carbocyanine neuronal tracing and immunohistochemistry using a cholesterol-specific detergent digitonin. *Journal of Neuroscience Methods* 174, 71–81. doi:10.1016/j.jneumeth.2008.07.003.

Neely, M. D., Stanwood, G. D., and Deutch, A. Y. (2009). Combination of diOlistic labeling with retrograde tract tracing and immunohistochemistry. *Journal of Neuroscience Methods* 184, 332–336. doi:10.1016/j.jneumeth.2009.08.016.

O'Brien, J. A., and Lummis, S. C. R. (2006). Diolistic labeling of neuronal cultures and

intact tissue using a hand-held gene gun. *Nature Protocols* 1, 1517–1521. doi:10.1038/nprot.2006.258.

Penzes, P., and Rafalovich, I. (2012). Regulation of the actin cytoskeleton in dendritic spines. *Adv. Exp. Med. Biol.* 970, 81–95. doi:10.1007/978-3-7091-0932-8_4.

Penzes, P., Cahill, M. E., Jones, K. A., VanLeeuwen, J.-E., and Woolfrey, K. M. (2011). Dendritic spine pathology in neuropsychiatric disorders. *Nature Publishing Group* 14, 285–293. doi:10.1038/nn.2741.

Pop, A. S., Levenga, J., Esch, C. E. F., Buijsen, R. A. M., Nieuwenhuizen, I. M., Li, T., Isaacs, A., Gasparini, F., Oostra, B. A., and Willemsen, R. (2012). Rescue of dendritic spine phenotype in Fmr1 KO mice with the mGluR5 antagonist AFQ056/Mavoglurant. *Psychopharmacology*. doi:10.1007/s00213-012-2947-y.

Ranjan, A., and Mallick, B. N. (2010). A modified method for consistent and reliable Golgi-cox staining in significantly reduced time. *Front Neurol* 1, 157. doi:10.3389/fneur.2010.00157.

Rochefort, N. L., and Konnerth, A. (2012). Dendritic spines: from structure to in vivo function. *Nature Publishing Group* 13, 699–708. doi:10.1038/embor.2012.102.

Rosenzweig, S. (2011). Analyzing dendritic growth in a population of immature neurons in the adult dentate gyrus using laminar quantification of disjointed dendrites. 1–8. doi:10.3389/fnins.2011.00034/abstract.

Ruszczycki, B., Szepesi, Z., Wilczynski, G. M., Bijata, M., Kalita, K., Kaczmarek, L., and Wlodarczyk, J. (2012). Sampling issues in quantitative analysis of dendritic spines morphology. *BMC Bioinformatics* 13, 213. doi:10.1186/1471-2105-13-213.

Schmitz, S. K., Hjorth, J. J. J., Joemai, R. M. S., Wijntjes, R., Eijgenraam, S., de Bruijn, P., Georgiou, C., de Jong, A. P. H., van Ooyen, A., Verhage, M., et al. (2011). Automated analysis of neuronal morphology, synapse number and synaptic recruitment. *Journal of Neuroscience Methods* 195, 185–193. doi:10.1016/j.jneumeth.2010.12.011.

Seabold, G. K., Daunais, J. B., Rau, A., Grant, K. A., and Alvarez, V. A. (2010). DiOLISTIC labeling of neurons from rodent and non-human primate brain slices. *JoVE*. doi:10.3791/2081.

Sherazee, N., and Alvarez, V. A. (2013). DiOlistics: delivery of fluorescent dyes into cells. *Methods Mol. Biol.* 940, 391–400. doi:10.1007/978-1-62703-110-3_28.

Smith, D. L., Pozueta, J., Gong, B., Arancio, O., and Shelanski, M. (2009). Reversal of long-term dendritic spine alterations in Alzheimer disease models. *Proceedings of the National Academy of Sciences* 106, 16877–16882. doi:10.1073/pnas.0908706106.

Staffend, N. A., and Meisel, R. L. (2011a). DiOlistic labeling in fixed brain slices: phenotype, morphology, and dendritic spines. *Curr Protoc Neurosci* Chapter 2, Unit 2.13. doi:10.1002/0471142301.ns0213s55.

Staffend, N. A., and Meisel, R. L. (2011b). DiOlistic Labeling of Neurons in Tissue

Slices: A Qualitative and Quantitative Analysis of Methodological Variations. *Front Neuroanat* 5, 14. doi:10.3389/fnana.2011.00014.

Terasaki, M., Slater, N. T., Fein, A., Schmidek, A., and Reese, T. S. (1994). Continuous network of endoplasmic reticulum in cerebellar Purkinje neurons. *Proc. Natl. Acad. Sci. U.S.A.* 91, 7510–7514.

Westmark, C. J., Westmark, P. R., O'Riordan, K. J., Ray, B. C., Hervey, C. M., Salamat, M. S., Abozeid, S. H., Stein, K. M., Stodola, L. A., Tranfaglia, M., et al. (2011). Reversal of fragile X phenotypes by manipulation of AβPP/Aβ levels in Fmr1KO mice. *PLoS ONE* 6, e26549. doi:10.1371/journal.pone.0026549.

Yuste, R. (2011). Dendritic spines and distributed circuits. *Neuron* 71, 772–781. doi:10.1016/j.neuron.2011.07.024.

CHAPTER 4:

ASTROCYTED-THROMBOSPONDIN-1 MODULATES SYNAPSE AND SPINE DEFECTS IN THE FRAGILE X MOUSE MODEL

Chapter 4

4.1. Preface to Chapter 4

This chapter consists of an author-generated version of an article prepared for submission to Molecular Brain entitled, "Astrocyte-Secreted Thrombospondin-1 Modulates Synapse and Spine Defects in the Fragile X Mouse Model". This paper was published and used with permission from the journal.

4.1.1. Declaration of Author Contributions

The author would like to acknowledge Sally Lau for her experimental contributions with the immunocytochemistry and Dr. Angela Scott for her editorial assistance. All other data collection, experiments and interpretation, preparation and writing of manuscripts were done by the author under the guidance of Dr. Laurie C. Doering.

4.1.2. Rationale

In the present study, the role of astrocyte-secreted thrombospondin-1 (TSP-1) in the regulation of spine and synapse development was assessed in FXS. Previous work in our laboratory has demonstrated a role for astrocytes in FXS (Pacey and Doering 2007). Astrocytes can prevent and rescue abnormal dendrite morphology and dysregulated synapses in *Fmr1* knockout hippocampal neurons (Jacobs and Doering 2010; Jacobs et al. 2010). While we have identified that astrocytes affect synapse development *in vitro*, it is unknown whether the observed effects can be attributed to soluble factors secreted by astrocytes that guide development. TSPs have been identified as necessary and sufficient

pro-synaptogenic components in astrocyte-conditioned medium (Christopherson et al. 2005). The purpose of these experiments was to determine the influence of the astrocyte-secreted TSP-1 on neuronal maturation and synaptic development. These experiments also sought out to support the hypothesis that *astrocyte-derived TSP-1 regulates synaptogenesis in the Fragile X mouse.* The established experiments provide insight into the cellular and molecular mechanisms of neuron-astrocyte interactions that govern normal morphological spine and synaptic profiles in FXS.

4.2 Astrocyte-secreted thrombospondin-1 modulates synapse and spine defects in the Fragile X mouse model

Connie Cheng[1,2], Sally K.M. Lau[2], Laurie C. Doering[1,2]*

[1]*McMaster Integrative Neuroscience Discovery and Study Program, McMaster University, Hamilton, Ontario, Canada.*
[2]*Department of Pathology & Molecular Medicine, McMaster University, Hamilton, Ontario, Canada.*

***Correspondence:**
Dr. Laurie C. Doering
McMaster University
Department of Pathology and Molecular Medicine,
1280 Main Street West, Hamilton, ON, L8S 4K1, Canada
doering@mcmaster.ca
Tel: +1(905)525-9140 ext. 22913

Journal: Molecular Brain

Running Title: Astrocyte-Secreted TSP-1 in Fragile X Neurobiology

Keywords: Fragile X Syndrome, Autism, Astrocytes, Secreted factor, Thrombospondin-1, Synapses, Dendritic Spines

4.2.1. Abstract

Astrocytes are key participants in various aspects of brain development and function, many of which are executed via secreted proteins. Defects in astrocyte signaling are implicated in neurodevelopmental disorders characterized by abnormal neural circuitry such as Fragile X syndrome (FXS). In animal models of FXS, the loss in expression of the Fragile X mental retardation 1 protein (FMRP) from astrocytes is associated with delayed dendrite maturation and improper synapse formation; however, the effect of astrocyte-derived factors on the development of neurons is not known. Thrombospondin-1 (TSP-1) is an important astrocyte-secreted protein that is involved in the regulation of spine development and synaptogenesis. In this study, we found that cultured astrocytes isolated from an *Fmr1* knockout (*Fmr1* KO) mouse model of FXS exhibit a significant decrease in TSP-1 protein expression compared to the wildtype (WT) astrocytes. Correspondingly, *Fmr1* KO hippocampal neurons exhibited morphological deficits in dendritic spines and alterations in excitatory synapse formation following long-term culture. All spine and synaptic abnormalities were prevented in the presence of either astrocyte-conditioned media or a feeder layer derived from FMRP-expressing astrocytes, or following the application of exogenous TSP-1. Importantly, this work demonstrates the integral role of astrocyte-secreted signals in the establishment of neuronal communication and identifies soluble TSP-1 as a potential therapeutic target for Fragile X syndrome.

4.2.2 Introduction

Fragile X syndrome (FXS) is the most common form of intellectual disability and is a leading cause of autism spectrum disorders [1], affecting about 1/4000 males and 1/8000 females. The causative mutation for the majority of cases is a trinucleotide CGG expansion in the promoter region of the fragile X mental retardation 1 gene (*FMR1*), which induces transcriptional gene silencing and the loss of the fragile X mental retardation 1 protein (FMRP). FMRP is an RNA-binding protein that is highly involved in binding and regulating the translation, transport and stability of a subset of mRNAs to synapses [2,3]. Fundamental research on the *Fmr1* knockout (KO) mouse has provided promising insights into the cellular and molecular underpinnings of the condition. A well-described characteristic feature of FXS is the presence of "immature" dendritic spines [4,5]. These dendritic spine abnormalities in *Fmr1* KO mice are most pronounced during development, but also persist into adulthood [6]. As spines are thought to be the site of functional changes that mediate memory storage, an immature or otherwise aberrant morphology could represent the critical effect of the FXS mutation that underlies learning impairments.

The appropriate formation of neural connections is vastly dependent on reciprocal neuronal and glial interactions. Until recently, the majority of research into the function of FMRP, and the consequences of its absence, has been focused on neurons. However, it is now known that FMRP is also expressed in cells of the glial lineage [7,8]. The expression of FMRP is typically highest in astrocytes within the first week of birth and subsequently declines to low or undetectable levels [8]. Based on these findings, work in

our laboratory investigated the role of astrocytes in the development of the abnormal neurobiology of FXS. Using an astrocyte-neuron co-culture system, hippocampal neurons showed developmental delays in dendritic growth patterns and also in the expression of excitatory synapses when interfaced with astrocytes lacking FMRP [9,10], suggesting that dysfunction in non-neuronal cells may be a contributing factor into the pathogenesis of FXS.

During development and in the mature brain, astrocytes are known to provide signals that guide synapse formation and neurite development [11-14]. Astrocytes can regulate the stability, dynamics and maturation of dendritic spines through the release of secreted factors [15,16]. In particular, astrocyte-derived thrombospondins (TSPs) are large extracellular matrix proteins (450 kDa) that have been identified as major contributors to astrocyte-regulated excitatory synapse formation [17]. The TSP family consists of two subfamilies, A and B, according to their organization and domain structure [18,19]; A includes the trimeric TSP-1 and TSP-2, while B includes the pentameric TSP-3, TSP-4 and TSP-5 [20,21]. Recently, the *THBS1* gene, which encodes the TSP-1 protein, has been identified as an autism risk gene [22]. In the central nervous system (CNS), TSP-1 is mostly enriched in glia and predominantly expressed by developing astrocytes during early postnatal development in the rodent cortex [23], which correlates with the onset of synaptogenesis. TSP-1 regulates excitatory synaptogenesis through the gabapentin receptor $\alpha 2\delta$-1 [24,25], and neuroligin-1 in hippocampal neurons [26]. Double TSP-1 and -2 knockout mice show a reduced number of excitatory synapses in the cortex [17] and display dendritic spine irregularities [27]. Given that FMRP and

TSP-1 are both expressed in immature astrocytes and have been associated with the timely development of synapses, there is reason to believe that the early regulation of synaptogenesis could be influenced by TSP-1.

Previously, our group has demonstrated that astrocytes modulate neuronal development in FXS; however, it is unknown whether the effects can be attributed to direct physical astrocyte-neuron interactions and/or to the release of extrinsic synaptic cues derived from astrocytes that are responsible for guiding development. Here, we determined the role of astrocyte-secreted TSP-1 on neuronal maturation and synaptic development in FXS. To explore the consequences of altered astrocyte signaling during development, we optimized an indirect (non-contact) astrocyte-neuron co-culture method with either astrocyte-conditioned medium or an astrocyte feeder layer to promote neuronal attachment and survival. Using this experimental paradigm, our results showed abnormal spine maturation and synapse development in normal hippocampal neurons grown with conditioned media and a feeder layer from FXS astrocytes. We also found that TSP-1 levels were markedly reduced in FXS cultured astrocytes and conditioned media. Further, the addition of TSP-1 to FXS cultures prevented synaptic and spine alterations. These findings provide insight into the significance of astrocyte-derived cues during early developmental periods in the brain that underlie the proper establishment of neural circuitry.

4.2.3. Materials & Methods

Animals

The FMRP mouse colony was established from breeding pairs of FVB.129P2(B6)-Fmr1^{tm1Cgr} mice. The wildtype (WT) and *Fmr1* knockout (KO) mice were maintained as individual strains and genotyped regularly. Both male and female mice were used in the experiments. The mice used for these experiments were housed and bred at the McMaster University Central Animal Facility. All experiments complied with the guidelines set out by the Canadian Council on Animal Care and were approved by the McMaster Animal Research Ethics Board.

Hippocampal Neuron Isolation

Hippocampal neurons were obtained from embryonic day E15-17 (day of sperm plug counted as E1) WT and *Fmr1* KO animals. Hippocampal tissue was isolated from at least six embryonic pups, digested with 2.5% trypsin, and triturated through a fire-polished glass Pasteur pipette. The neurons were subsequently plated on poly-$_L$-lysine (1 mg/ml, Sigma) and laminin (0.1 mg/ml, Invitrogen) coated glass coverslips in 24-multiwell plates immediately after dissociation at a density of 20 000 cells per well in Neural Growth Medium consisting of Neurobasal (NB) (Invitrogen) enriched with 0.5mM GlutaMAX (Invitrogen), and 2% B-27 Supplement (Invitrogen). Neurons remained in culture for 17 days in vitro (*DIV*) to allow for the development and maturation of dendritic spines. Immunocytochemical studies subsequently ensued to

identify alterations in spine density, morphology and length, and the formation of excitatory synapses.

Primary Cortical Astrocyte Cultures

Cortical astrocytes were prepared from four WT or *Fmr1* KO postnatal day 0 to day 2 (P0-P2) pups, as detailed previously by our laboratory [28]. Briefly, whole brains were extracted and cortical tissue was dissected and incubated with 2.5% trypsin (Invitrogen) and 15 mg/mL DNase (Roche) at 37°C. Following successive mechanical trituration using a serological pipette, the cells were passed through a 70 μm cell strainer (Fisher Scientific), dissociated into a single-cell suspension, and re-suspended in 10% Glial Media (GM) comprised of Minimum Essential Medium (MEM) (Invitrogen), 0.6% glucose and 10% horse serum (Invitrogen). The astrocytes were seeded in a T75 flask and maintained in culture for 7-12 days in a humidified 5% CO_2, 95% O_2 incubator at 37°C. Partial medium changes were performed every 2-3 days. Cultures consisted of at least 95% astrocytes as determined by glial fibrillary acidic protein (GFAP) immunocytochemistry.

Preparation of Astrocyte-Conditioned Medium (ACM)

After 4-5 days in culture and achieving 50-65% confluency, the monolayers of astrocytes were subjected to a Neuronal Growth Media (NGM) switch. The cultures were washed extensively with Neurobasal (Invitrogen) and the media was replaced with NB/B-27 culture medium to generate the ACM. In preparation for conditioning, ACM was

harvested for 4 days and collected. The media was filtered using a 0.22μm syringe filter for the removal of cellular debris and concentrated ten times by filtration through a 10 kDa molecular weight cut-off (MWCO) centrifuge concentrator (Satorius Stedim). ACM was stored at -80ºC and used at a final concentration of 5x. Notably, this procedure closely follows that of Christopherson et al. [17] used for the isolation of thrombospondins. The ACM was spun at 5000 rpm for 5 minutes to remove cell debris prior to protein quantification or plating with the neurons.

Astrocyte Feeder Layer

To evaluate astrocyte non-contact mediated influences on morphological parameters, ThinCert™ cell culture inserts from Greiner Bio-One were utilized and placed in 24-multiwell plates to facilitate the growth of the cortical astrocytes. These culture inserts consist of a 0.4μm porous, PET membrane support that forms a two-compartment system. In this set-up, cultures were co-cultivated with neurons and astrocytes in physically separated compartments to facilitate paracrine-signaling interactions involving diffusible astrocyte-secreted factors. For preparation of the astrocyte feeder layers (AFL), confluent astrocyte monolayer cultures were trypsinized with 0.05% Trypsin-EDTA to lift adherent cells and subsequently passaged. The dissociated cells (9000 cells) were seeded into the cell culture inserts (positioned above the bottom of the well) and maintained in 10% GM for 3 days. Media was switched to Neural Growth Media (NGM) at least one day before plating neurons. Subsequently,

hippocampal neurons supplemented with NGM were plated below the cell culture inserts on the coverslips. NGM was replenished every 3-4 days.

DiI Neuronal Labeling

Dendritic spines were identified using the well-characterized fluorescent marker DiI (1,1'-dioctadecyl-3,3,3',3'-tetramethylindocarbocyanine perchlorate), as described by Cheng et al. [29]. In brief, the neurons were fixed with 2% paraformaldehyde and stained with lipophilic DiI (Invitrogen). For the staining, 2-3 DiI crystals were applied to each coverslip. A small amount of Dulbecco's Phosphate Buffered Saline (DPBS, Invitrogen) was dispensed to the edge of the wells to prevent dehydration of the cells. The neurons were stained for 10 minutes on an orbital shaker and copiously washed with DPBS to remove all crystals. The cells were incubated in DPBS overnight at room temperature. The following day, the coverslips were rinsed with dH_2O, air-dried and mounted to slides with Prolong Gold Anti-fade (with DAPI) fluorescent mounting medium (Invitrogen). The cells were visualized 72 hours from the initial staining to allow for the complete migration of the dye into the dendritic spines.

Confocal Imaging

Visual imaging of dendritic spines was acquired using a Zeiss 510 confocal laser-scanning microscope (LSM 510). All images were taken using a 63x/1.2 water immersion lens. A 543nm Hene-1 Rhodamine laser was utilized to visualize the fluorescence emitted

by DiI with the filter channel 3 BP560-615 nm. To view the specimen with reflected fluorescent light, the reflector turret was programmed to position F set 15 in correlation to the Rhodamine laser, and the single-track configuration was chosen. We used 1024 x 1024 pixels for image size and set the scan speed at a setting of 6. Scan direction and line averaging were also adjusted to a setting of 6. The pinhole diameter was configured to 1 Airy unit (124 μm). Series stacks were collected from the bottom to the top covering all dendrites and protrusions, with an optical slice thickness of 0.5 to 1 μm. The resulting images (4-6) were then reconstructed according to z-stack projections of the maximum intensity.

Dendritic Spine Analysis

ImageJ software (RSB, NIH) was used for viewing the confocal images and for spine quantification. In order to increase the magnification for a better view of the spines without loss of image quality, the resolution of the stack image was increased by a factor of 5 in the X and Y directions with the plug-in Transform J Scale [30]. The length of a spine was obtained by drawing a line from its emerging point on the dendrite to the tip of its head. Approximately, 25 neurons were selected at random per condition across three coverslips from two batches of cultures per group were used for quantitative analysis. Secondary dendritic branches were selected for analysis. Density, morphology and length of spines were scored in dendritic segments 10 μm in length. Morphologically, two populations of spines were identified: (1) ‘mature’ stubby/mushroom-like spines, which are small, rounded spines with or without a short neck and (2) ‘immature’ filopodium-like

spines, which are typically longer, thin and lack a head. Two to three independent experiments were performed. For each independent culture, 40-50 dendritic segments (10 μm in length) were selected and evaluated for spine analysis.

Immunocytochemistry

Following 17 *DIV*, hippocampal neurons were fixed with ice-cold (-20ºC) acetone for 20 min and processed for immunocytochemistry. Cells were washed three times in PBS and permeabilized with 0.1% Triton X-100, respectively. Non-specific binding was blocked with 1% bovine serum albumin (BSA) with the appropriate normal animal serum for 30 min at room temperature (RT). Primary antibodies were applied to the coverslips and incubated overnight at 4ºC. The second day, following washes with PBS, secondary antibodies were incubated with the cells for 3 hours at RT. Lastly, the coverslips were mounted on to slides with Prolong Gold Anti-fade fluorescent mounting medium (Invitrogen) containing DAPI to stain for nuclei**.** The following antibodies, diluted in PBS, were used: monoclonal synaptophysin (clone SVP-38; 1:250; Sigma-Aldrich), mouse monoclonal postsynaptic density 95 (PSD-95) (clone 6G6-1C9; 1:200; Millipore Bioscience Research Reagents), donkey anti-mouse AlexaFluor 594 (1:1500, Life Technologies), and goat anti-rabbit FITC (1:100, Jackson ImmunoResearch).

Primary cortical astrocytes were also processed in a similar manner to visualize the localization of TSP-1 at 7 *DIV*. The following antibodies were used to label the astrocytes: mouse monoclonal thrombospondin-1 (A6.1; 1:100; ThermoFisher Scientific), polyclonal rabbit anti-GFAP (1:500, Dako), donkey anti-mouse AlexaFluor 594 (1:1500,

Life Technologies), and goat anti-rabbit FITC (1:100, Jackson ImmunoResearch).

Synaptic Puncta Analysis

Images were acquired using a Zeiss AxioImager.M2 at 40x magnification configured with the ApoTome.2 and Zeiss Zen Blue image acquisition software. Synapses were identified by the co-localization of the pre-(synaptophysin) and post-synaptic (PSD-95) puncta, using a custom written plug-in for ImageJ. After selecting a 50 μm segment along the dendrite, the image was processed using the above plug-in. Briefly, low frequency background from each channel (red and green) of the image was removed with the rolling ball background subtraction algorithm. Then, the puncta in each single-channel was **'**masked**'** by thresholding the image so that only puncta remained above threshold. Puncta were then identified in each channel by the **"** Puncta Analyzer**"** plug-in for Image J. Co-localization of the puncta in each channel was identified when the distance between the centers of the two puncta was less than the radius of the larger puncta. The number of co-localized puncta was then recorded as synapses. Two to three independent experiments were performed. Approximately 20-25 neurons from at least two coverslips were analyzed per condition/group. For each independent culture, 45-50 (50 μm long) segments along the dendrites were evaluated for synaptic protein co-localization. Multiple dendritic segments were sampled within a given neuron. The PSD95/synaptophysin-immunoreactive puncta along the dendrites in each photomicrograph were counted manually and normalized by dendrite length. The photography and analysis of immunoreactivity were conducted in an investigator-blinded

manner.

Measurements of TSP-1 Expression and Release

TSP-1 levels were determined in astrocyte cultures and astrocyte-conditioned medium (ACM). Confluent astrocyte cultures were incubated with 0.05% Trypsin-EDTA for 5 min at 37°C. Once cells were fully lifted, media with serum was added to stop the digestion. The cells were centrifuged at 250 g for 5 min, washed with ice-cold PBS, and lysed with cell lysis buffer containing 50mM Tris-HCl, 150mM NaCl, 1% Triton-X and 5mM EDTA with protease inhibitors (Roche). The lysates were collected in Eppendorf tubes, centrifuged at 12000 rpm in an Eppendorf microcentrifuge for 20 min at 4ºC, and the supernatants were used to determine the intracellular concentration of TSP-1. Aliquots of ACM from the same cultures were also processed to determine secreted, extracellular levels of TSP-1. TSP-1 protein measurements were determined using the Mouse Thrombospondin-1 ELISA kit (Biotang, Inc) following the vendor's instructions. Sample protein content normalization was based on total protein concentration, which was determined for each sample by Bradford assay.

Thrombospondin-1 Treatments

To assess the neuromodulatory effect of exogenous TSP-1 on spine development, hippocampal neuronal cultures derived from *Fmr1* KO mice were treated with human recombinant TSP-1 (R&D System) to stimulate spine formation. Recombinant TSP-1 was added to the neuronal media one day after plating, and replenished every 3 days for 17

days. A dose concentration of 250 ng/ml was used to restore TSP-1 levels [27]. Control cultures were incubated with heat-inactivated TSP-1 (TSP1-HI, 100°C for 5 min), or gabapentin (GBP; 32 μM) [24] to inhibit astrocyte induced spine and synapse formation.

Statistics

Statistics were performed using GraphPad Prism 5.0. Differences were detected using a Student's t-test or one-way analysis of variance (ANOVA). Following one-way ANOVA, post hoc differences were resolved using the Bonferroni correction. A p-value of <0.05 was considered significant. All values are expressed as mean ± SEM; n = number of neurons (unless otherwise specified); N = number of experiments.

4.2.4. Results

Fmr1 knockout neurons display dendritic spine and synaptic abnormalities relative to their wildtype counterparts.

Previous reports have established the critical role of astrocytes in FXS [9,10]; however, the role of astrocytes in regulating dendritic spine formation has not been elucidated. To investigate morphological differences, we first examined dendritic spine subtypes and length in dissociated hippocampal neuronal cultures labeled with DiI from *Fmr1* knockout (KO) and wildtype (WT) mice at 17 days *in vitro* (*DIV*). DiI is a fluorescent carbocyanine membrane dye that effectively illuminates the cellular architecture of neurons and individual processes, including dendrites and spines [31]. The morphological analysis of the neurons was conducted at 17 *DIV* to provide sufficient time for spine development and maturation, and circumvent the loss of neuronal processes due to the instability of long-term cultures. For simplicity, we categorized both the stubby and mushroom-shaped (mature) spines as ‘‘stubby’’, and thin and filopodium spines as ‘filopodia-like’ (immature) spines. Dendritic spine length of each individual dendritic spine was measured from its point of insertion in the dendritic shaft to the distal tip of the spine, while rotating the image in 3D. Fig 4.1A shows representative images of neurons and dendritic segments from *Fmr1* KO and WT mice.

Consistent with findings from the literature, we found a clear difference in dendritic spine length between WT and *Fmr1* KO hippocampal neurons. *Fmr1* KO neurons displayed remarkably longer spines (~1.5 fold increase) relative to their WT counterparts at 17 *DIV* (Fig 4.1B and 4.1C, $p<0.01$). The structural profiles of the spines

also differed considerably between the WT and *Fmr1* KO hippocampal neurons. *Fmr1* KO neurons displayed a higher density of immature thin/filopodia-like spines (Fig 4.1D, $p<0.05$), and a striking decrease in the number of mature stubby subtypes compared to WT hippocampal neurons (Fig 4.1E, $p<0.05$). The increased prevalence of elongated spines, characteristic of immature synapses, suggests that dendritic development is delayed in the *Fmr1* KO neurons. Notably, a slight decrease in the overall spine density was observed in the F*mr1* KO neurons; however, the differences were not statistically significant ($p>0.05$, Fig S4.1).

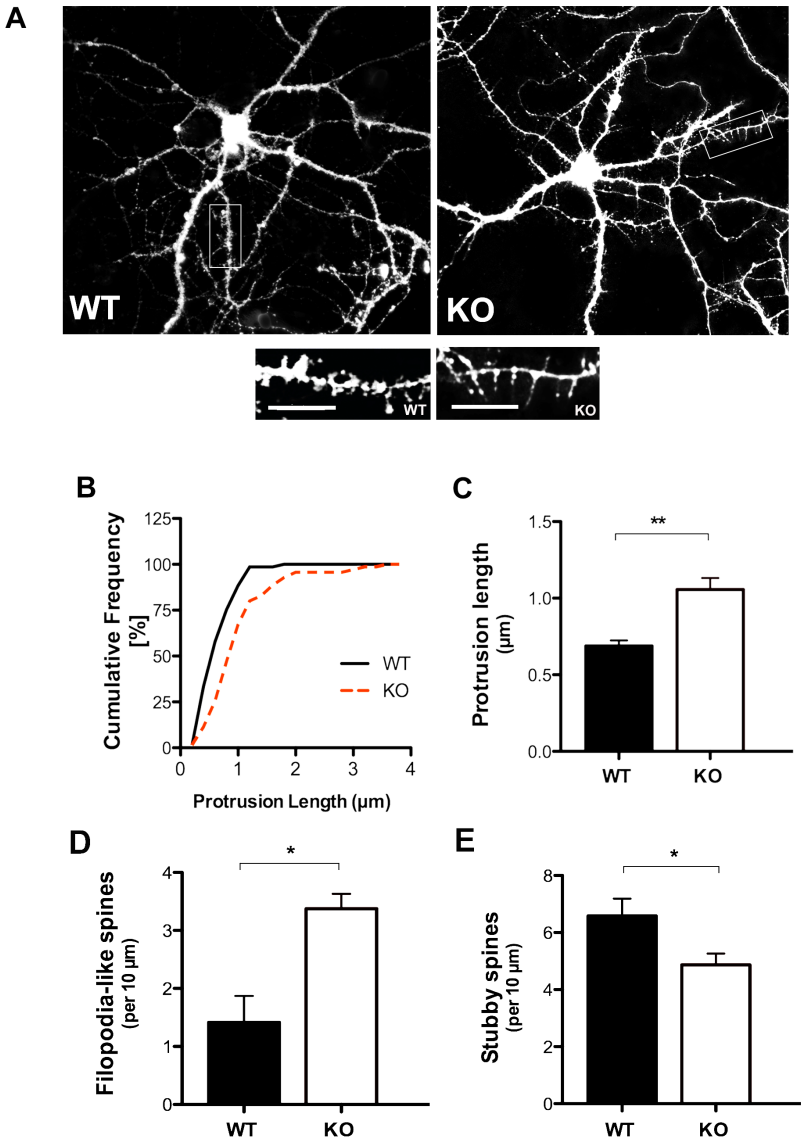

Figure 4.1: Spine length is altered in *Fmr1* KO hippocampal neurons at 17 *DIV*.

(A) Representative images of DiI labeled WT (left panel) and *Fmr1* KO (right panel) neurons highlighting dendrites and spines. Inset is an example of a 50 µm segment used for morphological analysis and quantification. Note the high prevalence of filopodium-like spines in the *Fmr1* KO dendritic segment (right panel) relative to the WT segment

(left panel). **(B)** Cumulative frequency distribution of spine lengths comparing *Fmr1* KO and WT neurons. **(C)** *Fmr1* KO neurons display increased dendritic spine length compared to their WT counterparts. **(D)** Assessment of spine morphology in *Fmr1* KO neurons shows a significant increase in the number of filopodia-like spines and **(E)** a reduction in the number of stubby spines. Data was analyzed by Student's t-test. Data are presented as the mean ± SEM, *p<0.05, **p<0.01; n = 75 neurons, N = 3 independent experiments. Scale bars: 10 μm.

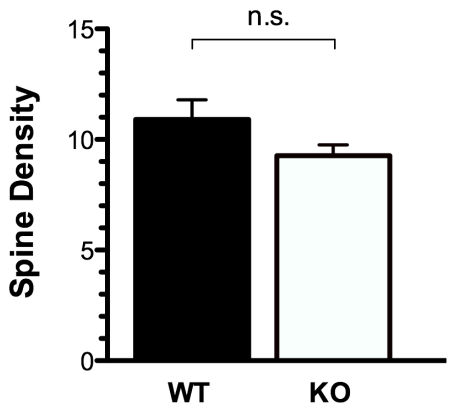

Supplementary Figure S4.1: Quantification of spine density between WT and *Fmr1* KO hippocampal neurons. *Fmr1* KO neurons display a decrease in spine density compared to WT neurons; although no significant statistical differences were detected (p>0.05).

Next, we sought to examine the role of FMRP in regulating excitatory synapse formation. The establishment of neural circuitry requires vast numbers of synapses to be generated during a specific window of brain development. We used immunocytochemistry with antibodies directed at synaptophysin (a presynaptic protein that exists as part of the synaptic vesicle membrane) and PSD-95 (a postsynaptic protein that forms part of the postsynaptic density) to identify synaptic protein aggregates in neurons at 17 *DIV*. Synapses were detected by yellow puncta (spots of intense staining), denoting the co-localization of immunoreactivity to pre- and postsynaptic protein markers. Each yellow punctum corresponded to the structural site of a single functional synapse (Fig 4.2A and B). At 17 *DIV,* the clustering of both pre- and postsynaptic proteins was decreased with less co-localization of puncta observed in *Fmr1* KO neurons relative to their WT counterparts (Fig 4.2C, $p<0.05$). These results suggest that excitatory synapse formation is altered in *Fmr1* KO hippocampal neurons.

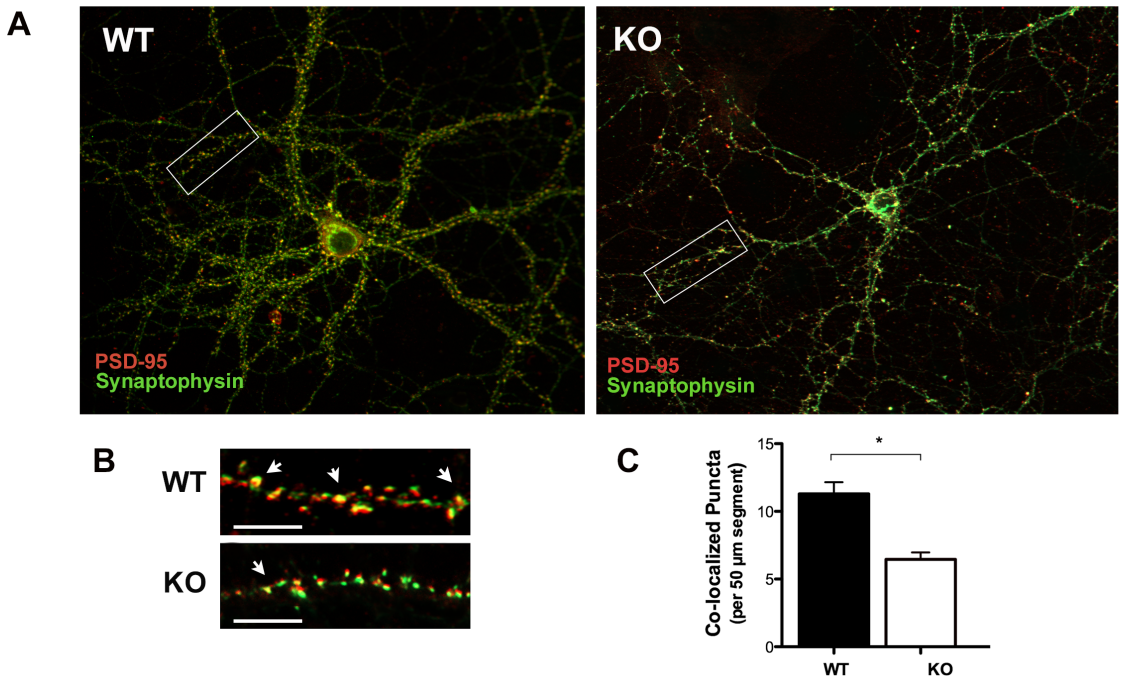

Figure 4.2: Quantification of excitatory synapse formation at 17 *DIV*.

(A) Representative images of WT and *Fmr1* KO neurons visualized using immunofluorescence. Inset is an example of a 50µm segment used for excitatory synapse quantification. **(B)** Excitatory synapses are denoted by the arrows representing the co-localization of pre-(synaptophysin, SYN, 1:250, green) and postsynaptic (PSD-95, 1:200, red) puncta (arrows). Synapses were identified using a custom written plug-in for ImageJ (http://rsbweb.nih.gov/ij/) – "Puncta Analyzer". **(C)** At 17 *DIV*, *Fmr1* KO neurons exhibit a reduction in the number of co-localized puncta relative to their WT counterparts. Data was analyzed by Student's t-test. Data are presented as the mean $\pm$ SEM, *$p<0.05$; $n = 75$, $N = 3$.

WT hippocampal neurons exhibit morphological spine and synaptic deficits and when grown with an Fmr1 KO astrocyte feeder layer.

Membrane-bound factors are known participants in synaptogenesis; however, the contributions of soluble factors on neuronal development in FXS have not been elucidated. To explore the possible role of diffusible factors secreted by astrocytes, we plated hippocampal neurons on glass coverslips positioned below a feeder layer of astrocytes (AFL), facilitating the exposure of soluble factors to neurons through a membrane without direct contact between these two cell types (Fig 4.3A). Using this non-contact co-culture approach, we found that deficits in FMRP in astrocytes affected the development of spines at 17 *DIV*. Although no significant effects were observed on spine density, we found that WT neurons exhibited morphological deficits when grown in the presence of an *Fmr1* KO feeder layer. WT hippocampal neurons cultured below an *Fmr1* KO feeder layer displayed abnormally longer spines (Fig 4.3B, ~1.6 fold increase) than WT neurons grown independently (Fig 4.3C, $p<0.001$) or with a WT feeder layer (Fig 4.3C, $p<0.001$). In addition, WT neurons exhibited a striking increase in the density of immature filopodia-like spines (Fig 4.3D, $p<0.001$) when cultured in combination with an *Fmr1* KO feeder layer. WT hippocampal neurons grown in the presence of an *Fmr1* KO feeder layer also presented with a reduced proportion of stubby spines that are typically indicative of mature spines (Fig 4.3E, $p<0.001$). Notably, WT neurons supplemented with a feeder layer of normal astrocytes displayed the highest proportion of stubby spines. Therefore, the increased frequency of 'immature' thin spine phenotypes, reminiscent of immature spine precursors, filopodia, suggests that *Fmr1* KO astrocytes alter the

appropriate formation of dendritic spines in WT neurons. Further, the observed spine phenotypes in the WT neurons cultured with the *Fmr1* KO feeder layer resemble the structural deficits observed in *Fmr1* KO neurons, demonstrating a role for secreted signals on spine development.

Next, we sought to ascertain the ability of ACM or astrocyte-feeding layers to induce the development of synapses in neurons (Fig 4.3F). WT neurons grown in the presence of an *Fmr1* KO feeder layer displayed significantly reduced co-localization relative to WT neurons cultured alone ($p<0.05$) or with a WT AFL ($p<0.001$). These results demonstrate that synaptic protein clustering is impaired when WT neurons are grown with a feeder layer derived from *Fmr1* KO astrocytes.

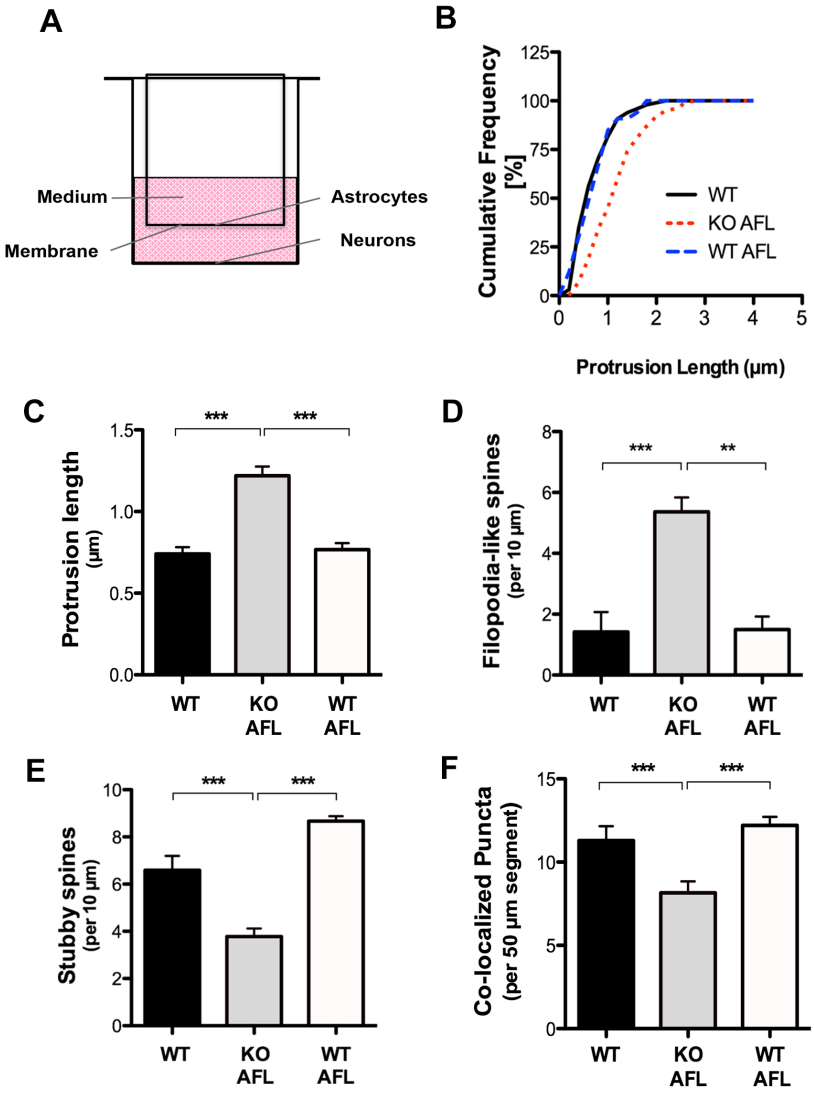

Figure 4.3: WT hippocampal neurons display morphological spine deficits when grown in the presence of an *Fmr1* KO astrocyte feeder layer.

(A) Schematic illustrating the indirect astrocyte-neuron co-culture set-up. Astrocytes were grown in a cell culture insert with a permeable membrane facing the neurons and sharing the same, defined medium. **(B)** Cumulative frequency distribution of spine

lengths comparing WT neurons grown independently and in co-culture with WT or *Fmr1* KO astrocyte feeder layers (AFL) at 17 *DIV*. **(C)** WT hippocampal neurons grown without direct contact with *Fmr1* KO astrocytes present with longer spines. (**D)** Assessment of spine morphology in *Fmr1* KO AFL/WT neuron co-cultures indicates a significant increase in the density of filopodia-like spines and **(E)** a decreased density of stubby spines. Spine density represents the average number of spines scored in a 10 μm dendritic segment. **(F)** *Fmr1* KO AFL/WT neuron co-cultures exhibit a reduction in the number of co-localized synaptic puncta relative to WT neurons cultured alone or with a WT AFL ($p<0.01$). Excitatory synapses represent the average number of co-localized puncta scored in a 50 μm dendritic segment. One-way ANOVA with Bonferroni correction was used to analyze the data. Data are presented as the mean $\pm$ SEM, $^{**}p<0.01$, $^{***}p<0.001$; n = 50 neurons per group, N = 2 independent experiments.

Spine and synaptic protein abnormalities are prevented in Fmr1 KO neurons by WT astrocyte conditioned media or a WT feeder layer.

Given that *Fmr1* KO astrocytes impact the dendrite morphology of cultured WT hippocampal neurons, we tested whether secreted molecules from WT astrocytes are able to prevent the abnormal spine development in *Fmr1* KO hippocampal neurons. We analyzed the structural morphology of dendritic spines in *Fmr1* KO neurons cultured with either conditioned media or a feeder layer derived from WT astrocytes. The application of ACM to cultures has been reported to be equally effective in inducing synapses as a feeder layer of astrocytes [32]. Synaptogenic factors are constitutively released from astrocytes grown in isolation in culture and do not require a neuronal signal to stimulate release [33,34]. Our results showed that *Fmr1* KO neurons displayed an overall increase in spine length (Fig 4.4A) compared to *Fmr1* KO neurons cultured with WT ACM ($p<0.05$) or a WT feeder layer ($p<0.05$). Remarkably, aberrations in spine length were mitigated in the *Fmr1* KO neurons when supplemented with either WT ACM by -1.2 fold (Fig 4.4B, $p<0.05$) or a WT feeder layer by -1.4 fold (Fig 4.4B, $p<0.01$). Furthermore, WT ACM significantly reduced the frequency of immature-appearing spine phenotypes in the *Fmr1* KO neurons (Fig 4.4C, $p<0.01$), restoring the density of unstable spine to normal levels. Similarly, a WT feeder layer considerably decreased the number of filopodia-like spines ($p<0.05$). WT ACM also promoted spine maturation by inducing the formation of stubby/mushroom spines in the *Fmr1* KO neurons following 2.5 weeks in culture (Fig 4.4D, $p<0.05$). Likewise, *Fmr1* KO neurons grown with a WT feeder layer significantly increased the density of stubby spines ($p<0.01$). Together, these results

suggest that astrocyte-mediated signaling is an important regulator of spine development and is sufficient to rescue deficits in neuronal connections associated with FXS.

Next, given that soluble factors derived from FMRP-deficient astrocytes affect excitatory synapse formation, we investigated whether normal astrocytes could prevent the alterations observed in *Fmr1* KO neurons. Consistent with previous studies showing that ACM induces synapse formation [17], we found that the addition of WT ACM to *Fmr1* KO neurons significantly increased the number of synaptophysin/PSD95 co-localized puncta per 50 μm length of dendrite (Fig 4.4E, $p<0.05$). Our results also showed that a greater number of synaptic contacts were formed in *Fmr1* KO neurons supplemented with a WT feeder layer ($p<0.01$). Together, these results demonstrate that synaptic protein clustering in *Fmr1* KO neurons can be restored to normal levels in the presence of FMRP-expressing astrocytes and further suggest a role for secreted factors in regulating synaptic development.

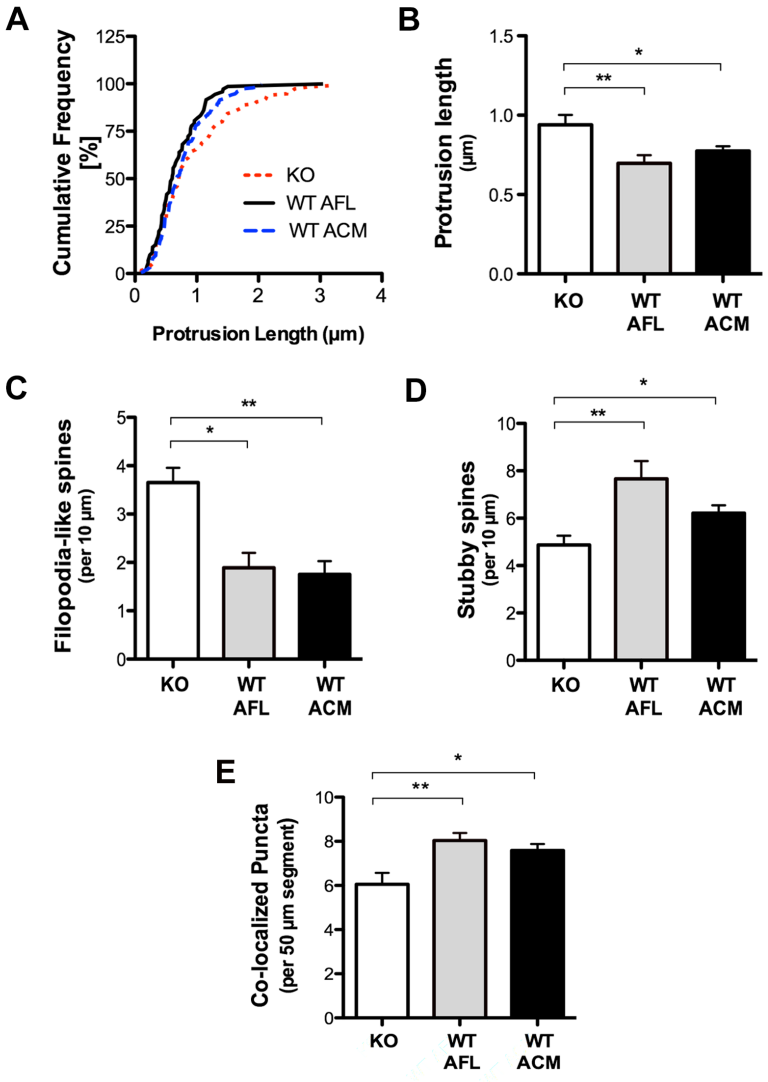

Figure 4.4: Morphological abnormalities in *Fmr1* KO hippocampal neurons are corrected by WT astrocytes with in-direct co-culture.

(A) Cumulative frequency distribution of spine lengths comparing *Fmr1* KO neurons grown in the presence of a WT AFL or supplemented with WT ACM at 17 *DIV*. **(B)** Spine length is significantly reduced in *Fmr1* KO neurons cultured with WT ACM or WT AFL. **(C)** Co-cultures with WT AFL or WT ACM reduced the proportion of immature

spine phenotypes in the *Fmr1* KO neurons. **(D)** Alternatively, WT ACM and WT AFL induced an increase in the formation of mature spines. **(E)** *Fmr1* KO neurons supplemented with WT ACM increases the co-localization of excitatory pre- and postsynaptic proteins, synaptophysin and PSD-95. Similarly, WT AFL/*Fmr1* KO neuron co-cultures enhance the number of co-localized puncta. One-way ANOVA with Bonferroni correction was used to analyze the data. Data are presented as the mean $\pm$ SEM, *$p<0.05$, **$p<0.01$; $n = 50$ neurons, $N = 2$ independent experiments.

Intracellular and extracellular TSP-1 expression levels are decreased in Fmr1 KO astrocytes.

TSP-1 is a matricellular protein synthesized and released by astrocytes during early development of the nervous system [35,36]. TSP-1 promotes neurite outgrowth and survival [37-39], neuronal migration [40] and synaptogenesis [17] *in vivo* and *in vitro*. It participates in synaptic remodeling following injury [41] and is required for synaptic and motor recovery after stroke [42], suggesting that TSP-1 also participates in neuronal plasticity. Since TSP-1 has been identified as a major contributor to astrocyte-regulated excitatory synapse formation [17,43], we determined if the expression of TSP-1 was altered in FXS cortical astrocytes. Here, we found relatively high levels of TSP-1 expression in cortical astrocytes (Fig 4.5A). However, quantification of TSP-1 protein levels by ELISA showed marked reductions in both cellular lysates and conditioned media derived from *Fmr1* KO astrocytes. In fact, *Fmr1* KO astrocytes express 5% less cellular TSP-1 compared to their WT counterparts (Fig 4.5B: 49.98 ± 13.24 ng/ml; $p<0.05$); and secrete 20% less TSP-1 into the media relative to their WT counterparts (Fig 5C: 208.12 $\pm$ 40.77 ng/ml; $p<0.05$). These results demonstrate that TSP-1 expression and release are both altered in *Fmr1* KO astrocytes, suggesting that a lack of FMRP expression prevents normal TSP-1 expression in cortical astrocytes during development.

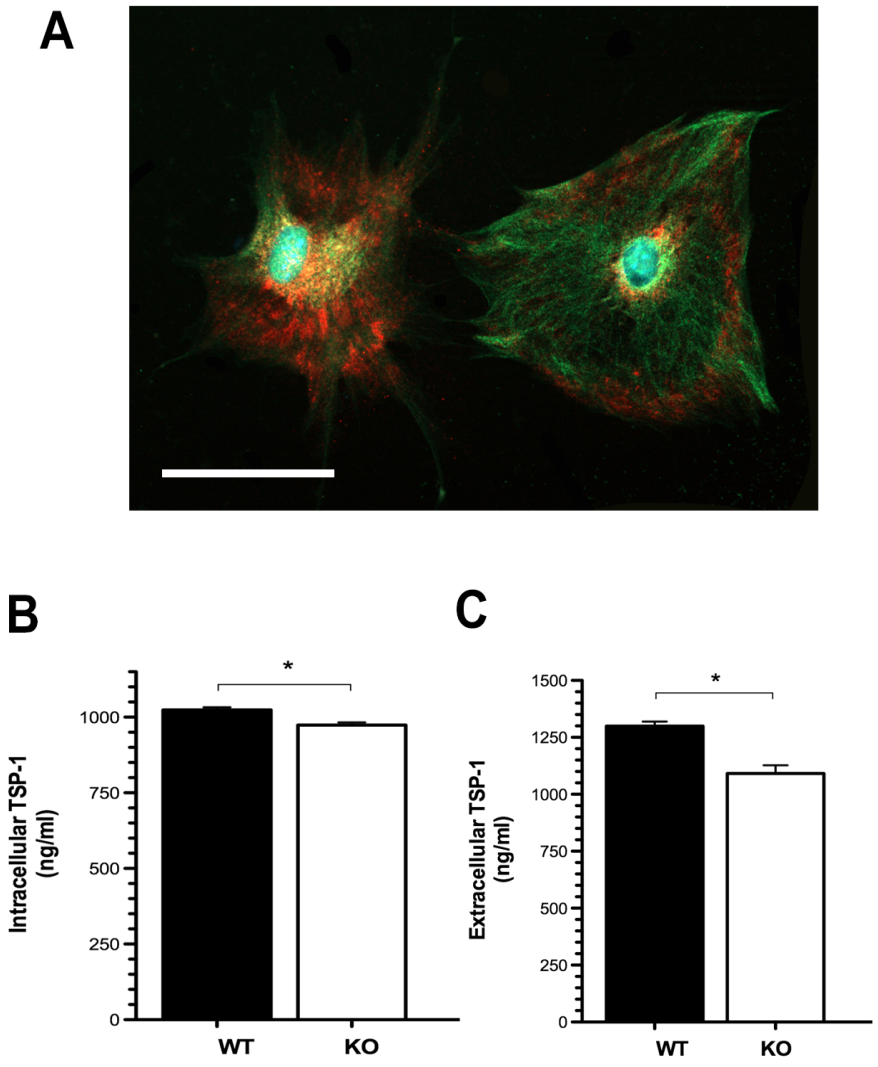

Figure 4.5: Reduced TSP-1 levels in cultured FXS cortical astrocytes.

(**A)** Representative staining of cultured cortical astrocytes co-labeled with GFAP and TSP-1. At 7 *DIV*, the cells were fluorescently labeled with anti-GFAP (glial fibrillary acidic protein, green) to visualize astrocytes and anti-TSP-1 (thrombospondin-1, red) to identify the intracellular expression of TSP-1 using a 20x objective. Nuclei were counterstained with DAPI (blue). Cultured cortical astrocytes express abundant levels of

TSP-1 at 7 *DIV*. Scale bars: 50 μm. (**B)** Quantification of intracellular TSP-1 protein levels by ELISA in cellular lysates. *Fmr1* KO astrocytes express lower levels of cellular TSP-1 compared to their WT counterparts. (**C)** Quantification of extracellular secreted TSP-1 in astrocyte-conditioned media. Measurements in TSP-1 protein levels in ACM revealed marked reductions in secreted TSP-1 by *Fmr1* KO astrocytes. Data was analyzed by Student's t-test. Data are presented as the mean $\pm$ SEM, *$p<0.05$; n=5 cultures per genotype.

Addition of TSP-1 corrects abnormal dendritic spine development and excitatory synapse formation in Fmr1 KO neurons.

Given the disruption in TSP-1 expression in *Fmr1* KO astrocytes and the aberrant growth of neurons in the presence of these cells, we examined the effects of exogenous TSP-1 on dendritic spine morphology in cultured hippocampal neurons. *Fmr1* KO hippocampal neurons were treated with human recombinant (rTSP-1; dosage of 250 ng/ml) to stimulate spine formation [27]. Treatment with TSP-1 was well tolerated by the hippocampal neurons, with no neurotoxicity at concentrations as high as 1000 ng/ml. Interestingly, the addition of rTSP-1 to *Fmr1* KO neurons mimicked the restorative effects of a WT feeder layer or WT ACM. Prior to rTSP-1 treatment, an increased frequency of long, thin spines were observed in *Fmr*1 KO neurons (Fig 4.6A and B, $p<0.01$). Following TSP-1 treatment, spine protrusion length was significantly reduced by 50% in *Fmr1* KO neurons (Fig 4.6B, $p<0.001$). Treatment with rTSP-1 decreased the proportion of thin spines (Fig 4.6C, $p<0.05$) and promoted the formation of mature spines in 2.5 week-old cultures (Fig 4.6D, $p<0.05$). To test whether the reduction in astrocytic TSP-1 was indeed responsible for the aberrant spine morphology, cultured neurons were treated with either heat inactivated TSP-1 (TSP1-HI) or rTSP-1 co-incubated with gabapentin (GBP), a competitive TSP-1 receptor antagonist. Notably, morphological spine anomalies were not corrected in *Fmr1* KO neurons treated with TSP1-HI or rTSP-1 (250 ng/ml) with gabapentin (GBP; 32 ug), further confirming the specific role of active TSP-1 on *Fmr1* KO hippocampal neurons.

To elucidate the neuromodulary effects of TSP-1 on excitatory synapse formation,

Fmr1 KO neurons were treated with a dose of 250 ng/ml of rTSP-1. At 17 *DIV*, an increase in the co-localization of pre-and postsynaptic puncta was observed when *Fmr1* KO neurons were treated with rTSP-1 (Fig 4.6F and G; $p<0.001$). Therefore, these results support the concept that rTSP-1 can increase the number of both presynaptic and postsynaptic protein clusters, contributing to the recovery of the alterations in synaptic protein expression in *Fmr1* KO neurons.

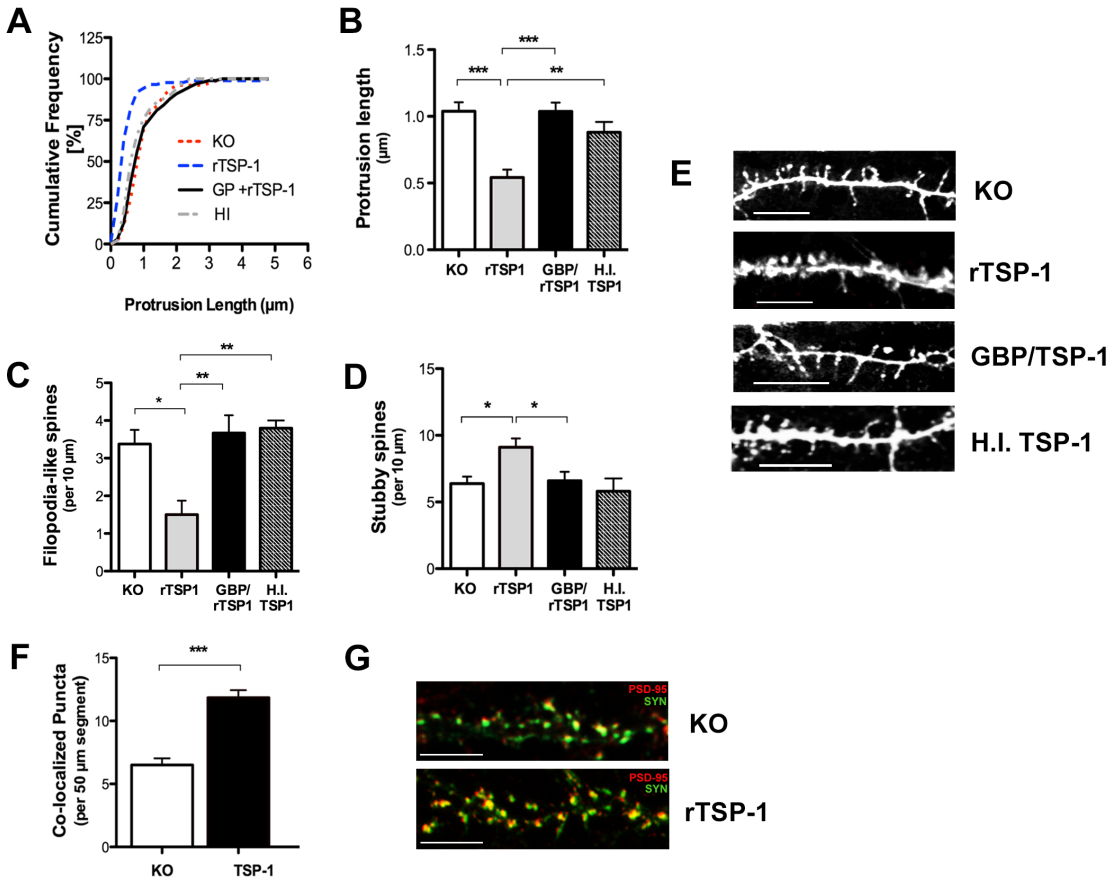

Figure 4.6: TSP-1 prevents spine and synapse alterations in *Fmr1* KO neurons.

Analysis of the effects of TSP-1 administration on dendritic spine morphology in *Fmr1* KO hippocampal neurons at 17 *DIV*. Continuous treatment with recombinant TSP-1 (250 ng/ml) averted the spine alterations in *Fmr1* KO neuronal cultures. **(A)** Cumulative frequency distribution of spine lengths. **(B)** rTSP-1 induced a significant reduction in spine length and **(C)** the density of filopodia-like spines in the *Fmr1* KO neurons. **(D)** A marked increase in the density of stubby spines was observed following the application of rTSP-1. Heat-inactivated human recombinant TSP-1 (HI-TSP1) or gabapentin (GBP; 32

ug) in combination with rTSP-1 did not exert a neuroprotective effect on spines. One-way ANOVA with Bonferroni correction was used to analyze the data. All data are expressed as mean ± SEM. *$p<0.05$; n = 75 neurons per group, N = 3 independent experiments. **(E)** Dendritic segments labeled with fluorescent DiI to illustrate typical spine morphologies found in *Fmr1* KO neurons and following treatment with exogenous TSP-1, GBP/TSP-1 or HI-TSP-1, respectively. Scale bars: 10 μm. **(F)** Excitatory synapse formation is normalized in *Fmr1* KO following rTSP-1 treatment. Data was analyzed by Student's t-test. Data are presented as the mean ± SEM, ***$p<0.001$; n = 75 neurons per group, N = 3 independent experiments. (G) Double immunofluorescence of dendritic segments with PSD-95 (red) and synaptophysin (green) to identify excitatory synapses. Scale bars: 10 μm.

4.2.5. Discussion

Dendritic spine abnormalities have long been recognized as structural correlates of learning impairments in FXS and various forms of ASDs [44,45]. However, the origin and mechanisms involved in spine dysgenesis are not well understood. In contrast to the expression of FMRP in neurons, relatively little is known about the function of FMRP in glial cells during CNS development. In these particular experiments, we investigated the role of astrocytes in the development of the abnormal dendritic spine morphology and synaptic aberrations seen in FXS. Primary hippocampal neurons were grown in a non-contact co-culture set-up with astrocytes for 17 *DIV*, allowing for the continuous exchange of molecules between both cell types via the shared defined medium. In this setting, we focused on the contribution of secreted CNS matricellular molecules to neuronal development and synapse formation using an *Fmr1* knockout (KO) Fragile X mouse model. Here, we show that: i) *Fmr1* KO astrocytes display deficits in TSP-1 levels; ii) An altered expression of astrocyte-secreted factors plays a significant role in dendritic spine dysgenesis and excitatory synapse formation; iii) Exogenous TSP-1 reverts *Fmr1* KO astrocyte-mediated spine and synaptic alterations to normal levels.

Role of Astrocytes in Fragile X Neurobiology

Astrocytes are important regulators of neuron growth and maturation, and are key players in the abnormal neurobiology of a number of developmental disorders, including FXS [27,46,47]. Several studies have recently linked the absence of FMRP in astrocytes to abnormal neuronal structure and function in FXS. Our previous work showed that the

loss of FMRP in astrocytes causes abnormal dendritic morphology, including aberrant dendritic branching and dysfunctional synapse development [9,10]. It has also been shown that the selective loss of FMRP from astrocytes (but not neurons) leads to the reduced expression of the glutamate transporter GLT-1 (EAAT2) and subsequent reduced glutamate uptake by these cells [48]. In this study, we confirmed that synapse formation between neurons is driven by factors released from astrocytes, and astrocytes devoid of FMRP affect proper spine development. More importantly, factors derived from normal astrocytes protect the loss of synapse formation, decrease the density of immature spines, and promote mature spine formation in *Fmr1* KO neurons.

Under normal conditions, the release of soluble factors from astrocytes guide neurite growth, synapse formation and maturation [34,49]. In FXS, dendritic contacts fail to mature and the result is aberrant neural connectivity. We hypothesized this was due to a deficit in astrocyte-derived factors since *Fmr1* KO astrocytes grown with WT neurons lacking direct contact contributed to the abnormal spine morphology, evidenced by a greater number of longer, thinner spines. In support of this, a recent study by Yang et al. [50] showed that elevated levels of neurotrophin-3 in *Fmr1 KO* astrocytes partially altered dendritic growth in neurons. Therefore, we aimed to identify potential additional astrocyte-derived soluble factors that contribute to the spine development and maturation impairment in FXS. Our study revealed that *Fmr1* KO astrocytes show a notable deficit in the expression of soluble factor TSP-1, resulting in dendritic spine dysgenesis in *Fmr1* KO neuronal cultures that can be corrected with the exogenous addition of TSP-1.

Thromobspondin-1 Contributes to Astrocyte-Regulated Synapse Formation

TSPs have been previously identified as important CNS synaptogenic molecules. TSP-1 and -2 are transynaptic organizers, highly expressed by immature astrocytes, which strongly promote structural synapse formation [51]. In particular, they act as permissive switches that time CNS synaptogenesis and enable neuronal molecules to assemble into synapses within a specific window of CNS development. This narrow developmental window typically coincides with the initiation of nascent synaptic contacts between dendrites and axons. Therefore, TSP-1 and -2 serve a transient function and are not required for maintenance of synapses in the adult. Both *in vitro* and *in vivo* studies have demonstrated the capacity of TSPs to increase synapse number, promote the localization of synaptic molecules, and refine the pre- and postsynaptic alignment [17,52]. Furthermore, TSP1/2-deficient mice display a significant decrease in the frequency of excitatory synapses [17]. TSPs have also been shown to regulate presynaptic function by limiting presynaptic release at glutamatergic synapses, serving as a protective mechanism against excitotoxicity [25]. Recently, two transmembrane molecules were uncovered in mediating TSP-induced synaptogenesis. Firstly, neuroligin 1 interacts with TSP-1 and mediates the acceleration of synaptogenesis in young hippocampal neurons [26]. Secondly, α2δ-1, a subunit of the L-type Ca^{2+} channel complex (LTCC), was also identified as the postsynaptic receptor of TSP in excitatory CNS neurons [24]. Interaction between TSP and α2δ–1 sequentially recruits synaptic scaffolding molecules and initiates synapse formation [53]. Several other known receptors for TSP include the CD47 integrin- associated protein (CD47/IAP), a variety of integrins, and the low-density

lipoprotein receptor-related protein LRP1; however, the role of each of these interacting proteins have not been elucidated.

Deficits in TSP-1 Affect Synapse and Dendritic Spine Development

Our findings revealed a decrease in TSP-1 protein expression in cellular lysates and in astrocyte-conditioned media from *Fmr1* KO astrocytes, which suggests that the lack of TSP-1 derived from FMRP-deficient astrocytes interferes with proper spine development and synapse formation in FXS. Likewise, deficits in TSP-1 expression in astrocytes has also been implicated in Down Syndrome (DS) from human brain tissue samples and DS cultured astrocytes [27]. In a study by Jayakumar et al. [54], a shortage of astroglial-derived TSP-1 contributed to synaptic dysfunction in hepatic encephalopathy, which was linked to a decrease in the neuronal expression of synaptophysin, synaptostagmin, and PSD-95, all of which are critically involved in maintaining the integrity of glutamatergic synapses. In line with these findings, we observed that a decrease in TSP-1 expression resulted in the reduced co-localization of pre- and post-synaptic synaptophysin and PSD-95 in *Fmr1* KO neurons.

Spine morphology is linked to synapse function and mushroom-shaped spines are considered to represent the most mature and stable spine morphology [55,56]. Several categories of spines have been identified based on their shape and size, including thin, stubby, cup, and mushroom-shaped. Recent studies suggest that excitatory synapses are a component of mushroom-shaped dendritic spines [57]. Thus, the increase in mushroom-shaped spines in response to TSP-1 treatment is consistent with our findings that TSP-1

stimulates the formation of excitatory synapses. In our study, we also found that spine length, a measure of synaptic immaturity, was increased in *Fmr1* KO mice, suggesting a delay in the development of spines. The prevalence of thin, elongated dendritic spine morphology in *Fmr1* KO mice is reminiscent of that observed during early synaptogenesis [58] in the developing brain, as well as the morphology seen following sensory deprivation [59,60]. The increase in immature-appearing spines could be due to augmented spine turnover [60], which fails to decrease in the early postnatal weeks in FXS [5]. Alternatively, the abundance of immature-looking spines in the *Fmr1* KO mice could be caused by a failure of a subset of spines to mature.

Interestingly, we did not observe significant differences in overall spine density between the WT and *Fmr1* KO neurons. Similar studies in *Fmr1* KO mice have also found normal hippocampal spine densities [61] and individual spines with longer lengths [62]. In contrast, others have reported decreased spine density in the *Fmr1* KO mice compared to WT littermates [63,64] and spines of normal length [63]. However, the discrepancies are likely attributed to the use of different staining and quantification methods of spines, and the choice of tissue source (cultured hippocampal neurons versus *in vivo* or *ex vivo* brain tissue). As we observed for hippocampal neurons, Braun et al. [62] also reported a lower abundance of excitatory synapses in Fmr1 KO hippocampal neurons relative to WT at 2 weeks in culture. The failure of excitatory synapse maturation has also been noted in cortical neurons of *Fmr1* KO mice [65-67], as well as in *Fmr1* KO cerebellar granule cells [68].

Severe learning deficits have been associated with synaptic dysfunction in FXS

and intellectual disabilities [69-71]. Here, we showed that deficits in the formation of dendritic spines in *Fmr1* KO neurons could be normalized with conditioned media or a feeder layer derived from normal astrocytes. Similarly, we demonstrated that the addition of exogenous TSP-1 to neuronal cultures markedly promoted the formation of mature (mushroom-shaped) dendritic spines and restored the number of synaptic protein clusters in *Fmr1* KO neurons comparable to the level that of WT neurons at 17 *DIV*. Notably, the application of ACM + TSP-1 has been shown to increase synaptic puncta to the same extent as either ACM or TSP-1 alone, indicating that TSP-1 alone is sufficient to recover synapse formation [17]. Mechanistically, TSP-1 may exert its restoring role in *Fmr1* KO neurons by specifically counteracting the loss in FMRP on the dendritic spines that are immature as a result of FMRP loss. Therefore, these findings identify TSP-1 as a critical astrocyte-secreted factor that modulates spine morphology and provide evidence that astrocytes are important contributors to synaptogenesis within the developing CNS. These results further reinforce that an absence of FMRP delays spine stabilization and maturation in FXS mice.

Conclusion

Abnormal or 'diseased' astrocytes are known regulators of many developmental disorders of the CNS, including FXS. Our findings highlight the important role for FMRP expression in astrocytes during the early postnatal weeks of synaptic development. Our results suggest that defects in the secretion of astrocyte-derived molecules, specifically TSP-1, during a crucial window of development contributes to the abnormal neurobiology seen in FXS. Neurons typically undergo a developmental switch to be able

to respond to soluble synaptogenic signals from astrocytes, and this switch can be induced by astrocytes [16,72]. In cultured hippocampal neurons, astrocytes have been shown to be a critical component for appropriate dendritic spine morphology and the ability of neurons to form synapses [73-76]. However, the full extent of the molecular interactions that govern indirect or contact-mediated synaptogenic signaling between astrocytes and neurons is not clear in FXS. For instance, WT neurons cultured with an astrocyte feeder layer from *Fmr1* KO mice exhibit less mature spines than WT neurons cultured alone. These results suggest that *Fmr1* KO astrocytes could potentially release inhibitory substances that prevent normal spine development. Given that profound changes in both excitatory and inhibitory neurotransmission have been reported in FXS [77], the mechanisms involving a lack of factor and/or the exertion of inhibitory effects should be differentiated and taken into consideration in future studies. Further, the potential therapeutic role of astrocyte-derived TSPs in excitatory synaptogenesis and their relevance to learning and memory in FXS will be an exciting avenue of future investigation. Additional studies exploring the contributions of other astrocyte-secreted factors and TSP family members may also provide important insights into the underlying mechanisms of FXS.

4.2.6. Acknowledgements

We genuinely thank Dr. Angela Scott for her editorial work on this manuscript. This work was supported by the Natural Sciences and Engineering Research Council of Canada (NSERC), Fragile X Research Foundation of Canada and the Brain Canada/Azrieli Neurodevelopmental Research Program.

4.2.7. References

1. Hagerman R, Hoem G, Hagerman P. Fragile X and autism: Intertwined at the molecular level leading to targeted treatments. Mol Autism. 2010;1:12.

2. Bagni C, Oostra BA. Fragile X syndrome: From protein function to therapy. Am. J. Med. Genet. 2013;161:2809–21.

3. Ascano M, Mukherjee N, Bandaru P, Miller JB, Nusbaum JD, Corcoran DL, et al. FMRP targets distinct mRNA sequence elements to regulate protein expression. Nature. 2012;492:382–6.

4. He CX, Portera-Cailliau C. The trouble with spines in fragile X syndrome: density, maturity and plasticity. Neuroscience. 2012.

5. Cruz-Martin A, Crespo M, Portera-Cailliau C. Delayed Stabilization of Dendritic Spines in Fragile X Mice. Journal of Neuroscience. 2010;30:7793–803.

6. Comery TA, Harris JB, Willems PJ, Oostra BA, Irwin SA, Weiler IJ, et al. Abnormal dendritic spines in fragile X knockout mice: maturation and pruning deficits. Proc. Natl. Acad. Sci. U.S.A. 1997;94:5401–4.

7. Gholizadeh S, Halder SK, Hampson DR. Expression of fragile X mental retardation protein in neurons and glia of the developing and adult mouse brain. Brain Research. 2015;1596:22–30.

8. Pacey LKK, Doering LC. Developmental expression of FMRP in the astrocyte lineage:

implications for fragile X syndrome. Glia. 2007;55:1601–9.

9. Jacobs S, Doering LC. Astrocytes prevent abnormal neuronal development in the fragile x mouse. Journal of Neuroscience. 2010;30:4508–14.

10. Jacobs S, Nathwani M, Doering LC. Fragile X astrocytes induce developmental delays in dendrite maturation and synaptic protein expression. BMC Neuroscience. 2010;11:132.

11. Dowell JA, Johnson JA, Li L. Identification of astrocyte secreted proteins with a combination of shotgun proteomics and bioinformatics. J. Proteome Res. 2009;8:4135–43.

12. Barres BA. The mystery and magic of glia: a perspective on their roles in health and disease. Neuron. 2008;60:430–40.

13. Nägler K, Mauch DH, Pfrieger FW. Glia-derived signals induce synapse formation in neurones of the rat central nervous system. The Journal of Physiology. 2001;533:665–79.

14. Ullian EM, Christopherson KS, Barres BA. Role for glia in synaptogenesis. Glia. 2004;47:209–16.

15. Risher WC, Eroglu C. Thrombospondins as key regulators of synaptogenesis in the central nervous system. Matrix Biol. 2012;31:170–7.

16. Jones EV, Bouvier DS. Astrocyte-secreted matricellular proteins in CNS remodelling during development and disease. Neural Plasticity. 2014;2014:321209.

17. Christopherson KS, Ullian EM, Stokes CCA, Mullowney CE, Hell JW, Agah A, et al. Thrombospondins Are Astrocyte-Secreted Proteins that Promote CNS Synaptogenesis. Cell. 2005;120:421–33.

18. Asch AS, Leung LL, Shapiro J, Nachman RL. Human brain glial cells synthesize thrombospondin. Proc. Natl. Acad. Sci. U.S.A. 1986;83:2904–8.

19. Adams JC, Lawler J. The Thrombospondins. Cold Spring Harb Perspect Biol. 2011;3:a009712–2.

20. Adams JC. Thrombospondins: multifunctional regulators of cell interactions. Annu. Rev. Cell Dev. Biol. 2001;17:25–51.

21. Bentley AA, Adams JC. The evolution of thrombospondins and their ligand-binding activities. Molecular Biology and Evolution. 2010;27:2187–97.

22. Lu L, Guo H, Peng Y, Xun G, Liu Y, Xiong Z, et al. Common and rare variants of the THBS1 gene associated with the risk for autism. Psychiatr. Genet. 2014;24:235–40.

23. Cahoy JD, Emery B, Kaushal A, Foo LC, Zamanian JL, Christopherson KS, et al. A Transcriptome Database for Astrocytes, Neurons, and Oligodendrocytes: A New Resource for Understanding Brain Development and Function. Journal of Neuroscience. 2008;28:264–78.

24. Eroglu C, Allen NJ, Susman MW, O'Rourke NA, Park CY, Özkan E, et al. Gabapentin Receptor α2δ-1 Is a Neuronal Thrombospondin Receptor Responsible for

Excitatory CNS Synaptogenesis. Cell. 2009;139:380–92.

25. Crawford DC, Jiang X, Taylor A, Mennerick S. Astrocyte-Derived Thrombospondins Mediate the Development of Hippocampal Presynaptic Plasticity In Vitro. Journal of Neuroscience. 2012;32:13100–10.

26. Xu J, Xiao N, Xia J. Thrombospondin 1 accelerates synaptogenesis in hippocampal neurons through neuroligin 1. Nature Publishing Group. Nature Publishing Group; 2009;13:22–4.

27. Garcia O, Torres M, Helguera P, Coskun P, Busciglio J. A Role for Thrombospondin-1 Deficits in Astrocyte-Mediated Spine and Synaptic Pathology in Down's Syndrome. Feany MB, editor. PLoS ONE. 2010;5:e14200.

28. Jacobs S, Doering LC. Primary dissociated astrocyte and neuron co-culture. Protocols for Neural Cell Culture: Fourth Edition. 2010.

29. Cheng C, Trzcinski O, Doering LC. Fluorescent labeling of dendritic spines in cell cultures with the carbocyanine dye "DiI". Front Neuroanat. 2014;8:30.

30. Pop AS, Levenga J, de Esch CEF, Buijsen RAM, Nieuwenhuizen IM, Li T, et al. Rescue of dendritic spine phenotype in Fmr1 KO mice with the mGluR5 antagonist AFQ056/Mavoglurant. Psychopharmacology. 2012;231:1227–35.

31. Sherazee N, Alvarez VA. DiOlistics: delivery of fluorescent dyes into cells. Methods Mol. Biol. 2013;940:391–400.

32. Pfrieger FW, Barres BA. Synaptic efficacy enhanced by glial cells in vitro. Science. American Association for the Advancement of Science; 1997;277:1684–7.

33. Geissler M, Faissner A. A new indirect co-culture set up of mouse hippocampal neurons and cortical astrocytes on microelectrode arrays. Journal of Neuroscience Methods. 2012;204:262–72.

34. Banker GA. Trophic interactions between astroglial cells and hippocampal neurons in culture. Science. 1980;209:809–10.

35. Iruela Arispe ML, Liska DJ, Sage EH, Bornstein P. Differential expression of thrombospondin 1, 2, and 3 during murine development. Developmental dynamics. Wiley Online Library; 1993;197:40–56.

36. Adams JC. Thrombospondin-1. The International Journal of Biochemistry & Cell Biology. 1997;29:861–5.

37. O'Shea KS, Liu LH, Dixit VM. Thrombospondin and a 140 kd fragment promote adhesion and neurite outgrowth from embryonic central and peripheral neurons and from PC12 cells. Neuron. 1991;7:231–7.

38. Yu K, Ge J, Summers JB, Li F, Liu X, Ma P, et al. TSP-1 Secreted by Bone Marrow Stromal Cells Contributes to Retinal Ganglion Cell Neurite Outgrowth and Survival. Reh TA, editor. PLoS ONE. 2008;3:e2470–11.

39. Ikeda H, Miyatake M, Koshikawa N, Ochiai K, Yamada K, Kiss A, et al. Morphine

modulation of thrombospondin levels in astrocytes and its implications for neurite outgrowth and synapse formation. Journal of Biological Chemistry. ASBMB; 2010;285:38415–27.

40. Blake SM, Strasser V, Andrade N, Duit S, Hofbauer R, Schneider WJ, et al. Thrombospondin-1 binds to ApoER2 and VLDL receptor and functions in postnatal neuronal migration. EMBO J. 2013;27:1–12.

41. Tyzack GE, Sitnikov S, Barson D, Adams-Carr KL, Lau NK, Kwok JC, et al. Astrocyte response to motor neuron injury promotes structural synaptic plasticity via STAT3-regulated TSP-1 expression. Nature Communications. 2014;5:4294.

42. Liauw J, Hoang S, Choi M, Eroglu C, Choi M, Sun G-H, et al. Thrombospondins 1 and 2 are necessary for synaptic plasticity and functional recovery after stroke. J Cereb Blood Flow Metab. 2008;28:1722–32.

43. Ullian EM. Control of Synapse Number by Glia. Science. 2001;291:657–61.

44. Kaufmann WE, Moser HW. Dendritic anomalies in disorders associated with mental retardation. Cerebral Cortex. 2000.

45. Budimirovic DB, Kaufmann WE. What can we learn about autism from studying fragile X syndrome? Dev Neurosci. 2011;33:379–94.

46. Ballas N, Lioy DT, Grunseich C, Mandel G. Non-cell autonomous influence of MeCP2-deficient glia on neuronal dendritic morphology. Nature Publishing Group.

2009;12:311–7.

47. Yang Y, Higashimori H, Morel L. Developmental maturation of astrocytes and pathogenesis of neurodevelopmental disorders. J Neurodevelop Disord. 2013;5:22.

48. Higashimori H, Morel L, Huth J, Lindemann L, Dulla C, Taylor A, et al. Astroglial FMRP-dependent translational down-regulation of mGluR5 underlies glutamate transporter GLT1 dysregulation in the fragile X mouse. Human Molecular Genetics. 2013;22:2041–54.

49. Eroglu C, Barres BA, Stevens B. Glia as active participants in the development and function of synapses. Springer; 2008;:683–714.

50. Yang Q, Feng B, Zhang K, Guo Y-Y, Liu S-B, Wu Y-M, et al. Excessive Astrocyte-Derived Neurotrophin-3 Contributes to the Abnormal Neuronal Dendritic Development in a Mouse Model of Fragile X Syndrome. Wang YT, editor. PLoS Genet. 2012;8:e1003172.

51. Johnson-Venkatesh EM, Umemori H. Secreted factors as synaptic organizers. Eur. J. Neurosci. 2010;32:181–90.

52. Eroglu C. The role of astrocyte-secreted matricellular proteins in central nervous system development and function. J. Cell Commun. Signal. 2009;3:167–76.

53. Kurshan PT, Oztan A, Schwarz TL. Presynaptic α2δ-3 is required for synaptic morphogenesis independent of its Ca2+-channel functions. Nature Publishing Group.

2009;12:1415–23.

54. Jayakumar AR, Tong XY, Curtis KM, Ruiz-Cordero R, Shamaladevi N, Abuzamel M, et al. Decreased astrocytic thrombospondin-1 secretion after chronic ammonia treatment reduces the level of synaptic proteins: in vitroand in vivostudies. Journal of Neurochemistry. 2014;131:333–47.

55. Bourne J, Harris KM. Do thin spines learn to be mushroom spines that remember? Current Opinion in Neurobiology. 2007;17:381–6.

56. Ethell IM, Pasquale EB. Molecular mechanisms of dendritic spine development and remodeling. Progress in Neurobiology. 2005;75:161–205.

57. Ochs SM, Dorostkar MM, Aramuni G, n CSO, Filser S, schl JPO, et al. Loss of neuronal GSK3. Nature Publishing Group; 2014;20:482–9.

58. Ren Z, Sahir N, Murakami S, Luellen BA, Earnheart JC, Lal R, et al. Neuropharmacology. Neuropharmacology. Elsevier Ltd; 2014;:1–9.

59. Friedlander MJ, Martin KA, Wassenhove-McCarthy D. Effects of monocular visual deprivation on geniculocortical innervation of area 18 in cat. J. Neurosci. 1991;11:3268–88.

60. Pan F, Aldridge GM, Greenough WT, Gan W-B. Dendritic spine instability and insensitivity to modulation by sensory experience in a mouse model of fragile X syndrome. Proceedings of the National Academy of Sciences. 2010;107:17768–73.

61. Grossman AW, Elisseou NM, McKinney BC, Greenough WT. Hippocampal pyramidal cells in adult Fmr1 knockout mice exhibit an immature-appearing profile of dendritic spines. Brain Research. 2006;1084:158–64.

62. Levenga J, Hayashi S, de Vrij FMS, Koekkoek SK, van der Linde HC, Nieuwenhuizen I, et al. AFQ056, a new mGluR5 antagonist for treatment of fragile X syndrome. Neurobiology of Disease. Elsevier Inc; 2011;42:311–7.

63. Braun K, Segal M. FMRP involvement in formation of synapses among cultured hippocampal neurons. Cereb. Cortex. 2000;10:1045–52.

64. Sun MK, Hongpaisan J, Lim CS, Alkon DL. Bryostatin-1 Restores Hippocampal Synapses and Spatial Learning and Memory in Adult Fragile X Mice. Journal of Pharmacology and Experimental Therapeutics. 2014;349:393–401.

65. Harlow EG, Till SM, Russell TA, Wijetunge LS, Kind P, Contractor A. Critical period plasticity is disrupted in the barrel cortex of FMR1 knockout mice. Neuron. 2010;65:385–98.

66. Till SM, Wijetunge LS, Seidel VG, Harlow E, Wright AK, Bagni C, et al. Altered maturation of the primary somatosensory cortex in a mouse model of fragile X syndrome. Human Molecular Genetics. 2012;21:2143–56.

67. Bureau I, Shepherd GMG, Svoboda K. Circuit and Plasticity Defects in the Developing Somatosensory Cortex of Fmr1 Knock-Out Mice. J. Neurosci. 2008;28:5178–88.

68. Wei H, Dobkin C, Sheikh AM, Malik M, Brown WT, Li X. The Therapeutic effect of Memantine through the Stimulation of Synapse Formation and Dendritic Spine Maturation in Autism and Fragile X Syndrome. Gillingwater TH, editor. PLoS ONE. 2012;7:e36981.

69. Westmark CJ, Westmark PR, O'Riordan KJ, Ray BC, Hervey CM, Salamat MS, et al. Reversal of fragile X phenotypes by manipulation of AβPP/Aβ levels in Fmr1KO mice. PLoS ONE. 2011;6:e26549.

70. de Vrij FMS, Levenga J, van der Linde HC, Koekkoek SK, De Zeeuw CI, Nelson DL, et al. Rescue of behavioral phenotype and neuronal protrusion morphology in Fmr1 KO mice. Neurobiology of Disease. 2008;31:127–32.

71. Zoghbi HY, Bear MF. Synaptic dysfunction in neurodevelopmental disorders associated with autism and intellectual disabilities. Cold Spring Harb Perspect Biol. 2012;4.

72. Chung W-S, Allen NJ, Eroglu C. Astrocytes Control Synapse Formation, Function, and Elimination. Cold Spring Harb Perspect Biol. 2015.

73. Hama H, Hara C, Yamaguchi K, Miyawaki A. PKC signaling mediates global enhancement of excitatory synaptogenesis in neurons triggered by local contact with astrocytes. Neuron. 2004;41:405–15.

74. Carmona MA, Murai KK, Wang L, Roberts AJ, Pasquale EB. Glial ephrin-A3 regulates hippocampal dendritic spine morphology and glutamate transport. Proceedings

of the National Academy of Sciences. 2009;106:12524–9.

75. Haber M. Cooperative Astrocyte and Dendritic Spine Dynamics at Hippocampal Excitatory Synapses. Journal of Neuroscience. 2006;26:8881–91.

76. Murai KK, Nguyen LN, Irie F, Yamaguchi Y, Pasquale EB. Control of hippocampal dendritic spine morphology through ephrin-A3/EphA4 signaling. Nature Neuroscience. 2002;6:153–60.

77. Huber KM, Gallagher SM, Warren ST, Bear MF. Altered synaptic plasticity in a mouse model of fragile X mental retardation. Proc. Natl. Acad. Sci. U.S.A. National Acad Sciences; 2002;99:7746–50.

CHAPTER 5:

DEVELOPMENTAL EXPRESSION OF THROMBOSPONDIN-1 DIMINISHES IN FRAGILE X ASTROCYTES

Chapter 5

5.1. Preface to Chapter 5

The work in the following chapter was submitted to Neuroscience and is currently under review (Submission #: NSC-16-833).

5.1.1. Declaration of Author Contributions

The author would like to acknowledge Sally Lau for her experimental contributions in assisting with the immunocytochemistry, cell counts and data analysis. All other data collection, experiments and interpretation, preparation and writing of manuscripts were done by the author with the assistance of Dr. Laurie C. Doering.

5.1.2. Rationale

Our earlier findings (Chapter 4) revealed that *Fmr1* KO astrocytes affect morphological features in spine and synapse development in WT hippocampal neurons through the altered secretion of soluble TSP-1. However, these TSP-1 measurements have not been verified *in vivo*. Using cellular and molecular techniques, we determined the relative spatial and temporal expression patterns of TSP-1 *in vitro* and *in vivo*. This study provides greater insight into the developmental trajectory of TSP-1 during crucial synaptogenic periods of brain development in FXS.

5.2. Developmental expression of thrombospondin-1 diminishes in Fragile X astrocytes

Connie Cheng[1,2], Sally K.M. Lau[1], Laurie C. Doering[1,2]*

[1]*Department of Pathology & Molecular Medicine, McMaster University, Hamilton, ON, Canada*

[2]*McMaster Integrative Neuroscience Discovery and Study (MiNDS), Hamilton, ON, Canada*

***Correspondence:**

Dr. Laurie C. Doering

McMaster University, Department of Pathology and Molecular Medicine

1280 Main Street West, Hamilton, ON, L8S 4K1, Canada

E-mail: doering@mcmaster.ca

Tel: +1(905)525-9140 ext. 22913

Running Title: Developmental Expression of TSP-1 in FXS Astrocytes

Keywords: Fragile X syndrome, FMRP, Secreted factor, TSP-1

Number of Figures: 4

Number of Tables: 2

5.2.1. Abstract

Fragile X syndrome (FXS) is the most prevalent form of intellectual disability and the leading cause of autism spectrum disorders. The fragile X mental retardation protein, FMRP, which is absent or expressed at substantially reduced levels, is involved in regulating the activity of key synaptic proteins. Thrombospondin-1 (TSP-1) is an astrocyte-secreted protein that is well known for its role in modulating synaptogenesis and neurogenesis. TSP-1 is expressed in immature astrocytes and its expression peaks during the first postnatal week in mice, which coincides with the expression of FMRP. Here, we examined the developmental trajectory of TSP-1 expression in cortical astrocytes of wildtype (WT) and *Fmr1* knockout (KO) mice at 7, 14 and 21 days *in vitro* (*DIV*). We assessed TSP-1 expression by semi-quantitative immunocytochemistry in cells co-labeled with the astrocyte markers, glial fibrillary acidic protein (GFAP) and aldehyde dehydrogenase 1 family, member L1 (ALDH1L1). TSP-1 protein levels were further confirmed in the cortex and hippocampus of mice at postnatal days P7, P14 and P21 by ELISA. Our results indicated that the proportion of TSP-1-expressing astrocytes is decreased in *Fmr1* KO cultures during early postnatal development. Furthermore, TSP-1 protein levels are significantly reduced in both the cortex and hippocampus of *Fmr1* KO mice in contrast to their WT counterparts. The differences observed in the developmental trajectory of astrocyte-derived TSP-1 in *Fmr1* KO mice likely contribute to the abnormal neurobiology seen in FXS.

5.2.2. Introduction

Fragile X syndrome (FXS) is a genetic disorder and a leading cause of cognitive impairment and autism spectrum disorder. The disorder is caused by a triplet repeat expansion in the 5' untranslated region of the *FMR1* gene, which induces a dramatic reduction or elimination of the expression of the encoded protein, fragile X mental retardation protein (FMRP). FMRP is an mRNA binding protein that controls the expression of hundreds of genes in the central nervous system (CNS) through multiple mechanisms including modulating ribosome stalling (Darnell *et al*., 2011). The expression of FMRP is developmentally regulated and is present at high levels in both neurons and astrocytes (Gholizadeh *et al.*, 2015). FMRP expression is highest in astrocytes typically within the first week of birth and subsequently declines to low or undetectable levels (Pacey & Doering, 2007). The abundant expression of FMRP at birth and during the first 1–2 postnatal weeks indicates that the functional requirement of FMRP in glia is highest during this critical period of early brain development. In FXS, the loss of FMRP in astrocytes is associated with delayed dendrite maturation and dysregulated synapse formation (Jacobs & Doering, 2010a; Jacobs *et al.*, 2010).

Recent evidence shows that astrocytes control the formation, maturation, function and elimination of synapses through various secreted and contact-mediated signals. Astrocytes produce an assortment of signals that promote neuronal maturation according to a precise developmental timeline. In particular, astrocyte-secreted thrombospondin-1 (TSP-1) has been shown to be important for the formation of excitatory synapses *in vitro* and *in vivo* (Christopherson *et al*., 2005; Eroglu *et al.*, 2009). TSP-1 is a matricellular

glycoprotein first discovered in activated platelets (Lawler *et al*., 1978). TSP-1 is the best-studied member of the TSP family (Adams & Lawler, 2011). The expression of TSP-1 in astrocytes is of crucial importance in regulating the established functions of astrocytes in synapse formation and neural plasticity (Crawford *et al.*, 2012; Risher & Eroglu, 2012). More specifically, during the early postnatal weeks in rodents when astrocyte support of neuron growth and synapse formation is vital, the lack of TSP-1 could contribute to the abnormal dendritic spine morphology and synapse development seen in FXS. Based on our previous findings, we revealed that primary cortical astrocytes derived from FXS mice display deficits in the intracellular expression and extracellular secretion of TSP-1 (*submitted*). We also showed that TSP-1 regulates synapse formation and spine maturation. However, is it unknown whether the orchestrated timing and signaling of TSP-1 is altered in FXS.

As an extension of our earlier findings, here we elucidated the distribution patterns of astroglia-derived TSP-1 during crucial periods of early postnatal development in wildtype (WT) and *Fmr1* knockout (KO) mice. The proportion of TSP-1 expressing astrocytes was assessed in WT and *Fmr1* KO cortical astrocyte cultures at 7, 14 and 21 *days in vitro (DIV)*. To profile the developmental trajectory of TSP-1, parallel studies confirming TSP-1 protein levels were also performed in the cortex and hippocampus at postnatal days P7, P14, and P21.

5.2.3. Materials & Methods

Animals

The FMRP mouse colony was established from breeding pairs of FVB.129P2(B6)-Fmr1^{tm1Cgr} mice. The wildtype (WT) and *Fmr1* knockout (KO) mice were maintained as individual strains and genotyped regularly. The mice used for these experiments were housed and bred at the McMaster University Central Animal Facility. All experiments complied with the guidelines set out by the Canadian Council on Animal Care and were approved by the McMaster Animal Research Ethics Board.

Primary Cortical Astrocyte Cultures

Cortical astrocytes were prepared from five WT or *Fmr1* KO postnatal day P0-P2 pups, as previously described (Jacobs & Doering, 2010b). Briefly, whole brains were extracted and cortical tissue was dissected and incubated with 2.5% trypsin and 15 mg/mL DNase (Roche Diagnostics, Laval, QC, Canada) at 37°C. Following successive mechanical trituration using a serological pipette, the cells were passed through a 70 μm cell strainer (Fisher Scientific, Whitby, ON, Canada), dissociated into a single-cell suspension, and re-suspended in 10% Glial Media (GM) comprised of Minimum Essential Medium (MEM) (Invitrogen, Burlington, ON, Canada), 0.6% glucose and 10% horse serum (Invitrogen, Burlington, ON, Canada). The astrocytes were seeded in a T75 flask and maintained in culture for 7-12 days in a humidified 5% CO_2, 95% O_2 incubator at 37°C. Partial medium changes were performed every 2-3 days. Cultures consisted of at least 95% astrocytes as determined by glial fibrillary acidic protein (GFAP)

immunocytochemistry. Confluent astrocyte cultures were incubated with 0.05% Trypsin-EDTA (Invitrogen, Burlington, ON, Canada) for 5 min at 37°C. Once cells were fully lifted, media with serum was added to stop the digestion. The cells were removed from the flask and counted to seed approximately 5000 cells on Poly-$_L$-Lysine (1 mg/mL, Sigma-Aldrich, Oakville, ON, Canada) and laminin (0.1 mg/mL, Invitrogen, Burlington, ON, Canada) coated glass coverslips in 24 multi-well plates. The cell cultures were maintained in 10% GM and grown for 7, 14 and 21 days.

Immunocytochemistry (ICC)

At 7, 14 or 21 *DIV*, the cells on the coverslips were fixed with ice cold (-20°C) acetone. Cell membranes were permeabilized using 0.1% Triton X-100. Coverslips were incubated in 1% bovine serum albumin to block non-specific binding. Primary antibodies were applied to the coverslips and incubated overnight at 4°C. Wells were washed with PBS the following day. Secondary antibodies were applied and incubated at room temperature for 3 hours. After three sets of washes with PBS and distilled water, the coverslips were dried and mounted onto slides with ProLong® Gold Antifade Mountant with DAPI (Life Technologies, Burlington, ON, Canada) to visualize the nuclei. The following primary antibodies, diluted in 0.01M PBS, were used: rabbit anti-ALDH1L1 (1:500, Abcam, Toronto, ON, Canada), rabbit anti-GFAP (1:500, Dako, Mississauga, ON, Canada), mouse anti-TSP-1 (1: 100, Thermo Scientific, Burlington, ON, Canada). The secondary antibodies used include: donkey anti-mouse AlexaFluor 594 (1:1500, Invitrogen, Burlington, ON, Canada), and goat anti-rabbit FITC (1:100, Jackson ImmunoResearch, West Grove, PA, USA).

Image Acquisition and Quantification

Images were acquired using a Zeiss AxioImager.M2 at 10x magnification configured with the ApoTome.2 and Zeiss Zen Blue image acquisition software. For each culture condition, three coverslips were set up and five individual frames (images) were taken from each coverslip (four corners and a central frame). For each frame per coverslip, approximately 120-150 cells were counted for each genotype, per timepoint. The proportion of co-labeling of TSP-1 and astrocyte markers GFAP or ALDH1L1 were manually counted using ImageJ (http://rsbweb.nih.gov/ij/) with the cell counter plug-in. Cells were categorized by the positive expression of an astrocytic marker (ALDH1L1 or GFAP) and whether they expressed TSP-1 at low levels (TSP-1+), at high levels (TSP-1++) or null (TSP-1-). In total, two independent experiments were performed.

Protein Extraction from Brain Tissue for ELISA

Cortical and hippocampal tissue were harvested from P7, P14 and P21 male mice. Tissues were dissected, weighed and suspended in 10 volumes of extraction buffer containing 10 mM Tris pH 7.4, 150 mM NaCl, 1% Triton X-100 and protease inhibitors per mg gram of tissue. Tissues were mechanically disrupted and incubated on ice for 1 hour. The homogenates were centrifuged at 13,000 RPM for 30 minutes at 4°C, and the supernatant was stored at -80°C until analyzed. Protein concentration of the supernatant was determined for each sample by DC Protein Assay. TSP-1 protein measurements for each sample were determined using the Mouse Thrombospondin-1 ELISA kit (Biotang, Inc, Waltham, MA, USA) following the vendor's instructions. The concentration of TSP-

1 was detected using the Multiskan™ GO Microplate Spectrophotometer and quantified using Thermo Scientific's SkanIt™ software.

Statistical Analysis

Statistics were performed using GrapPad Prism (v5.01). Data was analyzed using a Student's t-test. All values are expressed as mean ± SEM. In all analyses, the level of statistical significance was set at $p<0.05$. For the *in vitro* experiments, N represents the number of independent cultures per condition (genotype and days *in vitro* (*DIV*)) and n represents the total number of individual cells counted in each condition. For the TSP-1 protein measurements in cortical and hippocampal brain lysates, N represents the number of independent experiments and n represents the number of samples.

5.2.4. Results

To better understand the developmental temporal patterns of expression for TSP-1, immunocytochemical analysis was used to compare the presence of astrocyte-derived TSP-1 in WT and *Fmr1* cortical cultures at 7, 14 and 21 *DIV*. The timepoints correspond to the peak periods of synaptogenesis in culture, with specific reference to synapse formation. Astrocytes were immunolabeled with the glial-specific markers glial fibrillary acidic protein (GFAP) and aldehyde dehydrogenase 1 family, member L1 (ALDH1L1). As a control, cells stained with a secondary antibody showed no fluorescence. We quantified the total number of cells co-labeled with TSP-1 and GFAP or TSP-1 and ALDH1L1, and calculated the percentage of TSP-1-expressing astrocytes. Astrocytes expressing both strong and faint levels of TSP-1 staining were identified and included together in the analysis. All cultures yielded greater than 99% of cells stained with the astrocyte-specific markers ALDH1L1 or GFAP.

TSP-1-expressing astrocytes are decreased in Fmr1-KO cortical astrocyte cultures.

To elucidate the distribution patterns of astrocyte TSP-1, we first identified primary cortical astrocytes using the astrocyte markers GFAP and ALDH1L1 **(Figure 5.1).** These cells had the morphology of protoplasmic astrocytes and co-expressed TSP-1 with the astrocyte markers. We also found prominent surface localization of TSP-1 with similar subcellular localization and staining patterns in WT and *Fmr1* KO astrocytes (**Figure 5.1A**). For the GFAP-labeled cells, differences in the total proportion of astrocytes co-expressing TSP-1 were not observed between the WT and *Fmr1* KO cultures at 7 *DIV* (**Figure 5.1B**). However at 14 *DIV*, clear differences were revealed in

the proportion of double-labeling with GFAP and TSP-1 between the *Fmr1 KO* and WT cells. In particular, *Fmr1* KO cultures exhibited a striking 30% decrease in the proportion of TSP-1 labeled astrocytes in contrast to WT cultures ($p<0.05$). Similarly at 21 *DIV*, the proportion of double-labeled cells diminished by 45% relative to WT cells ($p<0.001$).

Notably, many of the immature (developing) astrocytes were not detected by GFAP. We therefore used the astrocyte-specific marker ALDH1L1 to identify the astrocytes, which provided more widespread labeling at early and later timepoints of development **(Figure 5.2A).** At 7 *DIV*, the expression of TSP-1 in ALDH1L1 labeled astrocytes was slightly reduced in *Fmr1* KO cultures ($p<0.05$) **(Figure 5.2B)**. At P14, deficits in the co-expression of ALDH1L1 and TSP-1 were also observed. In fact, the proportion of double-labeling drastically decreased by 50% in the *Fmr1* KO cultures compared to WT cultures at 14 *DIV* ($p<0.001$). Likewise at 21 *DIV*, the proportion of TSP-1-expressing astrocytes also diminished by nearly half (45%) in *Fmr1* KO cultures. This data suggests that the expression of TSP-1 by *Fmr1* KO astrocytes in the cortex is significantly altered during key synaptogenic periods of development *in vitro*.

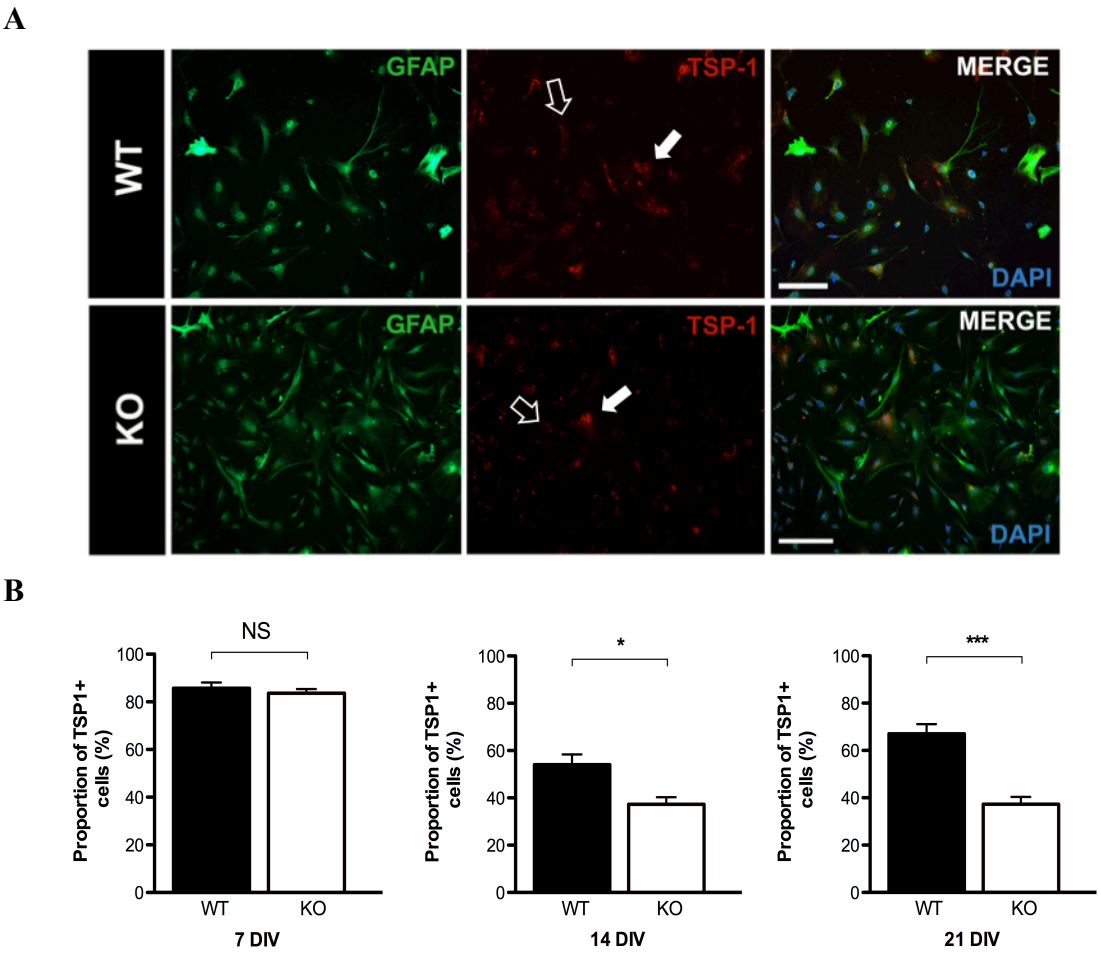

Figure 5.1: Representative images of WT and *Fmr1* KO cortical astrocytes co-labeled with TSP-1 and astrocyte marker GFAP.

(A) Primary cortical astrocytes from WT mice and *Fmr1* KO mice were labelled with anti-TSP-1 to visualize the intracellular expression of TSP-1(red) and anti-GFAP (green) visualize the astrocytes at 7 *DIV*. Cells were counterstained with DAPI (blue) to visualize the nuclei. Scale bars: 20 µm. TSP-1 is abundantly expressed in mouse cortical astrocytes

from WT and *Fmr1* KO mice at 7 *DIV*. Strong perinuclear staining is observed in the WT and *Fmr1* KO cells. The solid arrows denote strong TSP-1 labeling. The open arrows denote weak TSP-1 labeling. **(B)** Proportion of total TSP-1 expressing astrocytes labeled with GFAP at 7, 14 and 21 *DIV*. In total, 30 frames were taken per genotype, per timepoint. Decreased TSP-1 labeling is observed in the *Fmr1* KO astrocytes at 14 and 21 *DIV*. n = total cells counted. 7 *DIV*: n(WT) = 1817, n(KO) = 2106; 14 *DIV:* n(WT) = 2298, n(KO) = 3143; 21 *DIV:* n(WT) = 2057, n(KO) = 4569; N = 2 independent experiments.

A

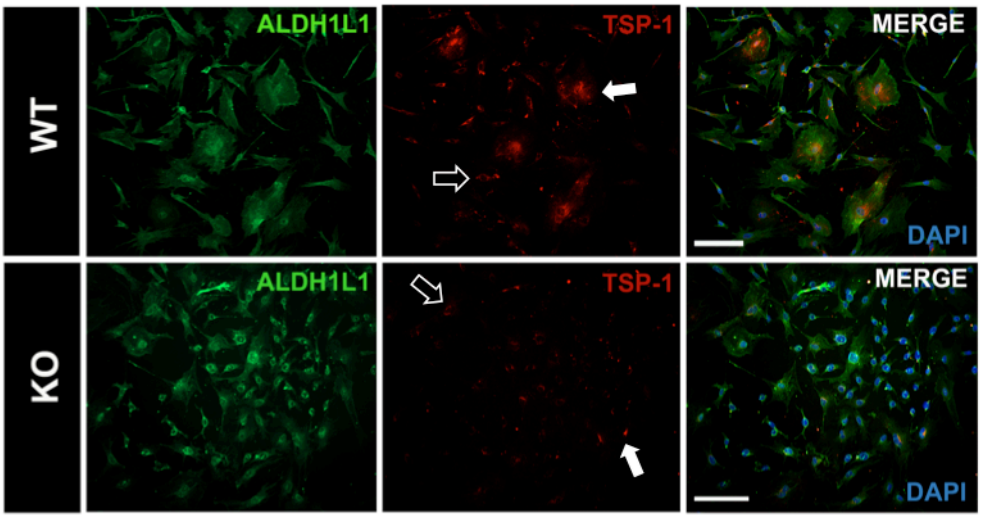

B

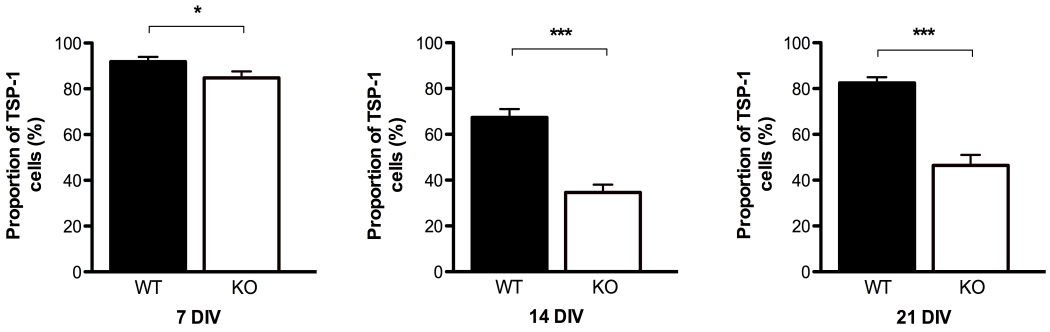

Figure 5.2: Representative images of WT and *Fmr1* KO cortical astrocytes co-labeled with TSP-1 and astrocyte marker ALDH1L1.

(A) Primary cortical astrocytes from WT and *Fmr1* KO mice were labelled with anti-TSP-1 to visualize the intracellular expression of TSP-1(red) and anti-ALDH1L1 (green) visualize the astrocytes at 7 *DIV*. Cells were counterstained with DAPI (blue) to visualize

the nuclei. Scale bars: 50 μm. The solid arrows denote strong TSP-1 labeling. The open arrows denote weak TSP-1 labeling. **(B)** Proportion of TSP-1 expressing astrocytes labeled with ALDH1L1 at 7, 14 and 21 *DIV*. In total, 30 frames were captured per genotype, per timepoint. Proportion of TSP-1 expressing astrocytes labeled with ALDH1L1 at 7, 14 and 21 *DIV*. Decreased TSP-1 labeling was observed in the *Fmr1* KO astrocytes compared to their WT counterparts at 7, 14 and 21 *DIV*. n = total cells counted, 7 *DIV*: n(WT) = 2610, n(KO) = 2500; 14 *DIV:* n(WT) = 2514, n(KO) = 2347; 21 *DIV:* n(WT) = 2430, n(KO) = 3676; N = 2 independent experiments.

Strong and faint TSP-1 labeling was observed in the distribution of astrocytes.

Tables 5.1 and **5.2** summarize the proportion of TSP-1 labeled astrocytes using GFAP and ALDH1L1 in two categories based on the intensity of TSP-1 labeling (weak or strong) at various stages of development. At 7 *DIV* for ALDH1L1 labeled astrocytes, strong TSP-1 labeling appeared to be more prominent in WT cultures compared to *Fmr1* KO cultures, during a period of development consistent with synapse formation (Table 1). In fact, *Fmr1* KO astrocytes exhibited a higher proportion of weak TSP-1 labeling, suggesting that TSP-1 may be expressed at lower levels compared to WT astrocytes. At 14 and 21 *DIV*, the proportion of strongly labeled TSP-1 astrocytes decreased in both the WT and *Fmr1* KO cells, suggesting that TSP-1 expression diminishes later in culture. However, WT astrocytes displayed increased proportions of both faint and intense TSP-1 labeling compared to their *Fmr1* KO counterparts at 14 and 21 *DIV*. Likewise, similar trends were also observed in the GFAP labeled cells at 7, 14, and 21 *DIV* between the WT and *Fmr1* KO astrocytes **(Table 5.2)**. These results suggest that TSP-1 is more highly expressed during the first week in culture, as indicated by a greater proportion of intensely labeled TSP-1 co-expressed in astrocytes. Furthermore, the intensity of TSP-1 expression appears stronger in the WT astrocytes compared to *Fmr1* KO cells across all timepoints *in vitro*.

Table 5.1: Proportion of cells co-expressing ALDH1L1 and TSP-1 (%).

	ALDH1L1+ cells		
	TSP-1+[a]	**TSP-1++[b]**	**TSP-1+ & ++[c]**
7 *DIV*			
WT	43.34 ± 3.185	48.53 ± 4.523	91.87 ± 2.098
KO	60.16 ± 3.405	24.60 ± 3.627	84.75 ± 2.887
14 *DIV*			
WT	56.45 ± 2.709	10.96 ± 2.438	67.40 ± 3.608
KO	32.95 ± 3.268	1.71 ± 0.5030	34.66 ± 3.349
21 *DIV*			
WT	59.34 ± 4.182	23.00 ± 3.882	82.34 ± 2.504
KO	42.53 ± 4.535	3.95 ± 1.093	46.48 ± 4.594

Note: All values are expressed as percentage of cells expressing the markers and as mean ± SEM.

[a]TSP-1+ represents astrocytes weakly labeled with TSP-1
[b]TSP-1++ represents astrocytes strongly labeled with TSP-1
[c]TSP1-1+&TSP-1++ represents total TSP-1 labeling (weak and strong)

Table 5.2: Proportion of cells co-expressing GFAP and TSP-1 (%).

	GFAP+ cells		
	TSP-1+[a]	**TSP-1++[b]**	**TSP-1+ & ++[c]**
7 *DIV*			
WT	54.46 ± 3.083	31.27 ± 3.825	85.73 ± 2.434
KO	59.53 ± 1.827	24.08 ± 2.491	83.61 ± 1.790
14 *DIV*			
WT	42.13 ± 2.833	11.94 ± 2.350	54.07 ± 4.267
KO	30.88 ± 2.593	6.456 ± 1.445	37.33 ± 2.971
21 *DIV*			
WT	48.23 ± 3.243	18.85 ± 4.642	67.08 ± 4.020
KO	32.57 ± 2.846	4.69 ± 0.8172	37.26 ± 3.145

Note: All values are expressed as percentage of cells expressing the markers and as mean ± SEM.

[a]TSP-1+ represents astrocytes weakly labeled with TSP-1
[b]TSP-1++ represents astrocytes strongly labeled with TSP-1
[c]TSP1-1+&TSP-1++ represents total TSP-1 labeling (weak and strong)

Cortical TSP-1 protein levels are downregulated in Fmr1 KO mice during early development.

To confirm that our previous findings were not simply due to the *in vitro* environment, we measured global TSP-1 levels in cortical lysates of WT and *Fmr1* mice at postnatal days P7, P14 and P21 by ELISA. Our results indicated that TSP-1 protein expression was highest after the first week of birth and gradually declined by P14 and P21 in both WT and *Fmr1* KO mice **(Figure 5.3)**. Significant alterations in TSP-1 were observed in the cortex at P7 and P14 between *Fmr1* KO and WT mice. At P7, cortical TSP-1 was downregulated by 20% in *Fmr1* KO mice in contrast to WT mice ($p<0.05$). At P14, clear differences in TSP-1 protein expression were also demonstrated between the two genotypes. In particular, *Fmr1* KO mice exhibited a 35% deficit in TSP-1 compared to their WT counterparts ($p<0.05$). At P21, cortical TSP-1 protein levels were also reduced relative to the observed levels at P7 and P14; however, significant differences were not detected between the genotypes. These results provide insight into the relative expression patterns of TSP-1 in the cortex during crucial synaptogenic periods of brain development.

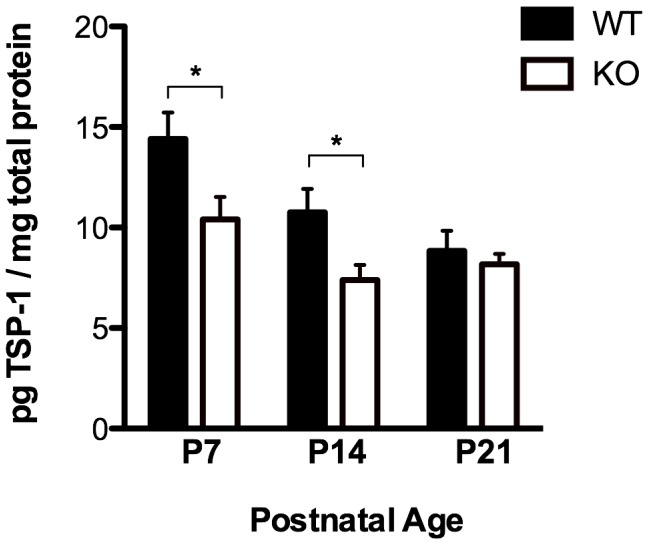

Figure 5.3: Quantification of TSP-1 protein levels by ELISA in the cortex of WT and *Fmr1* KO mice at postnatal days 7, 14 and 21.

TSP-1 protein expression peaks at P7 and gradually declines to low levels by P14 and P21. TSP-1 levels are significantly reduced in the cortex of the *Fmr1* KO mice relative to WT counterparts at P7 and P14. Pairwise comparison conducted using an independent Student's t-test. *$p<0.05$; n=6 for each genotype, per time point.

Hippocampal TSP-1 protein levels are significantly diminished in Fmr1 KO mice.

Since FMRP is highly abundant in the hippocampus and plays a major role in learning and memory, we were interested in exploring the expression patterns of TSP-1 in hippocampus of WT and *Fmr1* KO mice. To further validate the *in vitro* findings, we quantified TSP-1 protein levels in hippocampal lysates in a similar developmental sequence at P7, P14 and P21. At all developmental timepoints, the TSP-1 protein levels observed in the hippocampus were vastly higher than in the cortex, consistent with the expression patterns of FMRP (Pacey & Doering, 2007; Gholizadeh et al, 2015). Our findings also established that hippocampal TSP-1 protein levels were highest at P7, but dramatically declined by P14 and P21 in both WT and *Fmr1* KO mice **(Figure 5.4).** At P14, hippocampal TSP-1 levels substantially decreased in both WT (by 2.5 fold) and *Fmr1* KO (by 3 fold) mice relative to P7. However, hippocampal TSP-1 amounts remained low in both WT and *Fmr1* KO mice at P21.

Interestingly, striking deficits in TSP-1 levels were also observed across all developmental timepoints between the genotypes. In fact, at P7, TSP-1 levels were vastly downregulated by 25% in *Fmr1* KO mice in contrast to their WT counterparts ($p<0.05$). At P14, hippocampal TSP-1 levels were also substantially reduced by 50% in the *Fmr1* KO mice compared to WT mice ($p<0.01$). Similarly at P21, *Fmr1* KO mice exhibited 55% less TSP-1 in the hippocampus. These results propose that deficits in hippocampal TSP-1 during synaptogenic periods may significantly affect proper early postnatal development in FXS.

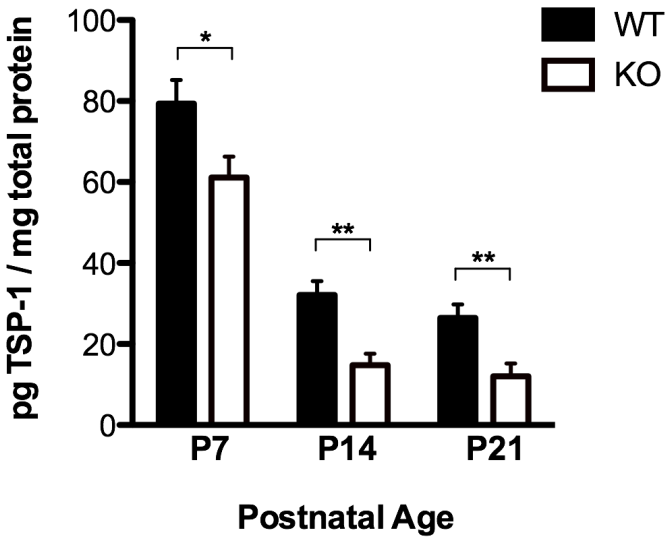

Figure 5.4: Quantification of TSP-1 protein levels by ELISA in the hippocampus of WT and *Fmr1* KO mice at postnatal days 7, 14 and 21.

TSP-1 protein expression is highest at P7 and gradually declines to low levels by P14 and P21 in both *Fmr1* KO and WT mice. Significant decreases in TSP-1 protein levels are observed in the hippocampus of *Fmr1* KO mice compared to WT mice at P7, P14 and P21. Pairwise comparison per time point conducted using an independent Student's t-test. *$p<0.05$, **$p<0.01$; P7, n=12; P14, n=8; P21, n=8 for each genotype, per time point.

5.2.5. Discussion

Astrocytes play a pivotal role in synapse formation and function. In the postnatal brain, their appearance at synapses coincides with periods of developmental plasticity when neural circuits are refined and established. Several studies have highlighted astrocytes and the TSPs that they secrete as major modulators of synapse formation (Ullian et al., 2001; Christopherson et al., 2005). In this study, we established a comprehensive developmental expression profile of TSP-1 in our FXS mouse model at various timepoints of development that correlate with synaptogenesis *in vivo* and *in vitro*. With double-labeling using astrocyte markers GFAP or ALDH1L1 in combination with TSP-1, we identified that the proportion of TSP-1 labeled cells was decreased in *Fmr1* KO astrocyte cultures during early postnatal development *in vitro*. We also found that TSP-1 protein expression peaked at P7 in the hippocampus and cortex, coinciding with synapse formation, and gradually declined to low levels by P14 and P21 in both WT and *Fmr1* KO mice. Interestingly, TSP-1 was present at higher levels in the hippocampus than the cortex. Lastly, TSP-1 protein levels were significantly diminished in the cortex and hippocampus of *Fmr1* KO mice compared to their WT counterparts across the various developmental timepoints. These findings infer an indirect role for FMRP in the regulation of TSP-1. In the absence of FMRP, a lack of TSP-1 may contribute to the neurobiological abnormalities seen in FXS.

GFAP and ALDH1L1 reliably label primary cortical astrocytes.

Astrocytes are the most abundant cells in the CNS. Astrocytes are not uniform as their functions and morphology differ largely depending on their location, subtypes, and the developmental stage (Lafon-Cazal et al., 2003). With the use of different markers, the characterization of astrocytes at various developmental stages can provide insight into astrocyte postnatal development in relation to the formation of abnormal neural circuitry. GFAP is an intermediate filament protein expressed in astrocytes that is typically used to distinguish astrocytes within the CNS. Although this marker has been used for decades as a standard to identify astrocytes, it has become clear that GFAP is not uniformly expressed in all astrocytes (Zhang and Barres, 2010; Oberheim et al., 2011). GFAP is expressed predominantly in mature and reactive astrocytes, making it a poor marker for identifying immature astrocytes in postnatal development (McCall et al., 1996). Since TSP-1 is highly synthesized by immature astrocytes (Christopherson et al., 2005), we required the use of a marker that would be capable of detecting developing astrocytes. ALDH1L1 is an enzyme that has been identified as a highly specific antigenic marker for astrocytes with a substantially broader pattern of expression than the conventional astrocyte marker GFAP (Cahoy et al., 2008). More importantly, ALDH1L1 is present in both immature and mature astrocytes. Therefore, we utilized both astrocyte markers in our immunocytochemical experiments. However, we were surprised to find that both markers sufficiently labeled primary astrocytes at early and late timepoint using immunocytochemistry. In fact, both ALDH1L1 and GFAP revealed that the cultures consisted of 99% astrocytes. This finding demonstrated that both markers were effective

and sensitive to labeling immature and mature astrocytes, although GFAP labeling appeared less intense in developing immature astrocyte1 relative to ALDH1L1.

Notably, differences in the proportion of TSP-1 expressing ALDH1L1-labeled astrocytes were detected as early as P7 between *Fmr1* KO and WT cultures. However, these changes were not observed in GFAP-labeled astrocytes until 14 and 21 *DIV*. Although consistent trends of decreased TSP-1 labeling were observed across the timepoints, the differences seemed to be delayed in the GFAP-labeled cells between 7 and 14 *DIV*, which may be attributed to an *in vitro* environment with slower growth. In addition, the cortical astrocytes were grown in isolation in the absence of neurons. Under normal circumstances, proper synapse development and function rely on dynamic neuron-glia interactions (Tran and Neary, 2006; Eroglu et al., 2009); thus the lack of neurons present in the microenvironment may exert an affect on TSP-1 expression, secretion and signaling in astrocytes.

TSP-1 is significantly reduced in the hippocampus and cortex of Fmr1 KO mice.

In the CNS, the expression of TSP-1 is driven by the presence of astrocytes and their developmental stage of maturity (Cahoy et al., 2008). TSP-1 is expressed in both cultured and developing astrocytes with its expression peaking during the first postnatal week (Christopherson et al., 2005), coinciding with synaptogenesis. In mature astrocytes, the expression of TSP-1 declines, although a low level is maintained throughout the brain and is particularly concentrated in areas of neurogenesis in the adult (Iruela Arispe et al., 1993; Cahoy et al., 2008; Lu and Kipnis, 2010).

Primary cultures of astroglia (McCarthy and de Vellis, 1980) have long served as an *in vitro* proxy for studying *in vivo* astrocytes; however, the relationship between preparations of cultured astroglia to normally functioning astrocytes is poorly understood. *In vivo*, newly generated immature astrocytes are formed during the first week of birth between P1-P8 in mice. Since TSP-1 is synthesized and secreted by immature astrocytes, this timepoint is of particular importance, specifically for synapse formation during synaptogenesis within the developing CNS. Astrocytes typically acquire their mature morphology at later stages when development is nearly complete at approximately P17-P21 (Bushong et al., 2004).

To verify our *in vitro* findings, we quantified the amount of TSP-1 protein present in hippocampal and cortical tissues of WT and *Fmr1* KO mice. Consistent with the semi-quantitative results from the primary cortical astrocytes, deficits in hippocampal and cortical TSP-1 were observed across the various developmental timepoints (P7, P4, and P21). We also demonstrated that both cortical and hippocampal TSP-1 protein levels in normal mice were highest at P7 and significantly declined by the second and third week after birth. These findings are supported by Christopherson *et al*. (2005), which detected the presence of TSP-1 in the postnatal cortex at P5 and downregulated levels in the adult cortex of rat cortical lysates. The present findings also coincide with the expression of FMRP, which is highly developmentally regulated during early postnatal development (Till 2010). Peak levels of FMRP are typically reached by the end of the first postnatal week, with expression gradually declining thereafter. Consistent with the high expression of FMRP (Pacey et al. 2007), we found that TSP-1 was more highly expressed in the

hippocampus (Jacobs & Doering, 2010; Christopherson et al., 2005). Interestingly, a study by Xu et al. (2009) demonstrated that TSP-1 is involved in accelerating the speed of synapse formation in young rat hippocampal neurons *in vitro*. Further, neurons grown in culture with TSP-1 KO astrocytes display alterations in spine morphology with a 50% reduction in the formation of mature spines (Garcia et al., 2010). Given that significant deficits in TSP-1 were observed in the hippocampus and cortex during critical time points of development in *Fmr1* KO mice, this may account for the developmental delays in neuronal maturation observed in FXS (Jacobs & Doering, 2010a; Jacobs et al., 2010).

Although the quantitative findings of TSP-1 were mostly consistent with the semi-quantitative outcomes *in vitro*, it is worthwhile to consider that TSP-1 protein levels were measured globally and not selectively in astrocytes from hippocampal and cortical tissue lysates. A variety of normal cells in the brain, including endothelial cells, oligodendrocytes, fibroblasts, and macrophages also secrete TSP-1 (Wight et al., 1985; Scott-Drew and ffrench-Constant, 1997). However, due to the high enrichment of astrocytes in the CNS (Sloan and Barres, 2014), it is unlikely that other cell subtypes accounted for the observed differences. In support of this, the TSP-1 protein levels observed in the hippocampus and cortex of the brain were consistent with our findings in cell culture. Therefore, it is conceivable that the differences observed in TSP-1 expression levels may be diluted by the presence of other neuronal and non-neuronal cell subtypes.

Conclusion

During early development, synapse formation is spatiotemporally controlled in the

CNS, suggesting the presence of regulatory mechanisms. The majority of excitatory synapses in the developing brain typically form during the second and third postnatal weeks (Eroglu et al., 2008; Eroglu and Barres, 2010). This window of development corresponds to the establishment of synapses and correlates with the appearance and maturation of astrocytes in the brain, which suggests that astrocytes may provide instructive cues that contribute to the initiation of excitatory synapse formation. Similarly, the identification of TSP-1 as CNS synaptogenic proteins has important implications. For instance, the abundance of TSPs *in vivo* is dynamically regulated during development, being low in late embryonic brain, higher in postnatal brain, and low or absent in the adult brain (Iruela-Arispe *et al.,* 1993). The downregulation of TSP-1 levels in later brain development also correlates with the relatively poor ability of the adult CNS to form new synapses. Therefore, significant alterations in astrocyte-derived TSP-1 during early development may contribute to contribute to long-term deficits in CNS wiring and synaptic function in FXS. Together, this study provides insight into the timing of the alterations in TSP-1 during crucial windows of early development that may be important for future therapeutic inventions in FXS and related neurodevelopmental disorders.

5.2.6. Acknowledgements

This work was supported by the Natural Sciences and Engineering Research Council of Canada (NSERC), Fragile X Research Foundation of Canada and the Brain Canada/Azrieli Neurodevelopmental Research Program.

5.2.7. References

Adams, J.C. & Lawler, J. (2011) The Thrombospondins. *Cold Spring Harb Perspect Biol*, **3**, a009712–a009712.

Bechara, E.G., Didiot, M.C., Melko, M., Davidovic, L., Bensaid, M., Martin, P., Castets, M., Pognonec, P., Khandjian, E.W., Moine, H., & Bardoni, B. (2009) A Novel Function for Fragile X Mental Retardation Protein in Translational Activation. *Plos Biol*, **7**, e1000016–13.

Bushong, E.A., Martone, M.E., & Ellisman, M.H. (2004) Maturation of astrocyte morphology and the establishment of astrocyte domains during postnatal hippocampal development. *International Journal of Developmental Neuroscience*, **22**, 73–86.

Cahoy, J.D., Emery, B., Kaushal, A., Foo, L.C., Zamanian, J.L., Christopherson, K.S., Xing, Y., Lubischer, J.L., Krieg, P.A., Krupenko, S.A., Thompson, W.J., & Barres, B.A. (2008) A Transcriptome Database for Astrocytes, Neurons, and Oligodendrocytes: A New Resource for Understanding Brain Development and Function. *Journal of Neuroscience*, **28**, 264–278.

Christopherson, K.S., Ullian, E.M., Stokes, C.C.A., Mullowney, C.E., Hell, J.W., Agah, A., Lawler, J., Mosher, D.F., Bornstein, P., & Barres, B.A. (2005) Thrombospondins Are Astrocyte-Secreted Proteins that Promote CNS Synaptogenesis. *Cell*, **120**, 421–433.

Crawford, D.C., Jiang, X., Taylor, A., & Mennerick, S. (2012) Astrocyte-Derived Thrombospondins Mediate the Development of Hippocampal Presynaptic Plasticity

In Vitro. *Journal of Neuroscience*, **32**, 13100–13110.

Darnell, J.C., Van Driesche, S.J., Zhang, C., Hung, K.Y.S., Mele, A., Fraser, C.E., Stone, E.F., Chen, C., Fak, J.J., Chi, S.W., Licatalosi, D.D., Richter, J.D., & Darnell, R.B. (2011) FMRP stalls ribosomal translocation on mRNAs linked to synaptic function and autism. *Cell*, **146**, 247–261.

Eroglu, C. & Barres, B.A. (2010) Regulation of synaptic connectivity by glia. *Nature*, **468**, 223–231.

Eroglu, C., Allen, N.J., Susman, M.W., O'Rourke, N.A., Park, C.Y., Özkan, E., Chakraborty, C., Mulinyawe, S.B., Annis, D.S., Huberman, A.D., Green, E.M., Lawler, J., Dolmetsch, R., Garcia, K.C., Smith, S.J., Luo, Z.D., Rosenthal, A., Mosher, D.F., & Barres, B.A. (2009) Gabapentin Receptor α2δ-1 Is a Neuronal Thrombospondin Receptor Responsible for Excitatory CNS Synaptogenesis. *Cell*, **139**, 380–392.

Eroglu, C., Barres, B.A., & Stevens, B. (2008) Glia as active participants in the development and function of synapses 683–714.

Iruela Arispe, M.L., Liska, D.J., Sage, E.H., & Bornstein, P. (1993) Differential expression of thrombospondin 1, 2, and 3 during murine development. *Developmental dynamics*, **197**, 40–56.

Jacobs, S. & Doering, L.C. (2010a) Astrocytes prevent abnormal neuronal development in the fragile x mouse. *Journal of Neuroscience*, **30**, 4508–4514.

Jacobs, S. & Doering, L.C. (2010b) Primary dissociated astrocyte and neuron co-culture 269–283.

Jacobs, S., Nathwani, M., & Doering, L.C. (2010) Fragile X astrocytes induce developmental delays in dendrite maturation and synaptic protein expression. *BMC Neuroscience*, **11**, 132.

Lawler, J.W., Slayter, H.S., & Coligan, J.E. (1978) Isolation and characterization of a high molecular weight glycoprotein from human blood platelets. *Journal of Biological Chemistry*, **253**, 8609–8616.

Lu, Z. & Kipnis, J. (2010) Thrombospondin 1--a key astrocyte-derived neurogenic factor. *The FASEB Journal*, **24**, 1925–1934.

McCall, M.A., Gregg, R.G., Behringer, R.R., Brenner, M., Delaney, C.L., Galbreath, E.J., Zhang, C.L., Pearce, R.A., Chiu, S.Y., & Messing, A. (1996) Targeted deletion in astrocyte intermediate filament (Gfap) alters neuronal physiology. *Proc. Natl. Acad. Sci. U.S.A*, **93**, 6361–6366.

McCarthy, K.D. & de Vellis, J. (1980) Preparation of separate astroglial and oligodendroglial cell cultures from rat cerebral tissue. *The Journal of Cell Biology*, **85**, 890–902.

Oberheim, N.A., Goldman, S.A., & Nedergaard, M. (2011) Heterogeneity of Astrocytic Form and Function. In *Methods in Molecular Biology*, *Methods in Molecular Biology*. Humana Press, Totowa, NJ, pp. 23–45.

Pacey, L.K.K. & Doering, L.C. (2007) Developmental expression of FMRP in the astrocyte lineage: implications for fragile X syndrome. *Glia*, **55**, 1601–1609.

Risher, W.C. & Eroglu, C. (2012) Thrombospondins as key regulators of synaptogenesis in the central nervous system. *Matrix Biol*, **31**, 170–177.

Scott-Drew, S. & ffrench-Constant, C. (1997) Expression and function of thrombospondin-1 in myelinating glial cells of the central nervous system. *J. Neurosci. Res*, **50**, 202–214.

Sloan, S.A. & Barres, B.A. (2014) Mechanisms of astrocyte development and their contributions to neurodevelopmental disorders. *Current Opinion in Neurobiology*, **27C**, 75–81.

Tran, M.D. & Neary, J.T. (2006) Purinergic signaling induces thrombospondin-1 expression in astrocytes. *Proc. Natl. Acad. Sci. U.S.A*, **103**, 9321–9326.

Ullian, E.M. & Dityatev, A. (2006) Extracellular matrix molecules and formation of CNS synapses. *Molecular Mechanisms of Synaptogenesis*.

Wight, T.N., Raugi, G.J., Mumby, S.M., & Bornstein, P. (1985) Light microscopic immunolocation of thrombospondin in human tissues. *J. Histochem. Cytochem*, **33**, 295–302.

Zalfa, F., Eleuteri, B., Dickson, K.S., Mercaldo, V., De Rubeis, S., di Penta, A., Tabolacci, E., Chiurazzi, P., Neri, G., Grant, S.G.N., & Bagni, C. (2007) A new function for the fragile X mental retardation protein in regulation of PSD-95 mRNA stability. *Nature Neuroscience*, **10**, 578–587.

Zhang, Y. & Ben A Barres (2010) Astrocyte heterogeneity: an underappreciated topic in neurobiology. *Current Opinion in Neurobiology*, **20**, 588–594.

Chapter 6: Discussion

The manuscripts presented in this dissertation were comprised of experiments that were designed to provide evidence for the central hypothesis of this thesis:

Alterations in astrocyte-secreted thrombospondin-1 contribute to the abnormal neurobiology in Fragile X syndrome.

The dissertation set out to **(1)** optimize novel labeling techniques using lipophilic DiI to identify dendritic spines in cultured hippocampal neurons, **(2)** examine the role of astrocyte-derived TSP-1 in the modulation of spine and synaptic deficits in the Fragile X mouse model, **(3)** compare the developmental expression of TSP-1 in Fragile X mice and cultured astrocytes relative to their wildtype counterparts. The results of this dissertation support the overall hypothesis.

In order to address the hypothesis, the present experiments were based on a set of six Specific Aims (See Section 2.1.3.). Each of the manuscripts in Chapters 3 through 5, contain experiments that were designed to address these Specific Aims. The major findings of each paper, and their contribution to the substantiation of the hypotheses are provided below.

6.1 Summary of Findings

6.1.1. Chapter 3

In this chapter, we optimized a technique using fluorescent DiI to effectively label dendritic spines and conduct our morphological spine analysis in Chapter 4. Among the most important parameters of this procedure, fixation properties impacted the success of labeling most profoundly. In the first set of experiments, the patterns of DiI labeling were investigated in dissociated hippocampal neurons fixed with laboratory prepared paraformaldehyde (PFA) in PBS or commercial grade formalin. The results indicated that laboratory prepared PFA samples outperformed commercial formalin by facilitating enhanced staining and clarity for the visualization of spines. In the next set of experiments, the findings showed that higher concentrations of PFA (4%) fixative resulted in less optimal DiI labeling compared to the use of lower concentrations of PFA (1.5% or 2%). Lastly, stronger fixative limited the diffusion of the dye in neuronal processes and affected the quantification of spine density, suggesting that variations in fixation approaches can alter the magnitude of DiI labeling in spines.

6.1.2. Chapter 4

This study presents evidence for the role of astrocyte-secreted TSP-1 in the dysregulation of dendritic spines and synapses in a mouse model of FXS, during a period when astrocytes are crucial for the proper establishment of neural circuitry in the CNS. In the first set of experiments, morphological differences in dendritic spine subtypes and length were examined in dissociated hippocampal neuronal cultures labeled with DiI from *Fmr1* knockout (KO) and wildtype (WT) mice at 17 days *in vitro* (*DIV*). *Fmr1* KO

neurons displayed an increase in dendritic spine length and filopodia-like subtypes characteristic of immature spines, and a subsequent decrease in mature stubby subtypes. *Fmr1* KO neurons also displayed reductions in excitatory synapse protein expression compared to their WT counterparts.

In the second set of experiments, the contributions of diffusible astrocytes factors on neuronal growth were investigated. Using a non-contact co-culture approach, WT neurons grown with *Fmr1* KO astrocyte feeder layer displayed enhanced immature spine morphologies and reduced synaptic densities than their WT counterparts; however, the spine/synaptic alterations could be recovered with WT astrocyte feeder layer or WT astrocyte-conditioned media (ACM), demonstrating an important role for secreted signals in the regulation of neuronal development.

In the next set of experiments, the role of astrocyte-secreted thrombospondin-1 (TSP-1) in the neurobiology of FXS was investigated. The results revealed that TSP-1 cellular expression and release in ACM were both altered in *Fmr1* KO astrocytes, suggesting that a lack of FMRP expression prevents normal TSP-1 expression in cortical astrocytes during development. However, supplementing *Fmr1* KO neurons with exogenous TSP-1 was sufficient to rescue the spine and synapse deficits. Two types of control experiments using gabapentin and heat-inactivated TSP-1 confirmed the effectiveness of the treatment. These findings support the hypothesis that astrocyte dysfunction underlies neuronal deficits observed in FXS and that altered TSP-1 levels in *Fmr1* KO astrocytes may contribute to the reported conclusions.

6.1.3. Chapter 5

As an extension of our findings from Chapter 4, we examined the expression of TSP-1 during early developmental periods in the brain that center on the proper formation and maturation of synapses in FXS. In our first study, the distribution patterns of TSP-1 were elucidated in WT and *Fmr1* KO primary cortical astrocytes. The results indicated that the proportion of TSP-1-expressing astrocytes was decreased in *Fmr1* KO cultures during early postnatal development at 14 and 21 *DIV*. These results support the findings from Chapter 4, which demonstrated that cellular and secreted levels of TSP-1 were diminished in *Fmr1* KO astrocytes.

In the next study, TSP-1 protein levels were further confirmed in the cortex and hippocampus of mice at postnatal days P7, P14 and P21. In both the WT and *Fmr1* KO mice, TSP-1 expression levels peaked in the cortex and hippocampus at P7 and significantly declined thereafter. However, TSP-1 protein levels were significantly reduced in both the cortex and hippocampus of *Fmr1* KO mice in contrast to their WT counterparts. Overall, the differences observed in the developmental trajectory of astrocyte-derived TSP-1 in *Fmr1* KO mice likely contribute to the alterations observed in synapse formation and delays in spine development.

Taken together, the novel findings of the thesis contribute and support the hypothesis that **astrocyte-secreted TSP-1 modulates synaptogenesis in the Fragile X mouse model.** More specifically, we provide evidence that the dysregulation of synapse formation and spine development are a consequence of deficient TSP-1 levels in FXS. Overall, these findings are the first to demonstrate that astrocyte-derived signals, specifically TSP-1 contribute to the abnormal neurobiology in Fragile X. The established experiments provide qualitative characteristics on dendritic spine and synaptic development and provide insight into the cellular and molecular mechanisms between astrocytes and neurons that govern normal synaptic profiles in FXS. These studies give us insight into where the alterations occur during crucial windows of early development that may be important for proper interventions in FXS. As such, this research provides exciting new avenues for FXS research and many novel possibilities for investigations into innovative therapeutic targets for the treatment of FXS, including a strategy for the exploration of astrocyte-based therapies involving secreted factors to correct abnormal patterns of development in FXS.

6.2. Future Directions

The author of this dissertation recognizes that these experiments are only the initial stepping stone towards validating the proposed hypothesis. Here, some of the limitations inherent in the experimental design are discussed, as well as some exciting areas of interest for future research.

6.2.1. Astrocyte-Mediated Mechanisms via Membrane-Associated Factors

The interface between astrocytes and neurons is necessary for normal synapse development, including synaptic pruning and maturation. In the experiments presented in Chapters 4 & 5, the contributions of astrocyte-secreted factors in neuronal development were established. While these studies have elucidated a role for the soluble factor TSP-1 on spine/synapse development in FXS, the role of contact-mediated mechanisms has not been elucidated. Membrane-bound factors have been identified as important participants in synaptogenesis. As such, the exploration of membrane-associated proteins would be useful in further identifying potential alterations in neuron-glia interactions in FXS.

For instance, an interesting link has emerged between TSP-1 and the neuronal cell surface adhesion protein neuroligin-1 (NL-1). TSP-1 interacts with NL-1 and plays a role in increasing the speed of synapse formation in young cultured rat hippocampal neurons (Xu et al. 2009). NL-1 has been identified as a direct target of FMRP (Darnell et al., 2011). Previous studies have reported abnormally low levels of NL-1 in *Fmr1* KO mice (Dahlhaus & El-Husseini 2009). Concomitantly, the findings in this dissertation showed deficits in the expression of astrocyte-derived TSP-1 at the cellular level, as well as in hippocampal and cortical tissues of *Fmr1* KO mice during early development. Given that TSP-1 and NL-1 are both downregulated in FXS, this may contribute to developmental delays in synapse formation and maturation. However, whether TSP-1 initiates synapses *de novo* or instead stabilizes dynamics also remains to be elucidated. Future studies could extend upon these findings to further delineate the specific underlying mechanisms of TSP-1 induced synapse formation in FXS.

Another example of direct astrocyte-neuron contact involves EphAR/ephrin-A signaling. More specifically, EphA4 receptors expressed on neurons and ephrin-A3 ligands located on the perisynaptic processes of astrocytes, play a role in maintaining normal dendritic spine morphology *in vivo* to regulate hippocampal function (Carmona et al. 2009). EphAR/ephrin-A interact downstream with members of the Rho/Ras pathways, suggesting that EphAR/ephrin-A interactions may underlie aspects of actin-driven astrocyte motility observed during synapse formation. Disruptions in these interactions would, therefore, result in the destabilization of newly formed spines. Hence, it may be interesting to explore contact-mediated mechanisms, specifically aspects of astrocyte and dendritic spine motility, to provide greater insight into signaling dynamics. A better understanding of the bidirectional signals between neurons and astrocytes would greatly advance our knowledge of neuronal circuit development in FXS.

6.2.2. Dendritic Spines and Synaptic Densities in Fmr1 KO Neurons

In FXS, ASDs and other forms of mental impairment, it has been suggested that the presence of unusually long and thin dendritic spines, reminiscent of filopodia, may be a sign of arrested dendritic development (Comery et al. 1997; Kaufmann and Moser 2000). However, significant discrepancies have been reported in the literature regarding changes in spine length, morphology and density. A major drawback when comparing similar studies can be attributed to a variety of factors, including the use of different staining (Golgi, diOlistic labelling, transfection) and quantification methods of spines, as well as the choice of tissue source (cultured hippocampal neurons versus *in vivo* or *ex vivo* brain tissue). Strain differences (FVB or C57BL/6) and environmental enrichment (Lauterborn

et al. 2013) can also influence spine morphology. The classification of dendritic protrusions into different categories, such as mature and immature, can vary from one study to another, resulting in diverse phenotypes. For instance, some studies look at the presence versus absence of a head, the ratio between the width and the length of the protrusion, and others, at the profile. As these criteria can be quite arbitrary, the study in Chapter 4 not only classified the spine profiles, but also used length as an objective measure. However, a "spinocentric" view would ignore another equally important aspect, which includes understanding the functional consequences of glial/neuronal abnormalities and how they are mediated in FXS. For instance, it is difficult to directly draw conclusions about how spine changes might contribute to neuronal excitability, or whether instead immature morphology and instability simply reflect the immaturity of circuits in the absence of FMRP (Cruz-Martin et al. 2010; Pan et al. 2010). Some have argued that motility and turnover are better indicators than morphological criteria (e.g., shape, length) at distinguishing immature filopodial protrusions from mature spines (Holtmaat and Svoboda 2009). By conducting functional studies with the use of electrophysiology, it would be possible to measure the activity at individual spines and identify synaptic and circuit defects in FXS.

In Chapter 4, the findings reported a lack of a spine density difference between *Fmr1* KO and WT neurons, but a significantly decreased synaptic density in the *Fmr1* KO neurons. *Fmr1* KO neurons also displayed an increase in the presence of thin, immature spines. Thin spines are thought to be less stable, tend to have higher turnover, and often lack a PSD (Knott and Holtmaat 2008). This could potentially give rise to a

reduced numbers of excitatory synapses that are structural in nature seen in the *Fmr1* KO neurons. Several studies have also demonstrated that different cells derived from the same region, and perhaps even individual cells within a class, can have dramatically different spine densities (Holtmaat and Svoboda 2009; Yoshihara et al. 2009). In an effort to reconcile this discrepancy, future experiments could assess the density and turnover of postsynaptic AMPA receptors. This approach may provide insight into the number of functional excitatory synapses formed.

It is also important to consider that in the experimental set up of the primary cultures, mixed genders were utilized to generate the astrocytes and neurons. However, sex differences exist in the occurrence and severity in FXS, particularly in males. This raises the possibility that some of the inconsistencies observed in spine morphology and synaptic densities may arise from random differences in male-to-female ratios between conditions.

Lastly, for the dendritic spine analysis, spines were manually counted on each dendritic segment. However, considerable overlap in the dendritic processes and spines was often observed. Consequently, some spines, particularly the shorter stubby spines, may have been concealed on the dendrites and gone undetected. The use of sensitive automated image processing and analysis software (i.e. Imaris) may provide a more robust analysis and accurately identify obscured or unresolved spines that may interfere with the quantification.

6.2.3. Extension of Findings (in vitro to in vivo)

The experiments presented in this dissertation were performed largely *in vitro* using a cell culture system with primary neurons and astrocytes. *In vitro* methods provide an excellent means for investigating the mechanisms underlying disease. They allow the study of disease processes in an environment isolated from the complexity of that *in vivo.* Our results with complete controls show compelling evidence for the role of TSP-1 in facilitating neuronal development. The advantage in an *in vitro* system allows one to study single growth factors and establish firm roles without the complication of multiple complex growth factor effects *in vivo*. Additionally, cells in culture are more accessible for experiments that require the visualization of spines and synapses, due to a lessening of the intricate networks present *in vivo.* However, this isolation has its limitations for the interpretation of the results *in vivo*. Firstly, in an *in vitro* environment, the cells are not subject to all aspects of the normal *in situ* environmental milieu. Secondly, the phenotypic characteristics of cultured cells differ significantly from their *in vivo* counterparts. In particular, astrocytes grown in culture often appear "reactive", exhibiting different structural characteristics and molecular profiles than astrocytes *in vivo* (Zamanian et al. 2012). Certain genes that are enriched in cultured astroglia may not be activated or expressed *in vivo* (Cahoy et al. 2008). Therefore, while the information obtained from *in vitro* studies is invaluable, investigations in an *in vivo* correlate are often desirable.

Further exploration of the astrocyte/spine relationship in FXS *in vivo* would be necessary to provide important new evidence that advances our knowledge beyond the *in vitro* findings and to confirm if similar affects can be observed *in vivo.* In order to provide

a more accurate measurement of astrocyte-specific TSP-1 levels in both normal and *Fmr1* KO mice, the purification of astrocytes by immunopanning would permit the prospective isolation of astrocytes from tissues in the rodent brain (Foo et al. 2011). Using these measurements, it would be possible to determine if the *in vivo* spine/synaptic phenotypes could be rescued by the restoration of TSP-1 levels in the *Fmr1* KO mouse.

Future efforts could also be directed toward determining whether FMRP re-introduction in astrocytes alone, or concomitantly in both astrocytes and neurons may provide enhanced benefit over that seen when expressed in neurons only. With the identification of astrocyte-specific markers and the molecules they release, the advent of optogenetics, *Fmr1* conditional KO mice and improvements in imaging techniques, it might now be possible to manipulate FMRP astrocytes in specific brain regions and at different times during development *in vivo*. These studies might shed new light on the contributions made by astrocytes to the formation of neural circuits in both healthy and FXS brains.

Another exciting area of research would be the study of human astrocytes to determine how they differ from their rodent counterparts. An understanding of the unique characteristics of human astrocytes might provide a new insight into the basis of human cognition. This molecular insight might also further our understanding of the pathological changes in astrocytes that lead to several neurodevelopmental disorders.

6.2.4. TSP-1 and Synapse Formation

In Chapter 4, the results demonstrated that *Fmr1* KO hippocampal neurons display abnormal morphological features in dendritic spines and synapses. However, the

application of astrocyte-conditioned media (ACM) or an astrocyte feeder layer (AFL) from normal FMRP-expressing mice rescued the spine and synaptic deficits in the *Fmr1* KO neurons, suggesting that WT astrocytes secrete factors that promote proper development. The study further reported decreased intracellular and secreted TSP-1 levels in FXS astrocytes. By restoring the deficits in TSP-1, the impairments in spine and synapse development could be corrected in the *Fmr1* KO neurons. In agreement with this, the results in Chapter 5 further confirmed that TSP-1 is downregulated at crucial developmental time points relevant for synapse formation in both cultured astrocytes and in the hippocampus and cortex of *Fmr1* KO mice. These results suggest TSP-1 functions as a permissive switch that helps to control the timing of CNS synaptogenesis. However, the specific mechanisms by which TSP-1 is secreted and what signals are involved in the release are not well understood. Investigation into how astrocytes respond to neuronal activity to regulate the release of secreted signals would provide greater insight into the molecular cues that control synapse formation and function.

In these studies, TSP-1 is the only astrocyte candidate screened. TSP-1 is able to promote synaptic adhesion and initiate the events that lead to the establishment of pre- and postsynaptic specializations. Interestingly, these TSP-induced synapses are ultrastructurally identical to fully developed synapses and are presynaptically active, but postsynaptically silent due to the lack of surface AMPA receptors (Christopherson et al. 2005). This suggests that astrocytes may secrete a second unrelated signal that is able to convert these silent synapses into fully active ones (Eroglu 2009). In recent years, a number of other astrocyte-secreted proteins have been identified with known effects on

synapse and spine formation and maturation (Clarke and Barres 2013b). Of those proteins, Hevin (SPARC-like 1) has been identified as an FMRP target. Hevin has been linked to autism and shown to play a role in spine formation and maturation (Kucukdereli et al. 2011). In contrast with the expression of TSP-1 which gradually declines during development, Hevin expression increases in agreement with synapse formation and is also present in adulthood (Risher et al. 2014). This suggests that Hevin likely participates in the maintenance of existing synapses and may be particularly important to consider. Future studies could also examine the role of other TSP family members, including TSP-2 which is also expressed early in brain development, as well as TSP-4 which is expressed in adulthood.

In Chapter 4, a potential inhibitory affect in the *Fmr1* KO astrocytes was identified when *Fmr1* KO astrocytes cultured in the presence of WT neurons resulted in spine and synaptic alterations. Thus, it is important to consider the possibility that *Fmr1* KO astrocytes could also be releasing inhibitory substances that prevent normal development. Profound changes in both excitatory and inhibitory neurotransmission have been reported in FXS (Huber et al. 2002). Thus, the differentiation between the two mechanisms involving a lack of factor and inhibitory effects is of particular importance. The investigation into other TSP family members and secreted synaptogenic molecules may also provide a broader understanding of the cellular and molecular regulatory mechanisms underlying the abnormal neurobiology in FXS.

6.4. Conclusion

Therefore, the results presented in the manuscripts included in this dissertation provide strong evidence for the central hypothesis of this thesis: *Astrocyte-secreted TSP-1 contributes to the development of the abnormal neurobiology seen in FXS*. These experiments are the first to suggest that defects in astrocyte function and secreted molecules during early development likely contribute to the abnormal neural development in FXS. As such, these findings present significant implications for future FXS research. They provide a new, and exciting, direction for studies investigating the underlying processes leading to the abnormal neuronal phenotype seen in FXS. Furthermore, and perhaps most importantly, the novel prospect for the role of astrocyte-derived molecules in the development of FXS will create many possibilities for new therapeutic targets and innovative treatment strategies for individuals with FXS. More detailed knowledge of the expression profiles of TSP-1 and other secreted factors will help facilitate the appropriate timing of interventions that may help promote optimal development in FXS.

7. References

Abbott NJ, Rönnbäck L, Hansson E. 2006. Astrocyte-endothelial interactions at the blood-brain barrier. Nat Rev Neurosci 7:41–53.

Adams JC, Lawler J. 2004. The thrombospondins. The International Journal of Biochemistry & Cell Biology 36:961–968.

Agah A, Kyriakides TR, Lawler J, Bornstein P. 2002. The lack of thrombospondin-1 (TSP1) dictates the course of wound healing in double-TSP1/TSP2-null mice. AJPA 161:831–839.

Akins MR, LeBlanc HF, Stackpole EE, Chyung E, Fallon JR. 2012. Systematic mapping of fragile X granules in the mouse brain reveals a potential role for presynaptic FMRP in sensorimotor functions. J. Comp. Neurol. 520:3687–3706.

Araque A, Carmignoto G, Haydon PG. 2001. Dynamic signaling between astrocytes and neurons. Annu. Rev. Physiol. 63:795–813.

Ascano M, Mukherjee N, Bandaru P, Miller JB, Nusbaum JD, Corcoran DL, Langlois C, Munschauer M, Dewell S, Hafner M, et al. 2012. FMRP targets distinct mRNA sequence elements to regulate protein expression. Nature 492:382–386.

Asch AS, Leung LL, Shapiro J, Nachman RL. 1986. Human brain glial cells synthesize thrombospondin. Proc. Natl. Acad. Sci. U.S.A. 83:2904–2908.

Ashley CT, Sutcliffe JS, Kunst CB, Leiner HA, Eichler EE, Nelson DL, Warren ST. 1993. Human and murine FMR-1: alternative splicing and translational initiation downstream of the CGG–repeat. Nature Genetics 4:244–251.

Ashley CT, Wilkinson KD, Reines D, Warren ST. 1993. FMR1 protein: conserved RNP family domains and selective RNA binding. Science 262:563–566.

Bagni C, Greenough WT. 2005. From mRNP trafficking to spine dysmorphogenesis: the roots of fragile X syndrome. Nat Rev Neurosci 6:376–387.

Bagni C, Tassone F, Neri G, Hagerman R. 2012. Fragile X syndrome: causes, diagnosis, mechanisms, and therapeutics. J. Clin. Invest. 122:4314–4322.

Bailey DB, Raspa M, Olmsted M, Holiday DB. 2008. Co-occurring conditions associated with FMR1 gene variations: findings from a national parent survey. Am. J. Med. Genet. 146A:2060–2069.

Bakker CE, de Diego Otero Y, Bontekoe C, Raghoe P, Luteijn T, Hoogeveen AT, Oostra BA, Willemsen R. 2000. Immunocytochemical and biochemical characterization of FMRP, FXR1P, and FXR2P in the mouse. Exp. Cell Res. 258:162–170.

Bakker CE, Kooy RF, D'Hooge R, Tamanini F, Willemsen R, Nieuwenhuizen I, De Vries BBA, Reyniers E, Hoogeveen AT, Willems PJ, et al. 2000. Introduction of a FMR1 transgene in the fragile X knockout mouse. Neuroscience Research Communications 26:265–277.

Banker GA. 1980. Trophic interactions between astroglial cells and hippocampal neurons in culture. Science 209:809–810.

Basu SN, Kollu R, Banerjee-Basu S. 2009. AutDB: a gene reference resource for autism research. Nucleic Acids Research 37:D832–6.

Bayraktar OA, Fuentealba LC, Alvarez-Buylla A, Rowitch DH. 2015. Astrocyte Development and Heterogeneity. Cold Spring Harb Perspect Biol 7:a020362.

Bear MF. 2005. Therapeutic implications of the mGluR theory of fragile X mental retardation. Genes Brain Behav 4:393–398.

Bechara EG, Didiot MC, Melko M, Davidovic L, Bensaid M, Martin P, Castets M, Pognonec P, Khandjian EW, Moine H, et al. 2009. A Novel Function for Fragile X Mental Retardation Protein in Translational Activation. Wickens M, editor. Plos Biol 7:e1000016–13.

Beckel-Mitchener A, Greenough WT. 2004. Correlates across the structural, functional, and molecular phenotypes of fragile X syndrome. Ment Retard Dev Disabil Res Rev 10:53–59.

Berry-Kravis E. 2014. Mechanism-Based Treatments in Neurodevelopmental Disorders: Fragile X Syndrome. Pediatr. Neurol. 50:297–302.

Berry-Kravis EM, Hessl D, Rathmell B, Zarevics P, Cherubini M, Walton-Bowen K, Mu Y, Nguyen DV, Gonzalez-Heydrich J, Wang PP, et al. 2012. Effects of STX209

(arbaclofen) on neurobehavioral function in children and adults with fragile X syndrome: a randomized, controlled, phase 2 trial. Science Translational Medicine 4:152ra127.

Blackwell E, Zhang X, Ceman S. 2010. Arginines of the RGG box regulate FMRP association with polyribosomes and mRNA. Human Molecular Genetics 19:1314–1323.

Bornstein P. 2001. Thrombospondins as matricellular modulators of cell function. J. Clin. Invest. 107:929–934.

Bornstein P, Agah A, Kyriakides TR. 2005. Corrigendum to "The role of Thrombospondins 1 and 2 in the regulation of cell–matrix interaction, collagen fibril formation and the response to injury." The International Journal of ….

Bourne J, Harris KM. 2007. Do thin spines learn to be mushroom spines that remember? Current Opinion in Neurobiology 17:381–386.

Bourne JN, Harris KM. 2008. Balancing structure and function at hippocampal dendritic spines. Annu. Rev. Neurosci. 31:47–67.

Brackett DM, Qing F, Amieux PS, Sellers DL, Horner PJ, Morris DR. 2013. Fmr1 Transcript Isoforms: Association with Polyribosomes; Regional and Developmental Expression in Mouse Brain. Silver DL, editor. PLoS ONE 8:e58296–11.

Bushong EA, Martone ME, Ellisman MH. 2004. Maturation of astrocyte morphology and the establishment of astrocyte domains during postnatal hippocampal development. International Journal of Developmental Neuroscience 22:73–86.

Cahoy JD, Emery B, Kaushal A, Foo LC, Zamanian JL, Christopherson KS, Xing Y, Lubischer JL, Krieg PA, Krupenko SA, et al. 2008. A Transcriptome Database for Astrocytes, Neurons, and Oligodendrocytes: A New Resource for Understanding Brain Development and Function. Journal of Neuroscience 28:264–278.

Carmona MA, Murai KK, Wang L, Roberts AJ, Pasquale EB. 2009. Glial ephrin-A3 regulates hippocampal dendritic spine morphology and glutamate transport. Proceedings of the National Academy of Sciences 106:12524–12529.

Ceman S, O'Donnell WT, Reed M, Patton S, Pohl J, Warren ST. 2003. Phosphorylation influences the translation state of FMRP-associated polyribosomes. Human Molecular Genetics 12:3295–3305.

Christopherson KS, Ullian EM, Stokes CCA, Mullowney CE, Hell JW, Agah A, Lawler J, Mosher DF, Bornstein P, Barres BA. 2005. Thrombospondins Are Astrocyte-Secreted Proteins that Promote CNS Synaptogenesis. Cell 120:421–433.

Clarke LE, Barres Ben A. 2013a. Emerging roles of astrocytes in neural circuit development. Nat Rev Neurosci 14:311–321.

Clarke LE, Ben A Barres. 2013b. Glia Keep Synapse Distribution under Wraps. Cell 154:267–268.

Coffee B, Ikeda M, Budimirovic DB, Hjelm LN, Kaufmann WE, Warren ST. 2008. MosaicFMR1 deletion causes fragile X syndrome and can lead to molecular

misdiagnosis: A case report and review of the literature. Am. J. Med. Genet. 146A:1358–1367.

Colak D, Zaninovic N, Cohen MS, Rosenwaks Z, Yang WY, Gerhardt J, Disney MD, Jaffrey SR. 2014. Promoter-Bound Trinucleotide Repeat mRNA Drives Epigenetic Silencing in Fragile X Syndrome. Science 343:1002–1005.

Comery TA, Harris JB, Willems PJ, Oostra BA, Irwin SA, Weiler IJ, Greenough WT. 1997. Abnormal dendritic spines in fragile X knockout mice: maturation and pruning deficits. Proc. Natl. Acad. Sci. U.S.A. 94:5401–5404.

Corty MM, Freeman MR. 2013. Cell biology in neuroscience: Architects in neural circuit design: Glia control neuron numbers and connectivity. The Journal of Cell Biology 203:395–405.

Cruz-Martin A, Crespo M, Portera-Cailliau C. 2010. Delayed Stabilization of Dendritic Spines in Fragile X Mice. Journal of Neuroscience 30:7793–7803.

Dansie LE, Ethell IM. 2011. Casting a net on dendritic spines: The extracellular matrix and its receptors. Prokop A; Reichardt LF, editors. Devel Neurobio 71:956–981.

Darnell JC. 2005. Kissing complex RNAs mediate interaction between the Fragile-X mental retardation protein KH2 domain and brain polyribosomes. Genes & Development 19:1–17.

Darnell JC, Klann E. 2013. The translation of translational control by FMRP: therapeutic

targets for FXS. Nature Publishing Group 16:1530–1536.

Darnell JC, Mostovetsky O, Darnell RB. 2005. FMRP RNA targets: identification and validation. Genes Brain Behav 4:341–349.

Darnell JC, Van Driesche SJ, Zhang C, Hung KYS, Mele A, Fraser CE, Stone EF, Chen C, Fak JJ, Chi SW, et al. 2011. FMRP stalls ribosomal translocation on mRNAs linked to synaptic function and autism. Cell 146:247–261.

De Boulle K, Verkerk AJ, Reyniers E, Vits L, Hendrickx J, Van Roy B, Van den Bos F, de Graaff E, Oostra BA, Willems PJ. 1993. A point mutation in the FMR-1 gene associated with fragile X mental retardation. Nature Genetics 3:31–35.

De Filippis B, Romano E, Laviola G. 2014. Aberrant Rho GTPases signaling and cognitive dysfunction: in vivo evidence for a compelling molecular relationship. Neuroscience and Biobehavioral Reviews 46 Pt 2:285–301.

Devys D, Lutz Y, Rouyer N, Bellocq JP, Mandel JL. 1993. The FMR-1 protein is cytoplasmic, most abundant in neurons and appears normal in carriers of a fragile X premutation. Nature Genetics 4:335–340.

Dictenberg JB, Swanger SA, Antar LN, Singer RH, Bassell GJ. 2008. A Direct Role for FMRP in Activity-Dependent Dendritic mRNA Transport Links Filopodial-Spine Morphogenesis to Fragile X Syndrome. Developmental Cell 14:926–939.

Dowell JA, Johnson JA, Li L. 2009. Identification of astrocyte secreted proteins with a

combination of shotgun proteomics and bioinformatics. J. Proteome Res. 8:4135–4143.

Dutch-Belgiam Fragile X Consortium. 1994. Fmr1 knockout mice: A model to study fragile X mental retardation. Cell 78.

Dury AY, Fatimy El R, Tremblay S, Rose TM, CÃ tÃ J, De Koninck P, Khandjian EW. 2013. Nuclear Fragile X Mental Retardation Protein Is localized to Cajal Bodies. Barsh GS, editor. PLoS Genet 9:e1003890–14.

Eberhart D. 1996. The fragile X mental retardation protein is a ribonucleoprotein containing both nuclear localization and nuclear export signals. Human Molecular Genetics 5:1–9.

Ebrahimi S, Okabe S. 2010. Biochimica et Biophysica Acta. BBA - Biomembranes 1838:2391–2398.

Eichler EE, Richards S, Gibbs RA, Nelson DL. 1993. Fine structure of the human FMR1 gene. Human Molecular Genetics 2:1147–1153.

Eliasson C, Sahlgren C, Berthold CH, Stakeberg J, Celis JE, Betsholtz C, Eriksson JE, Pekny M. 1999. Intermediate filament protein partnership in astrocytes. Journal of Biological Chemistry 274:23996–24006.

Eroglu C. 2009. The role of astrocyte-secreted matricellular proteins in central nervous system development and function. J. Cell Commun. Signal. 3:167–176.

Eroglu C, Allen NJ, Susman MW, O'Rourke NA, Park CY, Özkan E, Chakraborty C,

Mulinyawe SB, Annis DS, Huberman AD, et al. 2009. Gabapentin Receptor α2δ-1 Is a Neuronal Thrombospondin Receptor Responsible for Excitatory CNS Synaptogenesis. Cell 139:380–392.

Eroglu C, Barres BA, Stevens B. 2008. Glia as active participants in the development and function of synapses. :683–714.

Eroglu C, Barres Ben A. 2010. Regulation of synaptic connectivity by glia. Nature 468:223–231.

Ethell IM, Pasquale EB. 2005. Molecular mechanisms of dendritic spine development and remodeling. Progress in Neurobiology 75:161–205.

Fatemi SH, Folsom TD. 2011. Dysregulation of fragile X mental retardationprotein and metabotropic glutamate receptor 5in superior frontal cortex of individuals withautism: a postmortem brain study. Mol Autism 2:6.

Feng Y, Gutekunst CA, Eberhart DE, Yi H, Warren ST, Hersch SM. 1997. Fragile X mental retardation protein: nucleocytoplasmic shuttling and association with somatodendritic ribosomes. J. Neurosci. 17:1539–1547.

Fiacco T, Casper K, Sweger E, Agulhon C, Taves S, Kurtzer-Minton S, McCarthy KD. 2008. Molecular approaches for studying astrocytes. Boston, MA: Springer US. pp. 383–405; 23.

Foo LC. 2013. Purification of rat and mouse astrocytes by immunopanning. Cold Spring

Harb Protoc 2013:421–432.

Freeman MR. 2010. Specification and Morphogenesis of Astrocytes. Science 330:774–778.

Frotscher M, Studer D, Graber W, Chai X, Nestel S, Zhao S. 2014. Fine structure of synapses on dendritic spines. Front Neuroanat 8:94.

Gallagher A, Hallahan B. 2012. Fragile X-associated disorders: a clinical overview. J. Neurol. 259:401–413.

García-López P, García-Marín V, Freire M. 2010. Dendritic Spines and Development: Towards a Unifying Model of Spinogenesis—A Present Day Review of Cajal's Histological Slides and Drawings. Neural Plasticity 2010:1–29.

García-Marín V, García-López P, Freire M. 2007. Cajal's contributions to glia research. Trends in Neurosciences 30:479–487.

Gholizadeh S, Halder SK, Hampson DR. 2015. Expression of fragile X mental retardation protein in neurons and glia of the developing and adult mouse brain. Brain Research 1596:22–30.

Gold MG. 2012. A frontier in the understanding of synaptic plasticity: Solving the structure of the postsynaptic density. Bioessays 34:599–608.

Gross C, Hoffmann A, Bassell GJ, Berry-Kravis EM. 2015. Therapeutic Strategies in Fragile X Syndrome: From Bench to Bedside and Back. NURT 12:584–608.

Guo W, Allan AM, Zong R, Zhang L, Johnson EB, Schaller EG, Murthy AC, Goggin SL, Eisch AJ, Ben A Oostra, et al. 2011. Ablation of Fmrp in adult neural stem cells disrupts hippocampus-dependent learning. Nature Medicine 17:559–565.

Gürkan CK, Hagerman R. 2012. Targeted treatments in autism and fragile X syndrome. Research in Autism Spectrum Disorders 6:1311–1320.

Haber M. 2006. Cooperative Astrocyte and Dendritic Spine Dynamics at Hippocampal Excitatory Synapses. Journal of Neuroscience 26:8881–8891.

Hagerman PJ, Hagerman R. 2004. The fragile-X premutation: a maturing perspective. The American Journal of Human Genetics 74:805–816.

Hagerman R, Hoem G, Hagerman P. 2010. Fragile X and autism: Intertwined at the molecular level leading to targeted treatments. Mol Autism 1:12.

Halassa MM, Fellin T, Takano H, Dong J-H, Haydon PG. 2007. Synaptic islands defined by the territory of a single astrocyte. Journal of Neuroscience 27:6473–6477.

Haydon PG. 2006. Astrocyte Control of Synaptic Transmission and Neurovascular Coupling. Physiological Reviews 86:1009–1031.

He CX, Portera-Cailliau C. 2012. The trouble with spines in fragile X syndrome: density, maturity and plasticity. Neuroscience. 251:120–128.

Higashimori H, Morel L, Huth J, Lindemann L, Dulla C, Taylor A, Freeman M, Yang Y. 2013. Astroglial FMRP-dependent translational down-regulation of mGluR5 underlies

glutamate transporter GLT1 dysregulation in the fragile X mouse. Human Molecular Genetics 22:2041–2054.

Hinds HL, Ashley CT, Sutcliffe JS, Nelson DL, Warren ST, Housman DE, Schalling M. 1993. Tissue specific expression of FMR-1 provides evidence for a functional role in fragile X syndrome. Nature Genetics 3:36–43.

Holtmaat A, Svoboda K. 2009. Experience-dependent structural synaptic plasticity in the mammalian brain. Nat Rev Neurosci 10:647–658.

Honig MG, Hume RI. 1989. Dil and diO: versatile fluorescent dyes for neuronal labelling and pathway tracing. Trends in Neurosciences 12:333–5– 340–1.

Hotulainen P, Hoogenraad CC. 2010. Actin in dendritic spines: connecting dynamics to function. The Journal of Cell Biology 189:619–629.

Huang T, Li LY, Shen Y, Qin XB, Pang ZL, Wu GY. 1996. Alternative splicing of the FMR1 gene in human fetal brain neurons. Am. J. Med. Genet. 64:252–255.

Huber KM, Gallagher SM, Warren ST, Bear MF. 2002. Altered synaptic plasticity in a mouse model of fragile X mental retardation. Proc. Natl. Acad. Sci. U.S.A. 99:7746–7750.

Hughes EG, Elmariah SB, Balice-Gordon RJ. 2010. Astrocyte secreted proteins selectively increase hippocampal GABAergic axon length, branching, and synaptogenesis. Molecular and Cellular Neuroscience 43:136–145.

Irwin SA, Patel B, Idupulapati M, Harris JB, Crisostomo RA, Larsen BP, Kooy F, Willems PJ, Cras P, Kozlowski PB, et al. 2001. Abnormal dendritic spine characteristics in the temporal and visual cortices of patients with fragile-X syndrome: a quantitative examination. Am. J. Med. Genet. 98:161–167.

Jacobs S, Cheng C, Doering LC. 2012. Probing astrocyte function in fragile X syndrome. Results Probl Cell Differ 54:15–31.

Jacobs S, Cheng C, Doering LC. 2016. Hippocampal neuronal subtypes develop abnormal dendritic arbors in the presence of Fragile X astrocytes. Neuroscience 324:202–217.

Jacobs S, Doering LC. 2010. Astrocytes prevent abnormal neuronal development in the fragile x mouse. Journal of Neuroscience 30:4508–4514.

Jacobs S, Nathwani M, Doering LC. 2010. Fragile X astrocytes induce developmental delays in dendrite maturation and synaptic protein expression. BMC Neuroscience 11:132.

Jaffe EA, Ruggiero JT, Leung LK, Doyle MJ, McKeown-Longo PJ, Mosher DF. 1983. Cultured human fibroblasts synthesize and secrete thrombospondin and incorporate it into extracellular matrix. Proc. Natl. Acad. Sci. U.S.A. 80:998–1002.

Johnson-Venkatesh EM, Umemori H. 2010. Secreted factors as synaptic organizers. Eur. J. Neurosci. 32:181–190.

Kaufmann WE, Moser HW. 2000. Dendritic anomalies in disorders associated with mental retardation. Cerebral Cortex.

Kettenmann H, Verkhratsky A. 2008. Neuroglia: the 150 years after. Trends in Neurosciences 31:653–659.

Khandjian EW, Corbin F, Woerly S, Rousseau F. 1996. The fragile X mental retardation protein is associated with ribosomes. Nature Genetics 12:91–93.

Kim M, Bellini M, Ceman S. 2009. Fragile X mental retardation protein FMRP binds mRNAs in the nucleus. Molecular and Cellular Biology 29:214–228.

Knott G, Holtmaat A. 2008. Dendritic spine plasticity—Current understanding from in vivo studies. Brain Research Reviews 58:282–289.

Kreft M, Bak LK, Waagepetersen HS, Schousboe A. 2012. Aspects of astrocyte energy metabolism, amino acid neurotransmitter homoeostasis and metabolic compartmentation. ASN Neuro 4:e00086.

Kucukdereli H, Allen NJ, Lee AT, Feng A, Ozlu MI, Conatser LM, Chakraborty C, Workman G, Weaver M, Sage EH, et al. 2011. PNAS Plus: Control of excitatory CNS synaptogenesis by astrocyte-secreted proteins Hevin and SPARC. Proceedings of the National Academy of Sciences 108:E440–E449.

LaFauci G, Adayev T, Kascsak R, Kascsak R, Nolin S, Mehta P, Brown WT, Dobkin C. 2013. Fragile X Screening by Quantification of FMRP in Dried Blood Spots by a

Luminex Immunoassay. The Journal of Molecular Diagnostics 15:508–517.

Lauterborn JC, Jafari M, Babayan AH, Gall CM. 2013. Environmental Enrichment Reveals Effects of Genotype on Hippocampal Spine Morphologies in the Mouse Model of Fragile X Syndrome. Cereb Cortex 25:516–527.

Lawler JW, Slayter HS, Coligan JE. 1978. Isolation and characterization of a high molecular weight glycoprotein from human blood platelets. Journal of Biological Chemistry 253:8609–8616.

Levenga J, Hayashi S, de Vrij FMS, Koekkoek SK, van der Linde HC, Nieuwenhuizen I, Song C, Buijsen RAM, Pop AS, GomezMancilla B, et al. 2011. AFQ056, a new mGluR5 antagonist for treatment of fragile X syndrome. Neurobiology of Disease 42:311–317.

Li X, Newbern JM, Wu Y, Morgan-Smith M, Zhong J, Charron J, Snider WD. 2012. MEK Is a Key Regulator of Gliogenesis in the Developing Brain. Neuron 75:1035–1050.

Li YX, Schaffner AE, Walton MK, Barker JL. 1998. Astrocytes regulate developmental changes in the chloride ion gradient of embryonic rat ventral spinal cord neurons in culture. The Journal of Physiology 509:847–858.

Liauw J, Hoang S, Choi M, Eroglu C, Choi M, Sun G-H, Percy M, Wildman-Tobriner B, Bliss T, Guzman RG, et al. 2008. Thrombospondins 1 and 2 are necessary for synaptic plasticity and functional recovery after stroke. J Cereb Blood Flow Metab 28:1722–1732.

Lipton J, Sahin M. 2013. Fragile X syndrome therapeutics: translation, meet translational

medicine. Neuron 77:212–213.

Liu Q-S, Xu Q, Kang J, Nedergaard M. 2004. Astrocyte activation of presynaptic metabotropic glutamate receptors modulates hippocampal inhibitory synaptic transmission. Neuron Glia Biol 1:307–316.

Ludwig AL, Espinal GM, Pretto DI, Jamal AL, Arque G, Tassone F, Berman RF, Hagerman PJ. 2014. CNS expression of murine fragile X protein (FMRP) as a function of CGG-repeat size. Human Molecular Genetics 23:3228–3238.

Luo Y, Shan G, Guo W, Smrt RD, Johnson EB, Li X, Pfeiffer RL, Szulwach KE, Duan R, Barkho BZ, et al. 2010. Fragile X Mental Retardation Protein Regulates Proliferation and Differentiation of Adult Neural Stem/Progenitor Cells. Orr H, editor. PLoS Genet 6:e1000898.

Maiti P, Manna J, McDonald MP. 2015. Merging advanced technologies with classical methods to uncover dendritic spine dynamics: A hot spot of synaptic plasticity. Neuroscience Research 96:1–13.

Malinow R, Hayashi Y, Maletic-Savatic M, Zaman SH, Poncer J-C, Shi S-H, Esteban JA, Osten P, Seidenman K. 2010. Introduction of green fluorescent protein (GFP) into hippocampal neurons through viral infection. Cold Spring Harb Protoc 2010:pdb.prot5406.

Matus A. 2005. Growth of dendritic spines: a continuing story. Current Opinion in

Neurobiology 15:67–72.

McCall MA, Gregg RG, Behringer RR, Brenner M, Delaney CL, Galbreath EJ, Zhang CL, Pearce RA, Chiu SY, Messing A. 1996. Targeted deletion in astrocyte intermediate filament (Gfap) alters neuronal physiology. Proc. Natl. Acad. Sci. U.S.A. 93:6361–6366.

Molofsky AV, Krencik R, Krenick R, Ullian EM, Ullian E, Tsai H-H, Deneen B, Richardson WD, Barres BA, Rowitch DH. 2012. Astrocytes and disease: a neurodevelopmental perspective. Genes & Development 26:891–907.

Mosher DF, Doyle MJ, Jaffe EA. 1982. Synthesis and secretion of thrombospondin by cultured human endothelial cells. The Journal of Cell Biology 93:343–348.

Murai KK, Nguyen LN, Irie F, Yamaguchi Y, Pasquale EB. 2002. Control of hippocampal dendritic spine morphology through ephrin-A3/EphA4 signaling. Nature Neuroscience 6:153–160.

Myrick LK, Deng P-Y, Hashimoto H, Oh YM, Cho Y, Poidevin MJ, Suhl JA, Visootsak J, Cavalli V, Jin P, et al. 2015. Independent role for presynaptic FMRP revealed by an FMR1missense mutation associated with intellectual disability and seizures. Proceedings of the National Academy of Sciences 112:949–956.

Newman EA. 2003. New roles for astrocytes: Regulation of synaptic transmission. Trends in Neurosciences 26:536–542.

Nishida H, Okabe S. 2007. Direct Astrocytic Contacts Regulate Local Maturation of

Dendritic Spines. Journal of Neuroscience 27:331–340.

O'Shea KS, Liu LH, Kinnunen LH, Dixit VM. 1990. Role of the extracellular matrix protein thrombospondin in the early development of the mouse embryo. The Journal of Cell Biology 111:2713–2723.

Oostra BA, Willemsen R. 2009. FMR1: a gene with three faces. Biochim Biophys Acta 1790:467–477.

Pacey LKK, Doering LC. 2007. Developmental expression of FMRP in the astrocyte lineage: implications for fragile X syndrome. Glia 55:1601–1609.

Pacey LKK, Xuan ICY, Guan S, Sussman D, Henkelman RM, Chen Y, Thomsen C, Hampson DR. 2013. Delayed myelination in a mouse model of fragile X syndrome. Human Molecular Genetics 22:3920–3930.

Parri R, Crunelli V. 2003. An astrocyte bridge from synapse to blood flow. Nature Neuroscience 6:5–6.

Penzes P, Cahill ME, Jones KA, VanLeeuwen J-E, Woolfrey KM. 2011. Dendritic spine pathology in neuropsychiatric disorders. Nature Publishing Group 14:285–293.

Perea G, Araque A. 2010. GLIA modulates synaptic transmission. Brain Research Reviews 63:93–102.

Pfeiffer BE, Huber KM. 2009. The state of synapses in fragile X syndrome. Neuroscientist 15:549–567.

Pfrieger FW, Barres Barbara A. 1997. Synaptic efficacy enhanced by glial cells in vitro. Science 277:1684–1687.

Pontrello CG, Ethell IM. 2009. Accelerators, brakes, and gears of actin dynamics in dendritic spines. The open neuroscience journal 3:67-86.

Portera-Cailliau C. 2012. Which Comes First in Fragile X Syndrome, Dendritic Spine Dysgenesis or Defects in Circuit Plasticity? The Neuroscientist 18:28–44.

Purves D, Augustine G, Fitzpatrick D, Hall W, LaMantia AS, White L. 2012. Neuroscience Fifth Edition. Sunderland, MA: Sinauer Associates. 521-522.

Raugi GJ, Mumby SM, Abbott-Brown D, Bornstein P. 1982. Thrombospondin: synthesis and secretion by cells in culture. The Journal of Cell Biology 95:351–354.

Resovi A, Pinessi D, Chiorino G, Taraboletti G. 2014. Current understanding of the thrombospondin-1 interactome. Matrix Biol 37:83-91.

Riccomagno MM, Kolodkin AL. 2015. Sculpting neural circuits by axon and dendrite pruning. Annu Rev Cell and Dev Biol 31:770-805.

Risher WC, Patel S, Kim IH, Uezu A, Bhagat S, Wilton DK, Pilaz L-J, Singh Alvarado J, Calhan OY, Silver DL, et al. 2014. Astrocytes refine cortical connectivity at dendritic spines. Elife 3.

Rochefort NL, Konnerth A. 2012. Dendritic spines: from structure to in vivo function. Nature Publishing Group 13:699–708.

Rudelli RD, Brown WT, Wisniewski K, Jenkins EC, Laure-Kamionowska M, Connell F, Wisniewski HM. 1985. Adult fragile X syndrome. Clinico-neuropathologic findings. Acta Neuropathol 67:289–295.

Sala C, Segal M. 2014. Dendritic spines: the locus of structural and functional plasticity. Physiological Reviews 94:141–188.

Santoro MR, Bray SM, Warren ST. 2012. Molecular Mechanisms of Fragile X Syndrome: A Twenty-Year Perspective. Annu Rev Pathol Mech Dis 7:219–245.

Schaefer TL, Davenport MH, Erickson CA. 2015. Emerging pharmacologic treatment options for fragile X syndrome. Appl Clin Genet 8:75–93.

Shinohara Y. 2011. Quantification of postsynaptic density proteins: Glutamate receptor subunits and scaffolding proteins. Lubec G, editor. Hippocampus 22:942–953.

Shirao T, González-Billault C. 2013. Actin filaments and microtubules in dendritic spines. Journal of Neurochemistry 126:155–164.

Sittler A, Devys D, Weber C, Mandel JL. 1996. Alternative splicing of exon 14 determines nuclear or cytoplasmic localisation of fmr1 protein isoforms. Human Molecular Genetics 5:95–102.

Spencer CM, Alekseyenko O, Hamilton SM, Thomas AM, Serysheva E, Yuva-Paylor LA, Paylor R. 2011. Modifying behavioral phenotypes in Fmr1KO mice: genetic background differences reveal autistic-like responses. Crawley J; DiCicco-Bloom E;

Bailey AJ, editors. Autism Res 4:40–56.

Staffend NA, Meisel RL. 2011. DiOlistic Labeling of Neurons in Tissue Slices: A Qualitative and Quantitative Analysis of Methodological Variations. Front Neuroanat 5:14.

Tassone F, De Rubeis S, Carosi C, La Fata G, Serpa G, Raske C, Willemsen R, Hagerman PJ, Bagni C. 2011. Differential usage of transcriptional start sites and polyadenylation sites in FMR1 premutation alleles. Nucleic Acids Research 39:6172–6185.

Tucker RP. 2004. The thrombospondin type 1 repeat superfamily. The International Journal of Biochemistry & Cell Biology 36:969–974.

Verkerk AJMH, Pieretti M, Sutcliffe JS, Fu Y-H, Kuhl DPA, Pizzuti A, Reiner O, Richards S, Victoria MF, Zhang F, et al. 1991. Identification of a gene (FMR-1) containing a CGG repeat coincident with a breakpoint cluster region exhibiting length variation in fragile X syndrome. Cell 65:905–914.

Verkhratsky A, Nedergaard M, Hertz L. 2014. Why are Astrocytes Important? Neurochem Res 40:389–401.

Volterra A, Meldolesi J. 2005. Astrocytes, from brain glue to communication elements: the revolution continues. Nat Rev Neurosci 6:626–640.

Wijetunge LS, Chattarji S, Wyllie DJA, Kind PC. 2013. Fragile X syndrome: from targets

to treatments. Neuropharmacology 68:83–96.

Willemsen R, Levenga J, Oostra BA. 2011. CGG repeat in the FMR1 gene: size matters. Clinical Genetics 80:214–225.

Won H, Mah W, Kim E. 2013. Autism spectrum disorder causes, mechanisms, and treatments: focus on neuronal synapses. Front Mol Neurosci 6:19.

Xu J, Xiao N, Xia J. 2009. Thrombospondin 1 accelerates synaptogenesis in hippocampal neurons through neuroligin 1. Nature Publishing Group 13:22–24.

Yan QJ, Asafo-Adjei PK, Arnold HM, Brown RE, Bauchwitz RP. 2004. A phenotypic and molecular characterization of the fmr1-tm1Cgr fragile X mouse. Genes Brain Behav 3:337–359.

Yang Q, Feng B, Zhang K, Guo Y-Y, Liu S-B, Wu Y-M, Li X-Q, Zhao M-G. 2012. Excessive Astrocyte-Derived Neurotrophin-3 Contributes to the Abnormal Neuronal Dendritic Development in a Mouse Model of Fragile X Syndrome. PLoS Genet 8(12):e1003172.

Yang Y, Vidensky S, Jin L, Jie C, Lorenzini I, Frankl M, Rothstein JD. 2010. Molecular comparison of GLT1+ and ALDH1L1+ astrocytes in vivo in astroglial reporter mice. Glia 59:200–207.

Yoshihara Y, De Roo M, Muller D. 2009. Dendritic spine formation and stabilization. Current Opinion in Neurobiology 19:146–153.

Yuste R. 2011. Dendritic spines and distributed circuits. Neuron 71:772–781.

Zalfa F, Eleuteri B, Dickson KS, Mercaldo V, De Rubeis S, di Penta A, Tabolacci E, Chiurazzi P, Neri G, Grant SGN, et al. 2007. A new function for the fragile X mental retardation protein in regulation of PSD-95 mRNA stability. Nature Neuroscience 10:578–587.

Zamanian JL, Xu L, Foo LC, Nouri N, Zhou L, Giffard RG, Barres BA. 2012. Genomic Analysis of Reactive Astrogliosis. J. Neurosci. 32:6391–6410.

Zhang Y, Barres Ben A. 2010. Astrocyte heterogeneity: an underappreciated topic in neurobiology. Current Opinion in Neurobiology 20:588–594.

Zoghbi HY, Bear MF. 2012. Synaptic dysfunction in neurodevelopmental disorders associated with autism and intellectual disabilities. Cold Spring Harb Perspect Biol 4.